FEDERAL UNIVERSITY OF SANTA CATARINA
TECHNOLOGICAL CENTER
PROGRAM OF GRADUATE IN CHEMICAL ENGINEERING

Alisson Lopes Freire

# Application of Geopolymers in $CO_2$ Adsorption at Low Temperature

Florianópolis
2019

Alisson Lopes Freire

# Application of Geopolymers in $CO_2$ Adsorption at Low Temperature

Master thesis submitted to the Program of Graduate in Chemical Engineering of the Federal University of Santa Catarina to obtain the Degree of master in chemical engineering

Advisor: Profª. Dr. Regina de Fátima Peralta Muniz Moreira

Co-Advisor: Prof. Dr. Agenor de Noni Júnior

Co-Advisor: Profª. Dr. Maria Helena Araujo

Florianópolis
2019

Identification sheet of the work prepared by the author through the Automatic Program of the University Library of UFSC.

Freire, Alisson Lopes
Application of Geopolymers in CO2 Adsorption at Low Temperature / Alisson Lopes Freire ; orientadora, Regina de Fátima Peralta Muniz Moreira, coorientador, Agenor de Noni Junior, coorientadora, Maria Helena Araujo, 2019.
105 p.

Dissertação (mestrado) - Universidade Federal de Santa Catarina, Centro Tecnológico, Programa de Pós-Graduação em Engenharia Química, Florianópolis, 2019.

Inclui referências.

1. Engenharia Química. 2. Geopolymers. 3. Waste . 4. Reactive Oxides. 5. CO2 Capture . I. Moreira, Regina de Fátima Peralta Muniz . II. Junior, Agenor de Noni. III. Araujo, Maria Helena IV. Universidade Federal de Santa Catarina. Programa de Pós-Graduação em Engenharia Química. V. Título.

Alisson Lopes Freire

**Application of Geopolymers in $CO_2$ Adsorption at Low Temperature**

The present work at master level was evaluated and approved by an examining board composed of the following members:

Camilla Daniela Moura Nickel, Drª.
Federal University of Santa Catarina

Prof.ª Melissa Adeodato Gurgel Vieira, Drª.
State University of Campinas

Prof.ª Sandra Regina Salvador Ferreira, Drª.
Federal University of Santa Catarina

We certify that this is the original and final version of the final paper which was deemed appropriate to obtain the title of master in Chemical Engineering.

Documento assinado digitalmente
Cintia Soares
Data: 04/11/2019 10:54:07-0200
CPF: 020.401.629-09

Prof.ª Cíntia Soares, Drª.
Course Coordinator

Regina de Fatima Peralta Muniz Moreira:41393147968
Assinado de forma digital por Regina de Fatima Peralta Muniz Moreira:41393147968
Dados: 2019.11.04 09:35:25 -03'00'

Prof.ª Regina de Fátima Peralta Muniz Moreira, Drª.
Advisor

Florianópolis, 2019

This study is dedicated to my parents, José e Josidete, the greatest jewels of my life.

## ACKNOWLEDGMENTS

To God, for the opportunity of life, for never letting me think of giving up in the face of battles.

My advisor, Prof. Dr. Regina Peralta Muniz Moreira, for all the help and teaching passed on during the master period. You are inspiration.

To my co-advisors, Agenor de Noni Junior and Maria Helena Araujo, for all their support and dedication to me, were essential for the construction of this study.

To the members of the examining board for their availability and contribution to the improvement of this study.

To the Federal University of Santa Catarina, especially the Department of Chemical Engineering and Food Engineering (EQA), for providing all the support and infrastructure necessary to carry out the work.

To Central Laboratory of Electronic Microscopy (LCME), for the SEM analysis.

To André Ross and Prof. Dr. Philipe Gleize, for the XRD analysis.

To Professor Janaíde Rocha, for the XRF analysis.

To FAPESC (Santa Catarina State Research and Innovation Support Foundation), CAPES (Coordination for the Improvement of Higher Education Personnel) and CNPq (National Council for Scientific and Technological Development), for their financial support.

To my parents, José Milton Freire and Josidete Lopes Freire, for all their teaching, for always being by my side when I need them most. You are my reason for living. The distance only increases my love for you.

To my brothers, for all their support during these years, I hope that you will achieve all your dreams.

To my grandparents, Maria Neco, Pedro Lodonio (in memorian), Enedite Dantas and Francisco Dantas (in memorian) for all the good you want and for supporting me in my decisions. I love you.

My girlfriend Danyelle Gurgel for all the support, affection and love during this journey.

To my friends and colleges at the Laboratory of Energy and Environment (LEMA), who helped me and advised me in various ways, not only for the construction of the work, but for personal growth.

To all my friends, for the joyful moments and the support.

Finally, I thank everyone who contributed to this study.

“Acredite no improvável, acredite no
impossível, enxergue o que ninguém vê,
perceba o imperceptível
e enfrente o que, para muitos,
parece ser invencível...”

(Bessa, 2019)

## RESUMO

Este estudo relata pela primeira vez a obtenção de geopolímeros como material adsorvente utilizando cinza volante e cinza de casca de arroz como materiais precursores, substituindo em parte o metacaulim, para a obtenção de geopolímeros, onde foram avaliadas as capacidades de adsorção do dióxido de carbono, um dos gases majoritários do efeito estufa. Os materiais precursores foram caracterizados por distribuição de partícula, TGA, MEV, FRX, DRX-Rietveld e extração dos óxidos reativos ($SiO_2$, $Na_2O$, $Al_2O_3$). Com a quantificação dos óxidos reativos pode-se observar uma significante diferença entre a quantidade de óxidos apresentada no FRX e a extração, assim, podendo formular composições fidedignas dos geopolímeros. Dez diferentes formulações foram utilizadas na síntese de geopolímeros, variando-se as proporções e os tipos de materiais precursores, ou solução alcalina ativadora (S1: hidróxido de sódio-silicato de sódio, ou S2: hidróxido de sódio). Os geopolímeros foram caracterizados por DRX, MEV, resistência à compressão, absorção de água, densidade aparente, lixiviação de óxidos ($SiO_2$, $Na_2O$, $Al_2O_3$) e área superficial. A aplicação dos geopolímeros como adsorvente em processos de separação e captura de $CO_2$ foi estudada através do método gravimétrico, a 35 °C e 1 bar, tendo-se obtido a cinética de adsorção. Os resultados mostraram que a adição de silicato de sódio é fundamental para a obtenção de materiais com boas propriedades mecânicas. O geopolímero produzido pela adição de metacaulim e cinza volante apresentou elevada resistência à compressão e alta capacidade de adsorção, 11 MPa e 0,78 mmol/g, respectivamente, enquanto que a adição de cinza de casca de arroz não carbonizada reduz significativamente a resistência à compressão (5,5 Mpa) sem perda significativa da capacidade de adsorção de $CO_2$ (0,69 mmol/g). A combinação de cinzas de casca de arroz, cinza volante e metacaulim não apresentou grandes variações nas propriedades mecânicas e adsorção. A combinação de boa resistência e capacidade de adsorção de $CO_2$ obtida neste estudo sugere que os geopolímeros podem ser aplicados em processos de separação e captura de $CO_2$. A cinza de casca de arroz calcinada ativada por NaOH e silicato de sódio é o material precursor mais adequado para produzir geopolímeros adsorventes de $CO_2$. A capacidade de adsorção de $CO_2$ é 22,5% superior ao melhor adsorvente geopolimérico relatado na literatura até o momento, e 100% superior ao $CO_2$ adsorvido pelo valor médio ponderado das matérias-primas.



**Palavras-chave:** Geopolímeros. Resíduos. Óxidos reativos. Captura de $CO_2$.

## RESUMO EXPANDIDO

### Introdução

Os geopolímeros são materiais ligantes de aluminossilicatos tridimensionais amorfos que podem ser produzidos na faixa de temperatura de 20 a 120 °C por ativação alcalina de aluminossilicatos. Materiais geopoliméricos podem ser usados como agentes estabilizantes em aplicações de pavimentos, ou como adsorventes de metais pesados e corantes em efluentes ou tratamento de água. Sua capacidade de adsorção é o resultado de sua estrutura porosa e a presença de cargas negativas, localizadas em tetraedros de alumínio. No entanto, a aplicação de geopolímeros em processos de separação e adsorção de $CO_2$ ainda não foi explorada, embora existam algumas semelhanças entre esses materiais amorfos e os aluminossilicatos cristalinos. A remoção de $CO_2$ dos vapores gasosos tem uma grande relevância na utilização de biogás, e em processos de separação e captura de $CO_2$. Entre essas possibilidades, a adsorção física pode ser efetiva para a absorção de $CO_2$ na faixa de temperatura média baixa (20 a 200 °C), sob pressão atmosférica ou pressão mais alta. Este processo pode ser realizado utilizando um material adsorvente adequado, com uma grande área superficial e uma porosidade aberta bem desenvolvida. Na maioria dos casos, o sorvente é moldado em partículas ou grânulos para facilitar a operação no manuseio e armazenamento. Assim, o material utilizado deve ser mecanicamente resistente, resistente à abrasão e às rápidas variações de temperatura/pressão, quando são adotados métodos de oscilação de pressão ou temperatura para a regeneração. As zeólitas, os carvões ativados e os outros materiais mais novos, como os *Metal Organic Frameworks* (MOFs), são os adsorventes mais utilizados. Este trabalho relata pela primeira vez a síntese de geopolímeros como material adsorvente produzido utilizando cinzas volantes e cinza de casca de arroz e sua aplicação em processo de captura de $CO_2$. Os testes experimentais foram conduzidos a baixa temperatura (35 °C) através do método gravimétrico, para obtenção da cinética de adsorção e de dessorção.

### Objetivos

Os principais objetivos deste estudo são sintetizar, caracterizar e avaliar a utilização dos geopolímeros como materiais adsorventes em processos de captura do CO2.

### Metodologia

O caulim, a cinza volante e as cinzas de casca de arroz foram fornecidas pela Caulisa (SC), pelo Complexo Termoelétrico Jorge Lacerda, e pela empresa Fumacense Alimentos, respectivamente. O metacaulim foi obtido através do tratamento térmico (900 °C) do caulim. A cinza de arroz calcinada foi obtida via tratamento térmico da cinza da casca de arroz (500 °C por 3 h). Os materiais precursores foram caracterizados por distribuição de partículas, análises termogravimétrica e térmica diferencial (TGA e DTA), fluorescência de raio-X (FRX), difração de raio-X (DRX), quantificação Rietveld, extração de óxidos reativos por via alcalina (NaOH) e microscopia eletrônica de varredura (MEV). O estudo de Rowles e O'Connor (2003) foi utilizado como referência ($SiO_2$:$Na_2O$:$Al_2O_3$ = 0,62: 0,17: 0,21) para propor as composições dos geopolímeros deste estudo. As amostras de geopolímeros foram preparadas da seguinte maneira: materiais sólidos foram homogeneizados por 5 min a 600 rpm um agitador mecânico e o ativador alcalino também foram misturados separadamente por 5 min a 720 rpm usando um agitador magnético. As suspensões foram obtidas misturando mecanicamente o ativador alcalino, materiais sólidos e água a 2000 rpm por 10 min. As pastas foram transferidas para

moldes cilíndricos (20 mm x 40 mm). O processo de cura foi o seguinte: as amostras foram secas durante 48 h a 65 °C, arrefecidas a temperatura ambiente, removidas dos moldes e submersas em água deionizada durante 26 dias. Os geopolímeros foram caracterizados por DRX, MEV, resistência à compressão, condutividade elétrica, absorção atômica e área superficial (BET). O estudo da cinética de adsorção de $CO_2$ foi realizado utilizando um analisador termogravimétrico (DTG-60 Shimadzu). Uma amostra (aproximadamente 10 mg) foi colocada em um cadinho a 35 ºC por 1 h em atmosfera de nitrogênio a uma vazão de 100 mL/min, e a temperatura foi ajustada para 110 ºC para remover umidade e outras impurezas gasosas da superfície sólida. Após o pré-tratamento, a temperatura foi ajustada ao valor desejado (35 °C). Quando o sistema atingia a temperatura de 35 °C, o gás era trocado para $CO_2$ puro (100 ml/min, 99,0% de pureza, White Martins, Brasil) e o aumento de massa era continuamente monitorado. A etapa de dessorção era inicializada quando a massa permanecia constante por 1 hora, e então, o gás era substituído por $N_2$ puro (pureza de 99,996%, White Martins, Brasil) a 35 °C.

**Resultados e Discussão**

Os materiais precursores apresentaram $SiO_2$ e $Al_2O_3$ como majoritários. Os difratogramas obtidos por DRX confirmaram que os materiais apresentam uma grande quantidade de material não cristalino. O refinamento de Rietveld revelou que a cinza volante contém 80,5% de sílica amorfa, 13,1% de quartzo ($SiO_2$, JCPDS 46-1045) e 6,4% de mulita ($Al6Si_2O_{13}$, JCPDS 15-0776), enquanto o metacaulim contém 96,5% de sílica amorfa e 3,5% de quartzo ($SiO_2$, JCPDS 46-1045). As cinzas de casca de arroz e cinzas de casca de arroz calcinadas contêm diferentes materiais de fase amorfa, 75,9% e 73,1%, respectivamente, e uma fase cristalina (opalina) (BAYLISS; MALES, 1965). Com a quantificação dos óxidos reativos, $SiO_2$, $Al_2O_3$ e $Na_2O$, verificou-se que todos os óxidos presentes nas cinzas de casca de arroz e cinzas de casca de arroz calcinada são reativos. Por outro lado, na cinza volante e no metacaulim foi verificado uma diferença entre a quantidade obtida pelas técnicas de FRX e DRX-Rietveld após a extração dos óxidos reativos. A presença de uma larga protuberância de 20° a 40° 2θ é apresentada em alguns geopolímeros, este halo é característico da formação do gel de aluminossilicato, responsável pelas propriedades finais dos geopolímeros. Este fenômeno é mais intenso nos geopolímeros que utilizam cinza volante e metacaulim na composição. Pela imagem da morfologia pode-se observar que os geopolímeros que são obtidos com a mistura entre hidróxido de sódio e silicato de sódio apresentam precipitados bem dispersos, porém, mais homogêneos em relação aos que utilizam apenas hidróxido de sódio como ativador alcalino. Entretanto, são observadas rachaduras em todas as microestruturas dessas amostras e, embora as amostras tenham sido seladas, essas rachaduras podem ter sido causadas durante o processo de cura, devido à evaporação da água que produz contração das amostras. Os geopolímeros que apresentaram resistência foram os MF-1, MF-2, MR-1, MCR-1, MFR-1 e MFCR-1, sendo o MF-1 com o maior valor após 28 dias de cura, 11 MPa. Os geopolímeros MR-2, MCR-2, MFR-2 e MFCR-2 dissolveram durante o processo de cura submersa. A decomposição dos geopolímeros pode estar relacionada ao alto teor de cinza de casca de arroz e cinzas de casca de arroz calcinadas e a ausência de silicato de sódio, pois, dificultam o processo de geopolimerização e interferem nas propriedades mecânicas dos geopolímeros. Os geopolímeros apresentaram uma relativa absorção de água, contudo, esperado. Os geopolímeros que se dissolveram durante a cura submersa apresentaram os maiores valores de condutividade elétrica e lixiviação, confirmando que não ocorreu geopolimerização e os óxidos continuaram livres. Os geopolímeros apresentaram boa capacidade de adsorção de $CO_2$, sendo o MF-1 com a melhor relação de capacidade de adsorção (0,78 mmol/g) e resistência à compressão (11 MPa).

**Considerações Finais**

Com a utilização de cinzas volantes, cinza de casca de arroz e cinza de casca de arroz calcinada sob diferentes condições foi possível realizar o processo de geopolimerização. Um importante aspecto a ser considerado é que nem todos os óxidos presentes nesses materiais são efetivamente reativos e contribuem para o processo de geopolimerização e sua quantificação é fundamental para o controle do grau de geopolimerização. O material carbonoso presente na cinza da casca de arroz contribui para o aumento das propriedades mecânicas, mas não afeta a capacidade de adsorção de $CO_2$ de forma significativa. Geopolímeros contendo dois resíduos na mesma composição apresentaram decréscimo em relação as propriedades mecânicas, atribuído à diferença entre tamanhos de partículas, não permitindo uma boa compactação da matriz geopolimérica e observada em imagens de MEV. A utilização do silicato de sódio é fundamental para se alcançar geopolímeros com propriedades mecânicas e capacidade adsortiva adequada. Os geopolímeros que se dissolveram durante a cura submersa apresentaram as maiores porcentagens de óxidos lixiviados, observando que o gel de aluminossilicato não foi obtido. A capacidade de adsorção de $CO_2$ não apresentou uma relação direta com a extensão superficial do geopolímero, visto que, se mostraram sólidos pouco porosos.

**Palavras-chave:** Geopolímeros. Resíduos. Óxidos Reativos. Captura de $CO_2$.

## ABSTRACT

This study used residues of rice husk ash and fly ash as precursor materials, partly replacing metakaolin to obtain geopolymers, where the adsorption capacities of carbon dioxide, the greenhouse gas, was evaluated. The precursor materials were characterized by particle distribution, TGA, SEM, XRF, XRD-Rietveld and extraction of reactive oxides ($SiO_2$, $Na_2O$, $Al_2O_3$). With the extraction of oxides, the total oxides available for the geopolymerization reaction can be quantified. Ten geopolymers were produced, with different proportions and precursor materials, using two alkaline solutions, S1 (sodium hydroxide-sodium silicate) and S2 (sodium hydroxide). Geopolymers were characterized by XRD, SEM, compressive strength, water absorption, bulk density, oxide leaching ($SiO_2$, $Na_2O$, $Al_2O_3$) and surface area. The geopolymers were applied in carbon dioxide ($CO_2$) capture processes under the following conditions: 35 °C at 1 bar. Geopolymers that did not contain sodium silicate in their composition had impaired mechanical properties. The geopolymer with metakaolin and fly ash in its composition obtained the best values of compressive strength and adsorption capacity, 11 MPa and 0.78 mmol/g. The geopolymer with metakaolin and rice husk ash presented compressive strength of 5.5 MPa and adsorption capacity of 0.69 mmol/g. The combination of rice husk ash, fly ash and metakaolin did not show large variations in the mechanical properties and adsorption, where it was obtained approximately 5.5 MPa for compressive strength and approximately 0.68 mmol/g of adsorption capacity. Calcinated rice husk ash activated by NaOH and sodium silicate is the material precursor most suitable to produce a $CO_2$ geopolymeric adsorbent, and its $CO_2$ capacity is 22.5% higher than the best geopolymeric adsorbent reported in the literature up to now and 100% higher than the $CO_2$ which would be adsorbed by the weighted average value of the adsorptive capacity of the raw materials.



**Keywords:** Geopolymers. Waste. Reactive Oxides. $CO_2$ Capture.

## LIST OF FIGURES

## LIST OF EQUATIONS

## LIST OF TABLES

## LIST OF ABBREVIATIONS AND ACRONYMS

| Abbreviation/Acronyms | Definition |
|---|---|
| AAS | Atomic absorption spectroscopy |
| BET | Brunauer-Emmet-Teller |
| BJH | Barrett-Joyner-Halenda |
| EDS | Energy-dispersive spectroscopy |
| FA | Fly ash |
| GHG | Greenhouse gases |
| ICSD | Inorganic Crystal Structure Database |
| JCPDS | Joint Committee on Power Diffraction Standard |
| MK | Metakaolin |
| MOF | Metal organic frameworks |
| MPa | Megapascal |
| OPC | Ordinary Portland cement |
| ppm | Parts per million |
| RHA | Rice husk ash |
| RHAC | Rice husk ash calcined |
| rpm | Revolutions per minutes |
| SEM | Scanning electron microscopy |
| TGA | Thermogravimetric analysis |
| XRD | X-ray diffraction |
| XRF | X-ray fluorescence |

## LIST OF SYMBOLS

| Symbol | Meaning | Unit |
|---|---|---|
| $R^2$ | Correlation coefficient | - |
| $A_{H2O}$ | Water absorption | % |
| B | Bulk density | $g/cm^3$ |
| k | Rate constant pseudo-first order | $min^{-1}$ |
| $k_2$ | Rate constant pseudo-second order | $g\ mmol^{-1}\ min^{-1}$ |
| ki | Rate constant intra-particle diffusion model | $mmol\ g^{-1}\ min^{-0.5}$ |
| $m_S$ | Dry geopolymer mass | g |
| $m_{ST}$ | Saturated geopolymer mass | g |
| $m_{STI}$ | Immersed saturated geopolymer mass | g |
| $P_s$ | Average pore size | nm |
| Q | Mass variation | mmol/g |
| $q_e$ | Adsorption equilibrium | mmol/g |
| $q_t$ | Adsorption in t | mmol/g |
| $S_{BET}$ | Surface area | $m^2/g$ |
| t | Time | min |
| $V_p$ | Total pore volume | $cm^3/g$ |

**SUMMARY**

# 1 INTRODUCTION

There is a consensus that geopolymers have low carbon dioxide ($CO_2$) emissions since it is not required treatment at high temperatures to be produced compared to other inorganic binder (BAI; COLOMBO, 2018). Geopolymers are amorphous three-dimensional alumina-silicate binder materials that may be produced in the temperature range between 20–120 °C by alkaline activation of alumina-silicates (DAVIDOVITS, 1991a). The application of these materials as substitute of Portland cement is largely known, but new applications have been recently developed

Geopolymeric materials can be used as stabilizing agents in flexible pavement applications (HOY *et al.*, 2016), or as heavy metals (CHENG *et al.*, 2012) and dyes adsorbent in wastewater or water treatment (ONUTAI *et al.*, 2019). This adsorption capacity is the result of their porous structure and the presence of negative charges, located on aluminum tetrahedra, as well as their mechanical stability, cost-effectiveness, eco-friendliness and high efficiency. The utilization of geopolymers as $CO_2$ adsorbent is a very emergent technology to remove $CO_2$ from gaseous streams (NASVI; RANJITH; SANJAYAN, 2014)

The removal of $CO_2$ from gaseous steams has a great relevance in the use of e.g. biogas, in which the content of methane has to be upgraded, in order to be employed as renewable alternative to conventional fuels (SHEN *et al.*, 2018). In parallel, to considering climatic changes, it is required to decrease $CO_2$ emissions, by the implementation of carbon capture and sequestration processes. Among these possibilities, the physical adsorption can be effective for $CO_2$ uptake in the low-medium temperature range (20–200 °C), under atmospheric or higher pressure. This process can be carried out by using a suitable adsorbent material having large superficial area and a well-developed open porosity. In most cases, the sorbent is shaped in particles or granules for the sake of easy operation in handling and storage. Thus, the adopted material should have rather high mechanical resistance towards abrasion and be resistant to rapid changes of temperature/pressure, when pressure or temperature swing methods are adopted for the sorbent regeneration and $CO_2$ release (SAMANTA *et al.*, 2012). Zeolites, activated carbons, and the newly developed materials such as Metal Organic Frameworks (MOFs) are the most used adsorbents (D'ALESSANDRO; SMIT; LONG, 2010; MODAK; JANA, 2019)

The process for carbon capture and sequestration in enhanced oil (EOR) and gas (EGR) has become a relevant study. This technology has two main advantages: reducing the emission of $CO_2$ into atmosphere and recovering the oil and gas that is left after secondary processes (FAQIR *et al.*, 2017). However, the prolong interaction between the stored $CO_2$ with conventional Portland cement could lead to corrosion and embedded well tubular (NASVI *et al.*, 2014; PAIVA *et al.*, 2018). So, the substitution of Portland cement by geopolymer materials should be investigated.

A number of researches are using precursor materials in the synthesis of geopolymers such as kaolinitic, metakaolin, fly ash, biomass ash (rice husk ash, palm oil fuel ash and eucalyptus ash), blast furnace slag, such as mixtures of fly ash and metakaolin, fly ash and slag, metakaolin and ash biomass, metakaolin and slag, and fly ash and biomass ash. However, studies involving the incorporation of metakaolin, fly ash and rice husk ash in the synthesis of the geopolymer are not reported in the literature (PACHECO-TORGAL; CASTRO-GOMES; JALALI, 2008b)

Although the metakaolin is the most reactive raw material in alkaline environment, any alumino-silicate compound can undergo geopolymerization under tailored conditions. Fly ash and rice husk ash present relevant characteristics for application in the development of geopolymeric materials, impacting on a reduction of metakaolin in the formulation of geopolymers. Since the microstructures and properties of geopolymers depend on the nature of initial source materials, the final use of the geopolymer can be purposely designed.

Therefore, this work reports for the first time the characterization of geopolymers as adsorbent material produced using fly ash and rice husk ash for the capture of $CO_2$. The experimental results of tests carried out at low temperature (35 °C) by means of a gravimetric method are reported and discussed in the dissertation, along with the analysis of the ability of such material to reversely adsorb $CO_2$.

# 2 OBJECTIVES

## 2.1 GENERAL OBJECTIVES

The objective of this research is to synthesize, characterize and evaluate the use of geopolymeric materials, based on metakaolin, fly ash, rice husk ash and calcined rice husk ash, as adsorbent material to capture carbon dioxide at low temperature.

## 2.2 SPECIFIC OBEJECTIVES

The specific objectives are presented below:

•To quantify the content of reactive oxides available for the process of geopolymerization of precursor material, using the extraction (NaOH) process at 100 °C for 10 h;

•Formulate and prepare geopolymers using different precursor materials;

•Evaluate the characteristics of the geopolymers that influences the $CO_2$ adsorption capacity;

•Investigate the leaching process during submerged curing;

•Evaluate the impact of non-use of sodium silicate as an alkaline activator;

•Investigate the kinetics of $CO_2$ adsorption and desorption at 35 °C and pressure of 1 bar.

# 3 LITERATURE REVIEW

## 3.1 CARBON DIOXIDE ($CO_2$) EMISSIONS AND SEQUESTRATION BY $CO_2$ ADSORPTIVE PROCESS

Climate change has become a central concern on the planet. Studies show an increase in the earth temperature caused by the emission of greenhouse gases (GHG) and that severe effects may be irreversible (IPCC, 2014).

Among the gases emitted is carbon dioxide, whose concentration in the atmosphere has risen from 290 to 430 ppm since 1880 (NOAA, 2018). In Figure 1 it can be noted that the emission of $CO_2$ into the atmosphere by fossil fuels, cement and fires tripled from 1970-2011 in comparison with the period between 1750-1970, making them the main emitters of $CO_2$ (IPCC, 2014).

The progressive emission of carbon dioxide causes problems such as the loss of biodiversity and ecosystems, putting at risk the extinction of several animals, rising sea levels, causing floods and storms, and scarcity of food and water, making human life insecure.

Figure 1 – Cumulative $CO_2$ emissions.

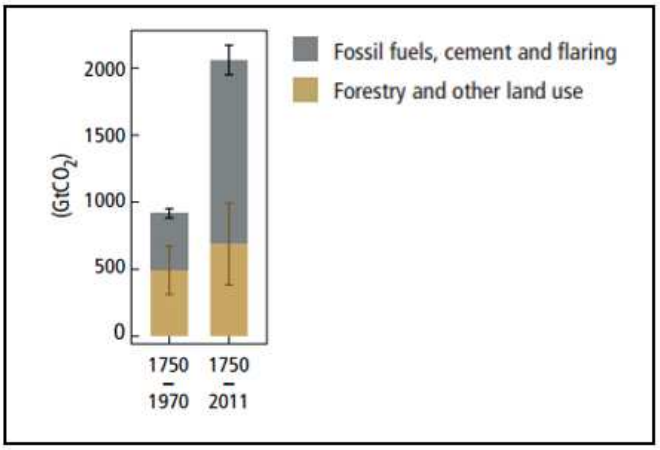


Source: Adapted from IPCC, 2014.

Faced with such problems, technologies such as wet chemical absorption, dry chemical absorption, physical adsorption and membrane separation are employed in order to reduce the impact caused by the emission of gases. The physical adsorption process is shown to be effective at a temperature below 200 °C under atmospheric pressure or higher. Materials that

have a high surface area, open porosity and high mechanical strength, can be used in the adsorption of $CO_2$ (WANG *et al.*, 2011).

Adsorption is described as the phenomenon in which some solids are able to attract molecules present in liquid or gaseous fluids to their surface. Enabling the separation of these elements from the fluid stream (THOMMES *et al.*, 2015).

The adsorption phenomena depends on the adsorbate concentration and the characteristics of the adsorbent, such as, surface area, size and volumes of porous (DANTAS, 2009). Two different process of adsorption may occur, chemisorption and physisorption.

In chemisorption the adsorbed molecules remain on the surface of the adsorbent material by covalent forces of the same kind as those occurring between atoms and molecules, that is, chemical interactions. Chemisorption is limited to the monolayer on the surface of the adsorbent (FOGLER, 2005; NIC; JIRAT; KOSATA, 2012).

The physisorption process is exothermic, and the adsorption heat is low, between 1 to 15 kcal/mol, the attraction forces between the molecules of the gas and the solid surface is weak. Two forces are involved on physisorption: specific molecular interactions such as polarization, field-dipole and field gradient-quadrupole, and van der Waals forces. The concentration of adsorbed gas on the surface of the adsorbent decreases with increasing temperature (FOGLER, 2005; THOMMES *et al.*, 2015).

Different adsorbent materials are used for carbon dioxide capture, such as carbonaceous materials, zeolites and metal-organic frameworks (MOF). Some criteria such as adsorption capacity, selectivity, adsorption/desorption kinetics, mechanical strength and cost must be satisfactory to make its application viable (SAMANTA *et al.*, 2012).

Activated carbons are widely used in adsorption processes such as water treatment and gas purification. These materials are inexpensive because they are widely available, have fast adsorption kinetics and low regeneration energy. However, the high pore volume hinders the carbon dioxide selectivity process and decreases in the adsorption process as the temperature rises (SAMANTA *et al.*, 2012)

Zeolites can be obtained from nature or synthesized and are usually used in gas separation and purification processes. Synthesized zeolites are the most used, since it is possible to modify the microstructure, altering the materials used in the synthesis, in view of their intended use. Adsorption kinetics are generally fast and have a good adsorption capacity, however, with increasing temperature their activity is negatively affected, and have a relatively

high cost depending on the materials required in the synthesis (D'ALESSANDRO; SMIT; LONG, 2010; WIRAWAN; CREASER, 2006). Metal Organic Frameworks are 3D networks made up of inorganic and organic units. Due to the possible incorporation of organic materials into the structure, an infinity of possibilities arise to control pore size and shape, as a result, the adsorption capacity and kinect process become better. However, the high cost to obtain those materials makes it impossible to use them in large scale industrial processes (MODAK; JANA, 2019; SAMANTA *et al.*, 2012).

Given the various negative factors among the adsorbents mentioned, there is a need for the development of new adsorbent materials that meet the industrial needs, thus, several studies have been developed for this purpose. Recent research shows the application of geopolymers as possible adsorbent materials.

Geopolymers are materials obtained from an aluminosilicate source and an alkaline activator, and it is possible to use various residues such as fly ash, slag, red mud and biomass ash as an aluminosilicate source, not requiring large industrial plants and machinery, which makes it a low cost material. Among the properties presented by geopolymers, the high surface area, considerable open porosity and high mechanical resistance makes it possible to evaluate the selectivity of this materials to different gases (DAVIDOVITS, 1991a).

Study developed by Minelli *et al.,* 2016, where they apply geopolymers to capture carbon dioxide, obtaining an adsorption capacity of 0.62 mmol/g which presents an excellent adsorption when compared to zeolite (Zeolitic imidazolate) and MOF (Metal Organic Frameworks), with-adsorptions of 0.59 and 0.68 mmol/g, respectively. The study was carried out at 35 °C and with a pressure of 1 bar.

In view of this, geopolymers become a viable material to be studied as $CO_2$ capture, as well as to evaluate different sources of precursor materials that can lead to materials with high adsorption capacity.

## 3.2 GEOPOLYMERS

Geopolymeric materials have gained a lot of interest in the last decades due to its characteristics, such as high mechanical strength, durability, ion exchange and resistance to high temperatures, allowing application in several areas.

The term, Geopolymers, was introduced by the French researcher, Joseph Davidovits, in 1979, where materials of an amorphous or semi-crystalline structural nature were obtained

(J., 2002; XU; DEVENTER, 2000), since them a variety of names were attributed to these materials, such as alkaline ceramics, hydroceramics among others (KOMNITSAS; ZAHARAKI, 2007). In 2008, Duxson and Provis proposed a broader term for geopolymers by classifying them as inorganic polymers materials from the reaction between an aluminosilicate powder and an alkaline activator (CARVALHO, 2008).

Davidovits, Joseph; Davidovics, Michael; Davidovits, (1994) proposed ideal limits for the molar ratios between the main oxides ($SiO_2$, $Al_2O_3$, and $Na_2O$) and sodium/water, which the formulations must contain in order to obtain high strength in the geopolymers. The relationships are shown below:

$$0.20 < Na_2O/SiO_2 < 0.48$$
$$3.30 < SiO_2/ Al_2O_3 < 4.50$$
$$0.80 < Na_2O/Al_2O_3 < 1.60$$
$$10 < H_2O/Na_2O < 25$$

However, the materials used in the synthesis of geopolymers do not always present a chemical composition that respects the values proposed by Davidovits, Joseph; Davidovics, Michael; Davidovits, (1994), thus, being necessary to incorporate materials to correct molar ratios (CARVALHO, 2008).

Davidovits (2002) presented several applications for geopolymeric materials in different areas (Figure 2), where the ratio $SiO_2/Al_2O_3$ is considered a determining factor for its applicability.

Figure 2 – Different applications of geopolymers as a function of $SiO_2/Al_2O_3$ ratio.

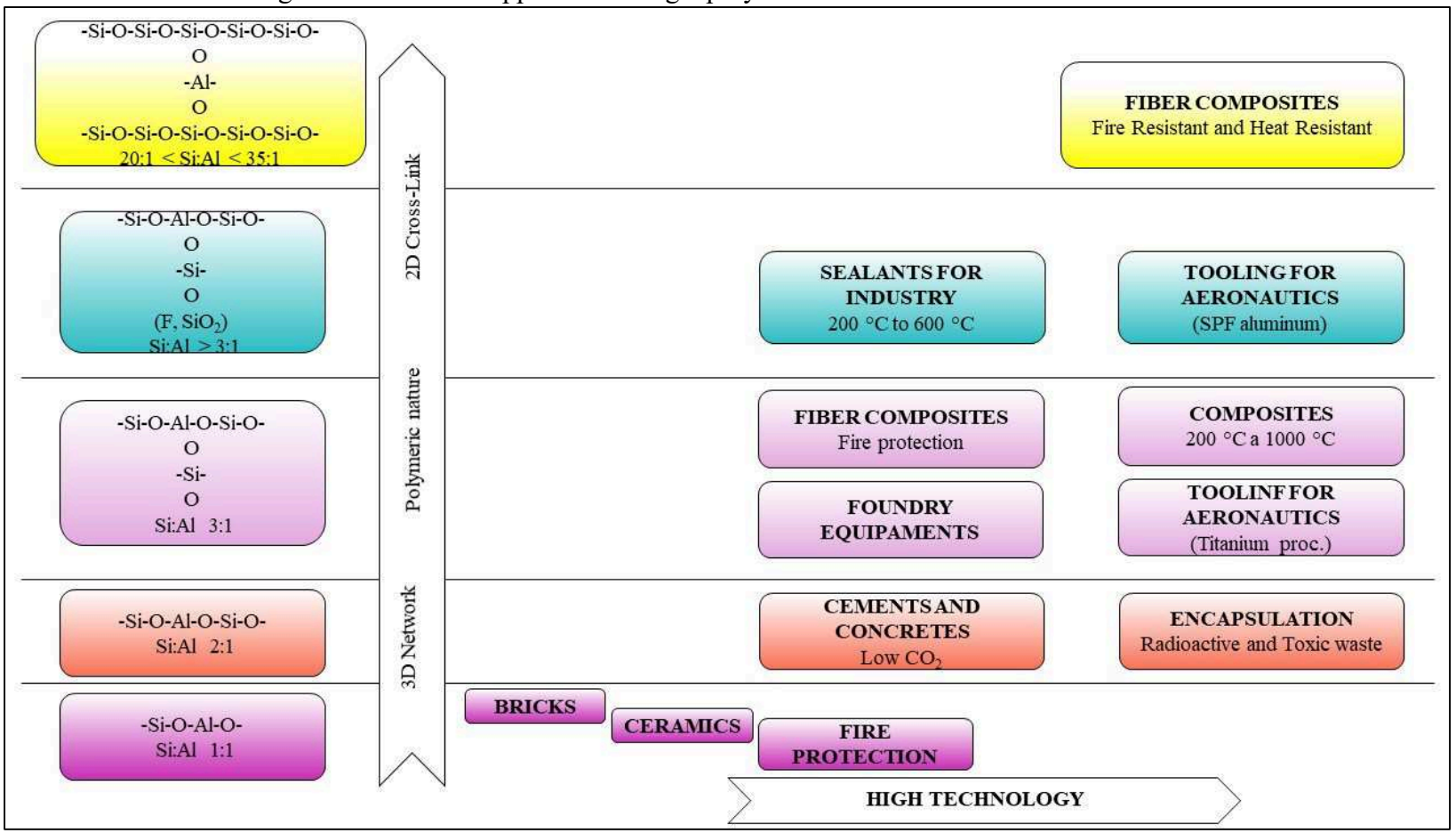


Source: Adapted from Davidovits, 2002.

The various areas of applicability of the geopolymeric materials cited by Davidovits are still under investigation by researchers which seek to understand the chemical, thermal and mechanical properties of the materials, the influence of different precursors used for the preparation of the geopolymers, the mechanism and kinetics of the polymerization reaction, and the molecular structure of geopolymers. (ZHANG *et al.*, 2016)

The polymeric structure of the geopolymers is formed by Si-O-Al. These chains are formed by alternating $[SiO_4]^{4-}$ and $[AlO_4]^{5-}$ tetrahedral, where they share oxygen atoms. To obtain chain stability due to the electrical charge of $Al^{3+}$ in coordination IV, the addition of cation such $Na^+$, $K^+$, $Li^+$, $Ca^{2+}$, $Ba^{2+}$, $NH_4^+$ and $H_3O^+$ is required (DAVIDOVITS, 1991b; KOLEŻYŃSKI; KRÓL; ŻYCHOWICZ, 2018; XU; DEVENTER, 2000). In view of this, the empirical formula of the geopolymers is as follows (KOMNITSAS; ZAHARAKI, 2007):

$$M_n \left\{ -\left(Si_iO_2\right)_Z - AlO_2 \right\}_n \cdot wH_2O \qquad (1)$$

Where:

M is the alkali cation (sodium or potassium);

n indicates the degree of polymerization;

z is the quantification factor of $SiO_2$ monomer units, which can be 1, 2 or 3.

w is the amount of water molecules associated (degree of hydration).

Depending on the value to be presented by the factor z, three different geopolymer structures can be obtained which are shown in Figure 3.

Figure 3 – Geopolymer structure according to the number of $SiO_2$ monomers. I – Polysialate; II – Polysialate-siloxo; III – Polysialate-disiloxo.

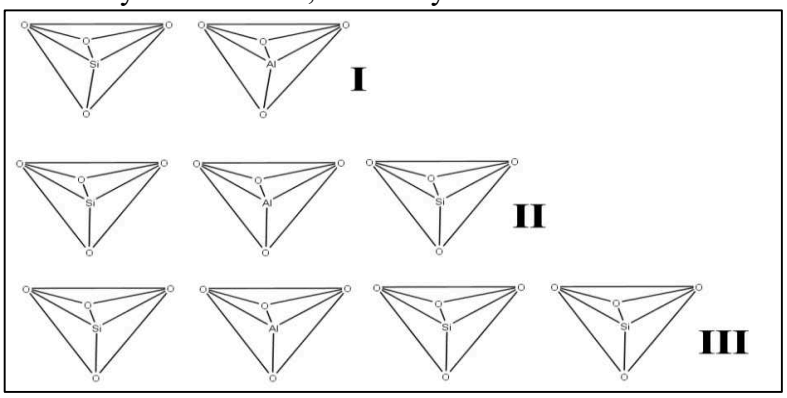


Source: Adapted from Davidovits, 1991.

### 3.2.1 Geopolymerization

The geopolymerization occurs through the reaction between aluminosilicate oxides and an alkaline activator, resulting in polymeric bonds of Si-O-Al-O (XU; DEVENTER, 2000). The mechanism that governs the process of geopolymerization is not totally understood (PACHECO-TORGAL; CASTRO-GOMES; JALALI, 2008a), but it is known that the reaction stages are based on three phases, which are: (I) dissolution of aluminosilicates due to hydroxyl ions, (II) orientation and transport, and (III) polycondensation, which was proposed by Glukhovsky (SHI; JIMÉNEZ; PALOMO, 2011; VAN JAARSVELD; VAN DEVENTER; LUKEY, 2002).

(I) Dissolution and Coagulation

In the initial stage of the process the dissolution of the solid and breakage of the Me-O, Si-O-Si, Al-O-Al and Al-O-Si bonds of the precursor material occurs, according to Shi; Jiménez and Palomo (2011). Glukhovsky have indicated that the disintegration of the solid phase can be governed by the formation of unstable complex products, with the change in the ionic strength of the medium being the main factor, which is caused by the addition of alkaline activator. Thus, a redistribution of the electron density around the silicon atoms occurs, making the Si-O-Si bond more vulnerable. The presence of alkali metal cations, leads to the neutralization of these anions, forming Si-O-$Na^+$ bonds, which makes the reaction irreversible, which favors the development of coagulated structure. The hydroxyl groups have the same effect on the Al-O-Si bond, whereby the aluminates present in the alkaline solution form complexes such as $Al(OH)_4^-$ or $Al(OH)_6^{3-}$, depending on the pH of the medium.

(II) Coagulation and Condensation

In this step, the concentration of disaggregated materials increases and thus leads to a greater contact between them, which gives rise to a coagulated structure where polycondensation occurs. The rate of the polycondensation process is determined by the state of the dissolved ions and by the existence of conditions that favor gel precipitation, such as the pH of the medium (SHI; JIMÉNEZ; PALOMO, 2011).

(III) Condensation and Crystallization

In this latter step, precipitation of the product is favored due to the presence of particles from the initial solid phase and microparticles resulting from the condensation process. The properties of the geopolymers are determined by the mineralogical composition of the initial phase (particle size, reactivity and amorphous phase), the nature and concentration of the

alkaline activator and the conditions of cure (DONG *et al.*, 2017; DUXSON *et al.*, 2007a; SHI; JIMÉNEZ; PALOMO, 2011).

Provis (2006) has developed a model in which it presents the processes of the reaction of geopolymerization using metakaolin as raw material, however, van Deventer *et al*. (2007) showed that the proposed model can also be applied to other precursor materials that present aluminosilicates in their composition, as can be seen in Figure 4.

Figure 4 – Schematic diagram of the processes involved in the geopolymerization reaction.

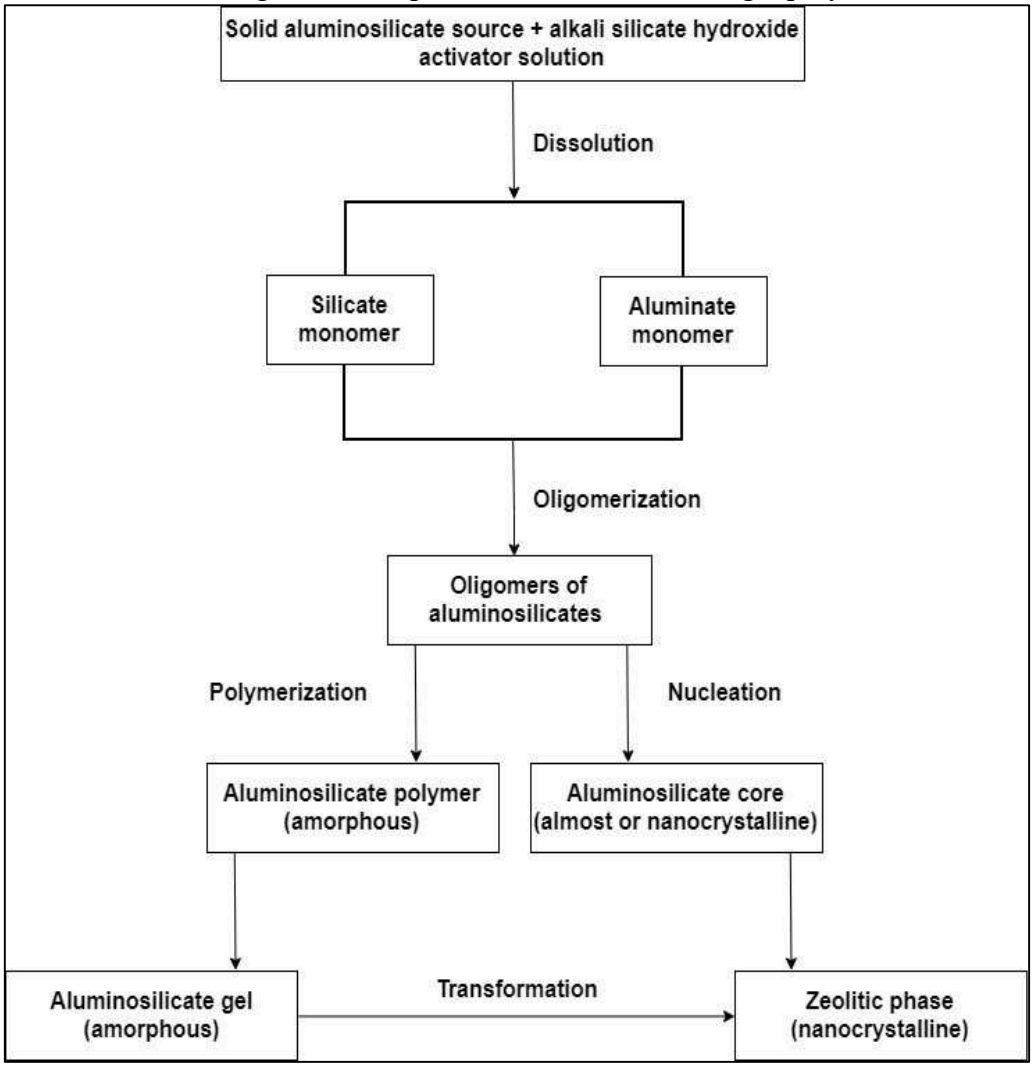


Source: Adapted from van Deventer *et al.*, 2007.

### 3.2.2 Precursor Materials

*3.2.2.1 Metakaolin*

Metakaolin is one of the most widely used materials in the production of geopolymers. It is obtained by heat treatment of kaolin, which is a mineral clay rich in kaolinite (WAN; RAO; SONG, 2017) and has secondary compounds such as humpisite, dicita anatase and quartz (ZHANG *et al.*, 2012). Studies by Zibouche *et al*., (2009) have verified that the presence of 30% by weight of secondary compounds does not inhibit the geopolymerization process. Figure 5 shows the thermal behavior of kaolinite, where:

- water loss occurs at 100 °C;
- the process of dehydroxylation is between 450 and 700 °C; and
- between 700 and 900 °C, the metakaolin is obtained.

Figure 5 – Thermal behavior of kaolinite.

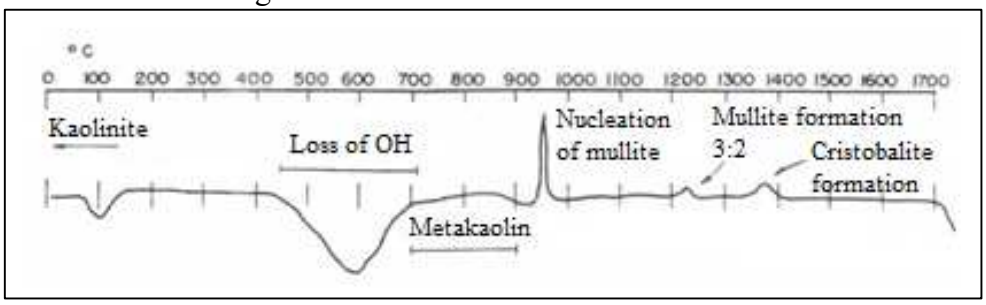


Source: Adapted from Santos, 1989.

The thermal processing of kaolinite gives rise to a disordered, amorphous and highly reactive material. This is due to the transformation of aluminum with octahedral coordination ($Al^{VI}$), in kaolin, to pentahedral ($Al^{V}$) and tetrahedral ($Al^{IV}$) (HELLER-KALLAI, 2006; MEDRI *et al.*, 2010). The dehydroxylation reaction of kaolinite is presented in Equation 2.

$$Al_2Si_2O_5(OH)_4 \xrightarrow{400\text{-}700^{\circ}C} Al_2O_3 \cdot 2SiO_2\,(\text{metakaolin}) + 2H_2O \qquad (2)$$

Source: Adapted from Redfern, 1987.

The metakaolin used to prepare geopolymers come from different regions of the earth, leading them to present different characteristics such as crystallinity, purity, particle size and

surface area, which directly influence their reactivity (PROVIS; YONG; DUXSON, 2009). Since the early days of the development of geopolymers, the use of metakaolin is necessary, but studies are being directed towards a partial or complete replacement by waste such as fly ash and slag, in order to reduce environmental impact and optimize costs. (PROVIS; BERNAL, 2014).

*3.2.2.2 Fly ash*

Fly ash comes from industries that use coal as a source of fuel (PROVIS; BERNAL, 2014), and it is estimated that the annual generation of fly ash is 750 million tons (MA *et al.*, 2018; YANG *et al.*, 2018a; ZHOU *et al.*, 2016). Considering the amount of fly ash generated, the use of this residue do produce new materials are very important to reduce its impact on the environment, among them the obtaining of geopolymeric materials. The reasons for the use of these materials are the presence of aluminosilicates, in amorphous and crystalline phase, and the geometry of the particles, in sphere forms, attributing a better workability to the geopolymer slurries (KOSHY *et al.*, 2019; YANG *et al.*, 2018b; ZHU *et al.*, 2019). Figure 6 shows that when searching the Scopus platform for geopolymer and fly ash there is a considerable increase of studies over the years.

Figure 6 – Publications regarding geopolymers using fly ash.

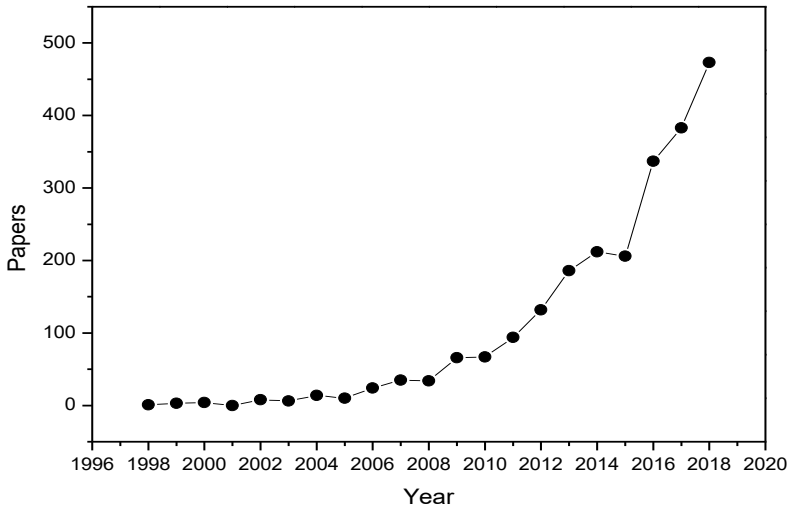


Source: SCOPUS, 2019. Advanced search in Scopus with title, abstract, keywords: geopolymer and fly ash.

The resistances presented by fly ash geopolymers are similar to those developed using metakaolin, 45 and 85 MPa (GOMEZ-ZAMORANO; VEGA-CORDERO; STRUBLE, 2016) as a precursor material and reported by Sun and Vollpracht (2019). For instance, geopolymers synthesized by Chindaprasirt *et al*., (2009) presented a resistance of 35 MPa using fly ash and a mixture of sodium silicate and 10 M NaOH as alkaline activator, with a cure of 65 °C for 48h. Palomo *et al*., (2008) obtained strength of 80 MPa, using in their formulation fly ash and an alkaline solution of 8 M (NaOH), with a cure of 85 °C for 14 days.

The difference of the resistance may be related to several factors, such as: i) cure time, since the resistance of geopolymers tend to increase in longer times; ii) concentration of the alkaline activator, since a higher concentration makes the activator more viscous, resulting in a more difficult leaching process of the aluminosilicate, which leads to a lower degree of geopolymerization (CHINDAPRASIRT *et al.*, 2009; PACHECO-TORGAL; CASTRO-GOMES; JALALI, 2008b).

The process of ash activation is presented in Figure 7, where Fernández-Jiménez, Palomo and Criado (2005) showed that in the initial part the chemical attack occurs on the surface of the particle, causing internal particles to be exposed and susceptible to total or partial dissolution of the ash.

Figure 7 – Alkaline activation pattern of fly ash.

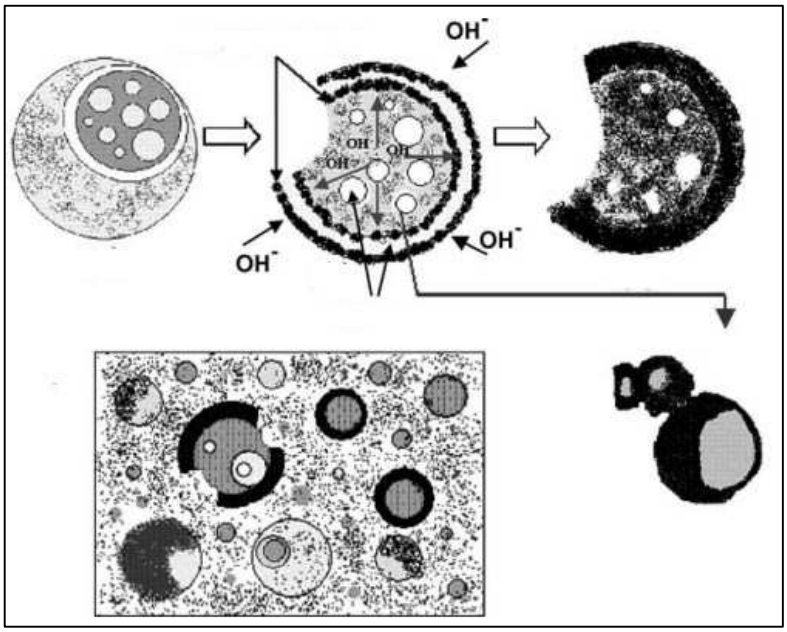


Source: Adapted from Fernández-Jiménez; Palomo; Criado, 2005.

Depending on the origin of the coal, the ash has variations in its chemical composition, but in general it is composed of alumina ($Al_2O_3$), silica ($SiO_2$), iron oxide ($Fe_2O_3$) and calcium oxide (CaO). The American Society for Testing & Materials (ASTM) classifies the ashes into two types, Class C and Class F, the specifications to qualify the type of ash is presented in Table 1 (ASTM, 2005).

Table 1 – Classification of ashes.

| | **Type** | |
|---|---|---|
| | **C** | **F** |
| **Silica ($SiO_2$) - Alumina ($Al_2O_3$) – Iron oxide ($Fe_2O_3$), min %** | 50 | 70 |
| **Calcium oxide (CaO), %** | > 20 | < 10 |
| **Loss on ignition (LOI), %** | 6 | 6 |

Fonte: Adapted from ASTM, 2005.

*3.2.2.3 Rice husk ash*

According to the United States Department of Agriculture (USDA), world rice production in the 2018/19 crop was around 487.35 million tons. Production in Brazil, in the same period, is estimated at 11.75 million tons (CONAB, 2018).

Rice husk ash comes from the processing industries, which use the husk of the rice as an energy generator in grain processing. After the burning process, the rice ash equals 20% of the rice husk, thus generating a high volume of ash (ZOU; YANG, 2019).

The chemical composition of the rice husk differs from one sample to another, due to rice type, climate, geographical conditions and harvest period. When burned at temperatures up to 700 °C the ashes are manly composed of high amorphous silica ($SiO_2$), which are beneficial for the geopolymerization reaction (AHSAN; HOSSAIN, 2018).

Studies developed by Antiohos *et al*., (2013) and Khan *et al*., (2012) show that replacing up to 40% of Portland cement by rice ash is quite effective, generating a product of good strength and a potential product for cementation.

Studies have been developed to investigate the incorporation of these ashes into the production of geopolymers. Sore *et al*., (2016) synthesized geopolymers containing 5% rice husk ash and 95% metakaolin, a 12 M NaOH alkaline solution and curing for 14 days, 7 at room

temperature and 7 at 60 °C, and obtained a mechanical strength of 25 MPa. Kusbiantoro *et al*., (2012) used a mixture of fly ash and rice ash, 93 and 7 %, respectively, a solution containing sodium silicate and 8 M NaOH as alkaline solution and curing for 28 days at 65 °C, where the final product presented a compressive strength of 70 MPa. Sturm *et al.*, (2016) developed rice ash-based geopolymers using sodium aluminate as activating solution and alumina source, being cured at 80 °C for 28 days, reaching a mechanical strength of 32.7 MPa.

Although the materials have different mechanical properties good strengths are obtained for geopolymers prepared using fly ash as the main material or as secondary material.

*3.2.2.4 Alkaline activator*

The alkaline activators are of fundamental importance in obtaining the geopolymers, which is the dissolution of the aluminosilicate and ionic stability (ZHUANG *et al.*, 2016). Several alkaline cations can be used in the preparation of geopolymers, but the most used are sources of sodium ($Na^+$) and potassium ($K^+$), the alkaline activator can be solutions of sodium hydroxide (NaOH), potassium hydroxide (KOH) or combinations with sodium silicate ($Na_2SiO_3$) or potassium silicate ($K_2SiO_3$) (DUXSON *et al.*, 2007a; KOMNITSAS; ZAHARAKI, 2007). Depending on the cation used, the geopolymer presents different characteristics, since the ions have different sizes and density charges, when using $K^+$ (ionic radius of 1.33Å) a fast solidification is noticed, but problems like cracks and low porosity are observed, this is due to difficulty of penetration of this ion, unlike the $Na^+$ ion (ionic radius of 0.98Å), which shows a better penetration and consequently tends to lead to a better reaction in the geopolymerization process (DUXSON *et al.*, 2005a; NURUDDIN *et al.*, 2014).

The concentration of the alkaline activator directly influences the final properties (strength and microstructure) of the geopolymer matrix. (RASAKI *et al.*, 2019). Studies show that the dissolution of the aluminosilicates is affected by the concentration of the alkaline activator, which exhibits an increasing rate as the concentration increases, caused by a higher amount of hydroxyl ions ($OH^-$) in the medium. (PANAGIOTOPOULOU *et al.*, 2007). However, Dimas; Giannopoulou, Panias (2009); Rattanasak; Chindaprasirt, (2009) and Samantasinghar; Singh, (2018) show that there is an optimum concentration of alkaline activator for the geopolymerization process, and it occurs when it maintains a balance between the dissolved ions ($Si^{4+}$ and $Al^{3+}$) and the cation ($Na^+$). High concentrations of the alkaline activator tend to decrease or remain constant the percentage of leached aluminosilicates, on the

other hand, if there is an excess of alkaline activator, the polycondensation process is affected causing less strength. Efflorescence is another negative factor with the high concentration of alkaline activator.

Efflorescence, a migration of a salt to the surface of a porous material, is a relevant problem originated during the geopolymer cure period, since it mainly affects the mechanical strength and durability of the samples. Among the factors responsible are excess of sodium oxide ($Na_2O$), reactivity precursor materials and cure conditions (NAJAFI KANI; ALLAHVERDI; PROVIS, 2012; ZHANG *et al.*, 2014).

The main products originated by this phenomenon are alkaline carbonates. Equation 3 presents the efflorescence mechanism in a geopolymer using sodium source as an alkaline activator. The leaching and carbonation processes are the mechanisms present in the reaction that gives rise to efflorescence, where the excess alkaline ions are deposited on the geopolymer surface through the diffusion phenomenon, thus causing precipitate formation, and upon entering in contact with air, water evaporates (MINJIGMAA *et al.*, 2016; ZHANG *et al.*, 2018).

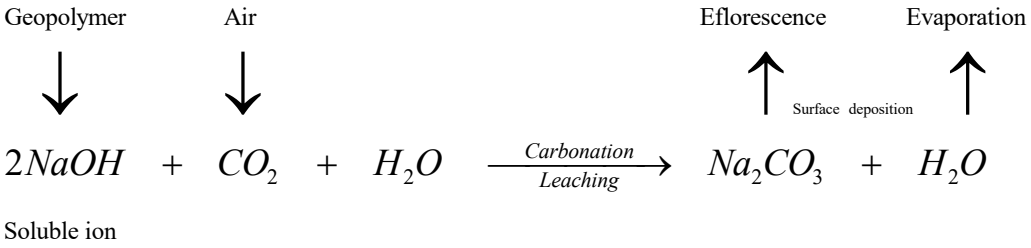


(3)

Source: Adapted from Zhang *et al*., 2018.

Several studies have been developed with the purpose of inhibiting efflorescence in the geopolymer matrix, among them are the control of the chemical formulation, particle size, type of activator and hydrothermal cure (ALLAHVERDI *et al.*, 2014; ŠKVÁRA *et al.*, 2009).

### 3.2.3 Reactivity

The reactivity of the materials is a prime factor to obtain a reliable quantification of the oxides used in the geopolymeric matrix, since the total composition of the material is not, however, reactive. Thus, precursor materials have been the subject of research in order to

elucidate doubts regarding the dissolution of aluminosilicates and how that affects the geopolymerization process (BURUBERRI *et al.*, 2019).

The amorphous phase contained in the raw material is the most relevant part for synthesizing the geopolymers, since it presents a higher reactivity, however, it is known that a fraction of this phase can not be attacked by the alkaline activator.

It is known that the dissolution of the aluminosilicates is initiated on the surface of the particle of the material and it is gradually relesead. With the progression of the dissolution and with higher concentration of Si and Al species, in the alkaline medium, the condensation reactions between aluminates and silicate monomer or between silicates monomer are initiated until the equilibrium of the condensation products is reached. The rate of dissolution is directly influenced by the surface area and concentration of the species, Si and Al, resulting from the alkaline activator (BURUBERRI *et al.*, 2019; RANJBAR *et al.*, 2014).

The combination techniques such as X-ray fluorescence (XRF) and X-ray diffraction (XRD) with phases quantification, atomic absorption spectroscopy (AAS), scanning electron microscopy (SEM) with energy-dispersive spectroscopy (EDS), aluminosilicates extraction combined with XRF, and inductively coupled plasma mass spectrometry (ICP-MS), are used for the appropriate quantification of amorphous and reactive material (MO *et al.*, 2014).

Due to its high purity and reactivity the metakaolin is the most widely used precursor for obtaining geopolymers. Generating a good geopolymer network and obtaining good mechanical strength properties (AUTEF *et al.*, 2013a; GHARZOUNI *et al.*, 2015).

The fly ash reactivity is given by the amount of amorphous aluminosilicate material, and this amount depends on the combustion conditions, type of coal and minerals contained, and particle size and shape (LEE *et al.*, 2017; WILLIAMS; VAN RIESSEN, 2010). However, not all amorphous material presented reacts during the geopolymerization process. Thus, the dissolution rate of aluminosilicates is a relevant factor in the production of geopolymers that use fly ash in their composition. With this, Fernández-Jiménez; Palomo; Criado (2005b) developed a model of the activation of fly ash, in which they describe that in the initial part they have the dissolution of the shell of the sphere, causing the inner part to be exposed to the attack of the activator. At the same time as the dissolution of the aluminosilicates occurs, the gel precipitation occurs due to the high concentration of the dissolved species, which is compacted in unreacted beads and in partially dissolved spheres, so that some of the beads are protected from the alkaline attack.

The rice husk ash, composed almost entirely of amorphous silica, is highly reactive and presents rapid dissolution in alkaline medium, therefore, it has been used to obtain geopolymers (BILLONG *et al.*, 2018; HAJIMOHAMMADI; VAN DEVENTER, 2015; ZOU; YANG, 2019).

Studies developed by Lee *et al*., (2017), Williams and Van Riessen (2010), where they quantify silica ($SiO_2$) and amorphous alumina ($Al_2O_3$) from precursor materials, show that the geopolymers presented better mechanical strength when compared to geopolymers prepared without phases quantification.

Quantification of the reactive oxides on the precursors materials, used in the production of the geopolymers, allows the use of the right amount of the alkaline activator, inhibiting problems such as efflorescence and high costs caused by the preparation of geopolymers with lower mechanical strength (LEE *et al.*, 2017).

### 3.2.4 Cure

The curing conditions employed in the geopolymeric slurry directly interfere in the dissolution of the aluminosilicates species and in the physical structure, which reflect in the strength and porosity of the geopolymers (MO *et al.*, 2014).

Geopolymers based on metakaolin were developed by Mo *et al*., (2014) and Muñiz-Villarreal *et al*., (2011), where they investigate the effect of the various curing conditions, concluding that when subjected to a temperature of 60 °C the geopolymer exhibits maximum strength. In fact, fly ash-based or rice husk ash-based geopolymerization rate increases as the temperature increases, as proved by others authors (Bakharev (2005), Palomo, A. and M. Grutzeck (1999), Strydom and Swanepoel (2002), Kaur; Singh; Kaur (2018) and Sturm *et al*., (2016b)).

## 3.3 KINECT MODELS APPLIED TO $CO_2$ ADSORPTION

The study of the mechanism of adsorption and desorption are essential, therefore, they provide an exact equation during the duration of the reaction. Thus, several kinetic models have been used to test experimental data, the most commonly used models are pseudo-first order,

pseudo-second order and intra-particle diffusion model (GUARÍN ROMERO; MORENO-PIRAJÁN; GIRALDO GUTIERREZ, 2018)

The kinetic parameters obtained from the models are of fundamental importance, since they allow to calculate the reaction time, process yield and quantity of material to be used in the process, relevant data for large scale applications.

Confirmation that the model fits the data is determined by the correlation coefficient ($R^2$), the closer to 1 the value is, the more satisfactory the model is.

### 3.3.1 Pseudo-first order

The pseudo-first order model was developed by Lagergren, 1898, and was initially used to describe the kinetic data of the adsorption process of oxalic and malonic acid in coal, the model reports the adsorption capacity of the adsorbent. The Langergren kinetic model is presented in Equation 4, where $q_t$ (mmol/g) is the adsorption capacity at time t, $q_e$ (mmol/g) is the equilibrium capacity, k ($min^{-1}$) is the constant of velocity and t (min) is the time (GUARÍN ROMERO; MORENO-PIRAJÁN; GIRALDO GUTIERREZ, 2018; HO; MCKAY, 1998)

$$q_t = q_e\left(1-e^{-kt}\right) \tag{4}$$

### 3.3.2 Pseudo-second order

The pseudo-second order model also reports the adsorption capacity of the adsorbent, however, throughout the process range. This model gained notoriety after Ho and Mckay (1999) analyzed data reported in the literature and found that the best fit was when using the pseudo-second order model. In equation 5, it is described the pseudo-second order model, where $q_t$ (mmol/g) is the adsorption capacity at time t, $q_e$ (mmol/g) is the equilibrium capacity, k (g $mmol^{-1}min^{-1}$) is the constant of velocity and t (min) is the time.

$$\frac{t}{q_t} = \frac{1}{k_2 q_e^2} + \frac{1}{q_e}t \tag{5}$$

### 3.3.3 Intra-particle diffusion model

The application of the kinetic model of intra-particle diffusion occurs when the adsorbent materials have a large particle size and highly porous, and when the diffusion rate is very small in relation to the intrinsic reaction. The model is derived from Fick Law, assuming that diffusion through the film of the fluid surrounding the adsorbent is negligible, so intra-particle diffusion becomes the limiting step of the process. The expression of the intra-particle model is presented in Equation 6, where $q_t$ (mmol/g) is the adsorption capacity at time t, $k_i$ (mmol $g^{-1}$ $min^{-0.5}$) is the constant of velocity and C is the value obtained through the intersection of straight with $q_t$ (GUARÍN ROMERO; MORENO-PIRAJÁN; GIRALDO GUTIERREZ, 2018)

$$q_t = k_i t^{1/2} + C \tag{6}$$

# 4 STATE OF ART

Table 2 presents some studies already developed to obtain geopolymers.

Geopolymers were initially developed using metakaolin as the main precursor material. However, with the evolution of research several materials, mainly residues such as fly ash, rice husk ash and red mud, which contains in its matrix aluminosilicates were used to obtain the geopolymers. (KOMNITSAS; ZAHARAKI, 2007). However, most research does not use more than three aluminosilicate sources to obtain geopolymers.

The alkaline activator used geopolymerization process normally is sodium hydroxide (NaOH), potassium hydroxide (KOH) or combinations with sodium silicate ($Na_2SiO_3$) or potassium silicate ($K_2SiO_3$) (DUXSON *et al.*, 2007b). Few studies are developed using a renewable source of silicon, such as rice husk ash, to replace commercial.

The curing conditions used in the geopolymeric slurry directly interfere in the dissolution of the aluminosilicates species and in the physical structure. Thermal curing and room temperature are the most used in the process of obtaining the geopolymer. However, it is known that unreacted ions during the curing process are free in the matrix and may react after the curing time when used in applications such as carbon dioxide capture or heavy ion adsorption. Thus, studies analyzing the removal of free ions during the cure time are necessary to obtain geopolymers with good chemical stability (MO *et al.*, 2014).

As shown (Table 2), the various parameters, such as precursor material, alkaline activator, molar ratio and curing conditions, directly affect the final properties of geopolymers such as compressive strength.

Studies using geopolymers as adsorbent material for the $CO_2$ capture process are recent. Study developed by Minelli *et al.,* 2016 (Table 3), where they apply geopolymers to capture carbon dioxide, obtaining an adsorption capacity of 0.62 mmol/g. However, the geopolymer is obtained using metakaolin as a precursor material, which increases the cost of operation. Therefore, studies that verify the behavior of geopolymers that use residues in their composition are subject to further studies.

Table 2 – State of art of geopolymers.

| Aluminosilicate | Alkaline activator | Ratio | Cure | Compressive strength | Reference |
|---|---|---|---|---|---|
| metakaolin | sodium hydroxide/sodium silicate | Si/Al=2.50 | 75 °C for 24h/7 days room temperature | 60 Mpa | Rowles *et al*., 2003 |
| metakaolin | sodium hydroxide/sodium silicate | Si/Al=2.00 | room temperature for 7 days | 67 Mpa | Lahoti *et al*., 2018 |
| fly ash | sodium hydroxide/sodium silicate | Si/Al=2.10 | 75 °C for 24h/24h room temperature | 33 MPa | Yousefi *et al*., 2017 |
| fly ash and rice husk ash | sodium hydroxide/sodium silicate | Si/Al=2.50 | 35 °C for 28 days | 35 Mpa | Hwang *et al*., 2015 |
| rice husk ash | sodium aluminate | Si/Al=1.74 | room temperature for 3 days | 33 Mpa | Sturm *et al*., 2016 |

Source: Author's own elaboration.

Table 2 (continue)

| Aluminosilicate | Alkaline activator | Ratio | Cure | Compressive strength | Reference |
|---|---|---|---|---|---|
| red mud | sodium hydroxide/sodium silicate | Si/Al=2.5 | 75 °C for 10 days | 43 MPa | Toniolo *et al.*, 2018 |
| red mud | sodium hydroxide/sodium silicate | Si/Al=3.0 | 75 °C for 10 days | 46 MPa | |
| red mud | sodium hydroxide/sodium silicate | Si/Al=3.5 | 75 °C for 10 days | 32 MPa | |

Source: Author's own elaboration.

Table 3 – $CO_2$ adsorption on geopolymers.

| Adsorbent | $CO_2$ Capture (mmol/g) 35 °C – 1 bar | Precursor material | Reference |
|---|---|---|---|
| G10 | 0.62 | Metakaolin | Minelli *et al*., 2016 |
| G13 | 0.58 | Metakaolin | |
| G23 | 0.57 | Metakaolin | |

Source: Author's own elaboration.

# 5 MATERIAL AND METHODS

This chapter presents the materials and methods used in the synthesis of geopolymers, the characterization techniques used in precursor materials and geopolymers, finally the methodology used in the $CO_2$ capture process. Figure 8 shows the methodologies applied in the study.

Figure 8 – Flowchart of the developed studies.

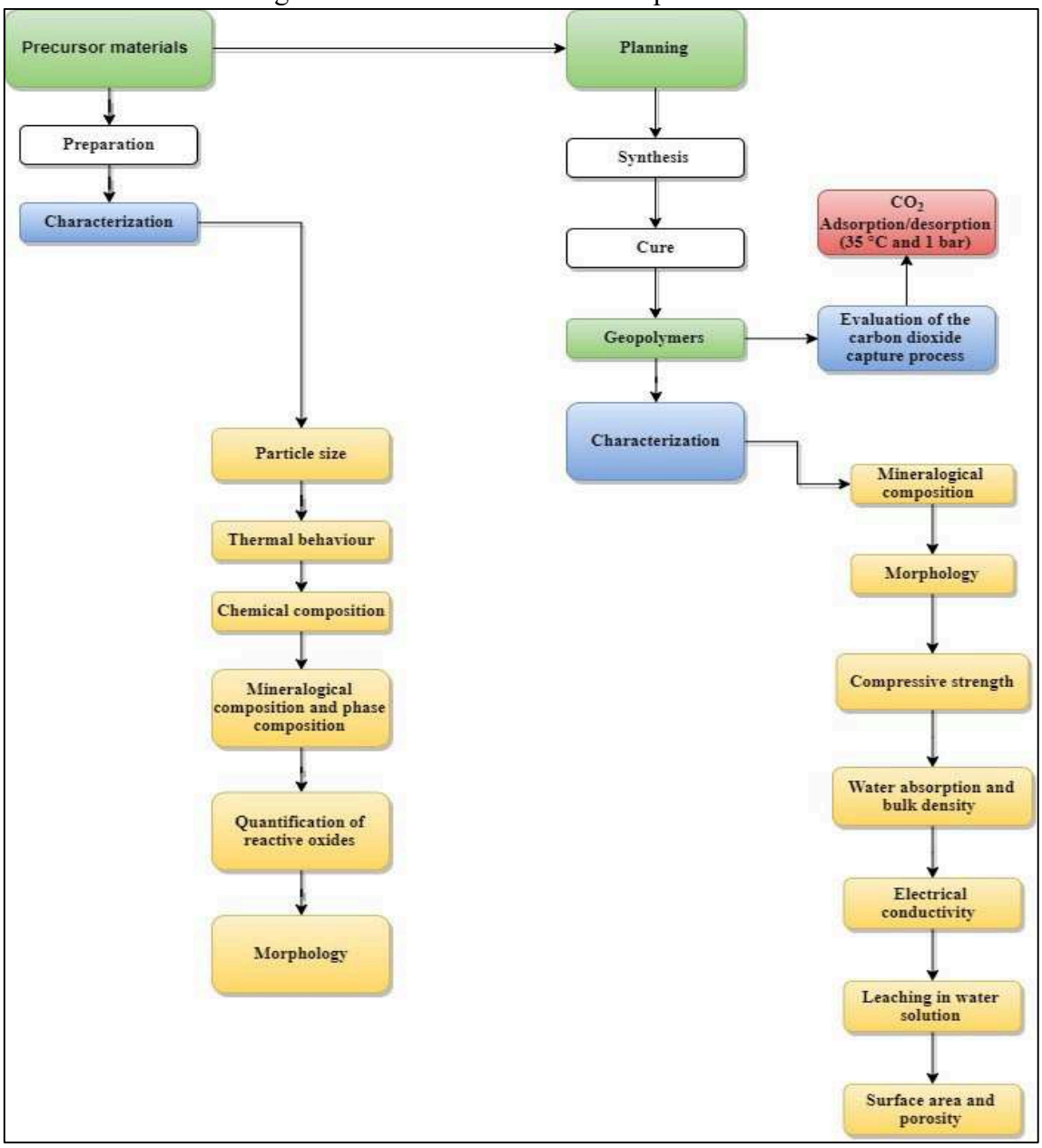


Source: Author's own elaboration.

## 5.1 MATERIALS

The materials used in the production of geopolymers are:

- Caulisa Kaolin Industry (Campina Grande, PB, Brazil);
- Fly ash (FA), waste from the burning of coal used as energy source, supplied by company Jorge Lacerda Thermoelectric Power Plant;
- Rice husk ash (RHA), waste from the burning of rice husks as a source of energy in the processing industries provided by the company Fumacense Alimentos (Morro da Fumaça, SC, Brazil);
- Neutral sodium silicate, with $SiO_2/Na_2O$ ratio of 3.2 obtained from commercial Quimidrol; and
- Sodium hydroxide (NaOH) in micro pearls, 97% purity, obtained from commercial NEON.

## 5.2 CHARACTERIZATION TECNIQUES

### 5.2.1 Particle size

The particle size distribution was performed on the precursor materials. The analysis was performed in the Engineering and Technology Institute-UNESC, using the CILAS-1064 in liquid medium.

### 5.2.2 Thermal behavior

The mass variation was determined by Thermogravimetric analysis (TGA) with $N_2$ atmosphere, the programming used for kaolin was as follows: ambient temperature up to 900 C at a rate of 10 °C/min. The programming for RHA was as follows: ambient temperature up to 500 °C at a rate of 10 °C/min, after reaching 500 ºC the sample was heated for 240 min. It was used a thermogravimetric analyzer DTG 60/60H (Shimadzu).

The analysis was performed at the Laboratory of Energy and Environment (LEMA) of UFSC-Florianópolis.

### 5.2.3 Chemical composition

The chemical analysis of X-ray fluorescence (XRF) spectrometry was used to quantify the oxides present in the raw materials. The analysis was carried out in the Laboratory of Materials Development and Characterization (LDCM) of Senai-Criciúma. The equipment used was the Panalytical-AXIOS Max.

### 5.2.4 Mineralogical composition and phase quantification

The mineralogical composition was determined by X-ray diffraction (XRD) The experimental conditions were: Cu-Kα incident radiation (25 kV/25 mA), 2θ scanning from 3 to 65° and speed of 1°/min.

The phases quantification was calculated using Materials Analysis Using Diffraction (MAUD) software by the Rietveld method. The fluorite was used as internal standard.

The analysis was performed in the Engineering and Technology Institute-UNESC, using the Shimadzu-XRD 6000.

### 5.2.5 Quantification of reactive oxides

The analysis of the extraction of reactive oxides aimed to quantify the percentage of oxides available in the precursor materials for the reaction. The procedure was carried out at the Laboratory of Energy and Environment (LEMA) of UFSC-Florianópolis.

The experimental procedure was carried out following the steps below:

1. 20 g of the sample (MK, FA, RHA or RHAC), 26.60 g of sodium hydroxide and 100 g of water;
2. The three components were allowed to react for 10 h at 100 °C;
3. A filtration was performed to separate the liquid phase from the solid;
4. The liquid phase was neutralized with sulfuric acid ($H_2SO_4$); and
5. The phases, liquid and solid, were taken for drying in oven for posterior analysis of XRF.

The reactive oxides for the rice husk ash and the calcined rice husk ash was determined by weighting the resulting mass after extraction, because silica ($SiO_2$) is the only chemical component to be dissolved. However, the determination of the reactive oxides of fly ash and metakaolin can not be totally determined by mass difference, considering that aluminosilicate materials, when subjected to dissolution with alkali hydroxides, at 100 °C for 3 h, also leads to the formation of type A zeolite (DAVIDOVITS, 1994). Thus, the determination of the reactive oxides of these two materials is given by the sum of the dissolved oxides and the amount that reacts to produce the zeolite.

### 5.2.6 Morphology

Scanning electron microscopy (SEM) was necessary to evaluate the microstructure of precursor materials and geopolymers. The analyses were performed at the Central Laboratory of Scanning Electron Microscopy (LCME) at UFSC-Florianópolis using a JEOL JSM-6390LV microscope. The samples were coated with gold, thus making it more conductive and allowing better analysis.

### 5.2.7 Compressive strength

The uniaxial mechanical strength test was performed at the Laboratory of Nanotechnology - Nanotec at UFSC-Florianópolis. The equipment used was from universal test systems of the brand Instron and model 5569.

The analyzes were carried out in triplicate and with saturated geopolymers, after 7 and 28 d of curing, the application rate of charge was 1 mm/min.

### 5.2.8 Electric conductivity

The electrical conductivity analysis was performed at the Laboratory of Energy and Environment (LEMA) of UFSC-Florianópolis. The equipment used was the conductivity meter of the brand Digimed model DM 32. The data were collected during the period in which the samples were immersed (curing process). From the analysis of electrical conductivity, it is possible to determine the dissolution of salts, which may not have reacted during the formation of the geopolymers.

### 5.2.9 Leaching in water solution

The concentrations of sodium, silicon, alumina, potassium, calcium and magnesium, dissolved during the geopolymers immersed curing process were determined by atomic absorption spectrophotometry using an Agilent 240 FSA spectrophotometer. The analysis was performed at the Laboratory of Energy and Environment of UFSC-Florianópolis. The samples were previously acidified with nitric acid ($HNO_3$).

### 5.2.10 Water absorption and bulk density

The analyses were determined by the Arquimeds method, in the geopolymers, after 28 days of cure. For this experiment it is necessary to obtain the mass of the dry geopolymer ($m_S$), which was achieved by drying it in an oven for 24 h at 100 °C, then the geopolymer is immersed in water for 24 h to obtain the immersed saturated geopolymer mass ($m_{STI}$) and saturated ($m_{ST}$). To obtain the $m_{STI}$, the solid is suspended in a beaker containing water. The sample weight will be equal to the volume of displaced fluid. To obtain the $m_{ST}$ the excess water is removed from the surface using a damp cloth.

The water absorption is established as the percentage gain of mass in the geopolymer and is given by Equation 7.

$$A_{H_2O(\%)} = \frac{m_{ST} - m_S}{m_S} \times 100 \quad (7)$$

Equation 8 refers to bulk density

$$B_{(g/cm^3)} = \frac{m_S}{m_{ST} - m_{STI}} \quad (8)$$

### 5.2.11 Surface area and porosity

The specific surface area, pore size and total pore volume were obtained through the nitrogen adsorption-desorption isotherms at 77 K, the analyses were performed at the Engineering and Technology Institute-UNESC, using a Quantachrome equipment, model Nova 1200e. Degassing process was carried out under vacuum at 300 °C for 3 h.

## 5.3 METHODS

The study was divided into three stages: preparation of precursor materials, synthesis of geopolymers, and, finally, evaluation of the carbon dioxide ($CO_2$) capture process.

### 5.3.1 Preparation of precursor materials

The precursor materials used were prepared for later obtaining the geopolymers.

The kaolin was subjected to the calcination process to obtain metakaolin, in a muffle oven of the Fornitec brand, model F2-DM. The calcination temperature was 900 °C, heating rate 5 ºC/min for a period of 60 min.

The magnetic ions of the fly ash were removed and the obtained material was dried in an oven at 100 °C for 24h.

The rice husk ash (RHA) was subjected to the calcination process to remove the carbonaceous material, obtaining the ash from the rice husk ash (white), a muffle oven of the Fornitec brand, model F2-DM was used. The calcination temperature was 500 °C, heating rate of 5 °C and the sample was left at this temperature for 180 min.

### 5.3.2 Synthesis of geopolymers

Initially, for the geopolymer synthesis process required studies that used similar precursor materials and obtained good physical properties (HWANG; HUYNH, 2015a; LAHOTI *et al.*, 2018; ROWLES; O'CONNOR, 2003; STURM *et al.*, 2016b; YOUSEFI ODERJI; CHEN; JAFFAR, 2017).

The study developed by Rowles and O'connor, (2003) ($SiO_2$:$Na_2O$:$Al_2O_3$= 0.62:0.17:0.21) was selected as the basis for obtaining the percentage of each material to be

used in the formulations. The choice was made because the study is within the optimum limits, suggested by (DAVIDOVITS, JOSEPH; DAVIDOVICS, MICHAEL; DAVIDOVITS, 1994), because it presents a better flexibility in the incorporation of the materials used, and because it presents a higher percentage of silica, which is also found in the materials used in the study. With the determination of the reference study, a triaxial diagram containing the main oxides ($SiO_2$, $Al_2O_3$ and $Na_2O$) was plotted.

The Figure 9 shows the triaxial diagram, on the base of reactive oxides, which contains the materials used in the synthesis (squares), as well as the selected study as base (red dot), with this, ten target formulations of study were elaborated. Table 2 shows the experimental design developed. The compositions were encoded as follows: MF-1, MF-2, MR-1, MR-2, MCR-1, MCR-2, MFR-1, MFR-2, MFCR-1 and MFCR-2, where M is metakaolin, F is fly ash, R is rice husk ash, CR is calcined rice husk ash, S1 is sodium hydroxide mixture with sodium silicate solution and S2 is sodium hydroxide.

Formulations MF-1 and MF-2 are composed of metakaolin, fly ash, S1 (NaOH-$Na_2O$●$3.2SiO_2$) and S2 (NaOH), differing that in MF-1 if S1 and MF-2 S2 is used. Formulations MR-1 and MR-2 have the use of metakaolin, rice husk ash, S1 and S2 incorporating S1 in MR-1 and S2 in MR-2. Formulations MCR-1 and MCR-2 consist of metakaolin, calcined rice husk ash, S1 and S2, used S1 in MCR-1 and S2 in MCR-2. Formulations MFR-1 and MFR-2 are composed of metakaolin, fly ash, rice husk ash, S1 and S2, where uses S1 in MFR-1 and S2 in MFR-2. Formulations MFCR-1 and MFCR-2 are already prepared containing metakaolin, fly ash, calcined rice husk ash, S1 and S2, where S1 is incorporated in MFCR-1 and S2 in MFCR-2.

As one of the objectives of the work is to use a higher percentage of residues, the comparison between S1 and S2 is justified, since in S2 is not used the sodium silicate, being necessary the use of a greater percentage of the ashes of rice husk because, where it presents a high source of silica. On the other hand, the use of rice husk ash and calcined rice husk ash is aimed at evaluating the best dissolution of the silica oxides in the reaction medium and, because of the large specific area, the evaluation of the carbon dioxide capture process.

Figure 9 – Triaxial diagram to obtain the mass percentages of geopolymers.

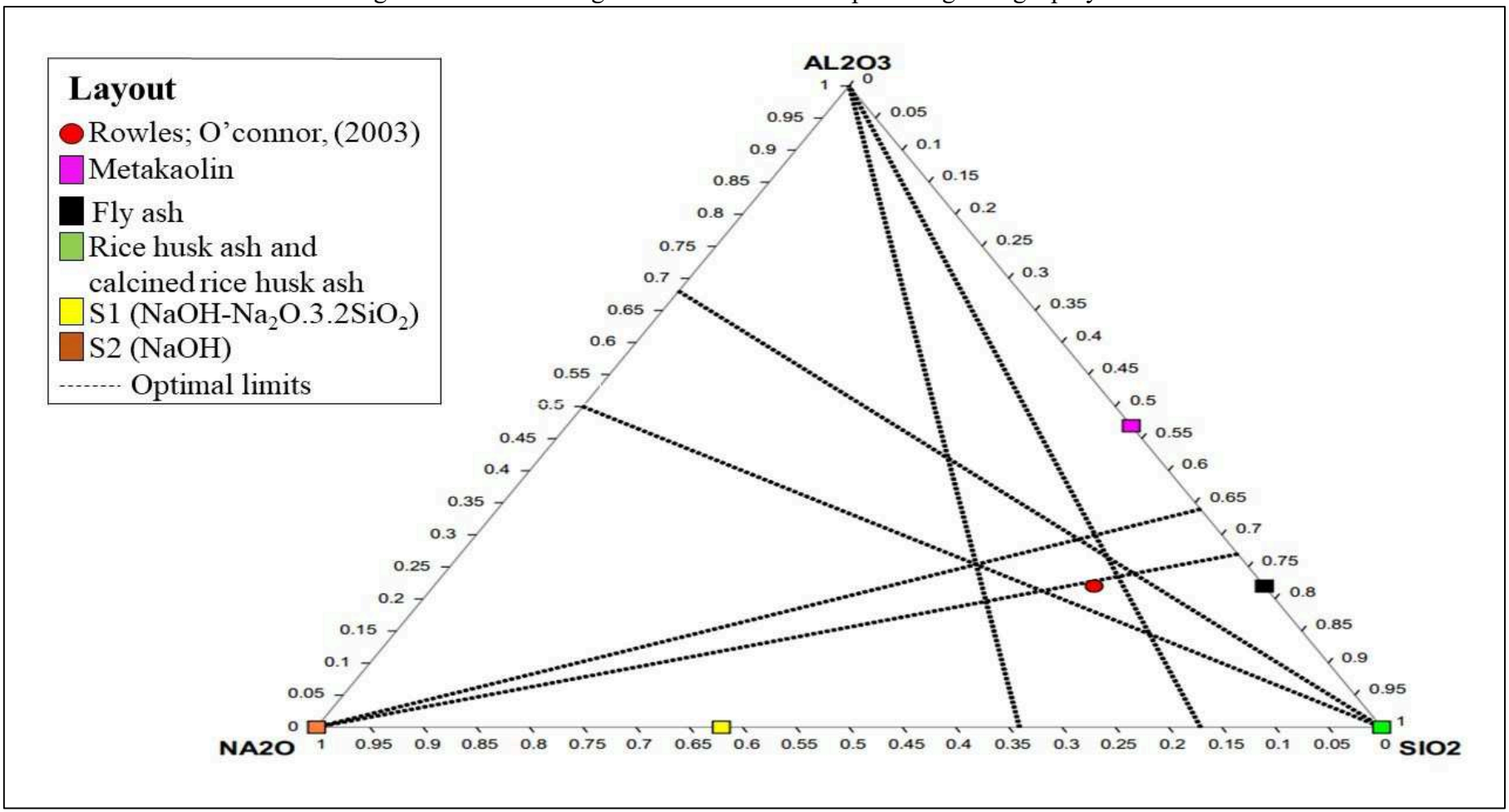


Source: Author's own elaboration

From the elaboration of the experimental planning it is possible to obtain the mass percentage of the components based on the reactive oxides, using the Excel software solver tool. The percentages are show in Table 4.

Table 4 – Materials percentages of mass.

| Geopolymer | Precursor materials | | | | | | Extra water (g) |
|---|---|---|---|---|---|---|---|
| | | | | | Alkaline activator | | |
| | Metakaolin | Fly ash | RHA | RHAC | S1 | S2 | |
| **MF-1** | 14 | 45 | - | - | 41 | - | - |
| **MF-2** | 9 | 65 | - | - | - | 26 | 15 |
| **MR-1** | 32 | - | 21 | - | 47 | - | 10 |
| **MR-2** | 36 | - | 32 | - | - | 32 | 30 |
| **MCR-1** | 33 | - | - | 19 | 48 | - | 15 |
| **MCR-2** | 37 | - | - | 30 | - | 33 | 30 |
| **MFR-1** | 27 | 14 | 14 | - | 45 | - | 5 |
| **MFR-2** | 27 | 21.5 | 21.5 | - | - | 30 | 25 |
| **MFCR-1** | 27 | 13.5 | - | 13.5 | 46 | - | 10 |
| **MFCR-2** | 28 | 20.5 | - | 20.5 | - | 31 | 22 |

M. metakaolin; F. fly ash; R. rice husk ash (black); CR. rice husk ash (white)

Source: Author's own elaboration.

After obtaining the mass percentages of the precursors the geopolymers were synthesized, 100 g batches were made to obtain the geopolymers. The following steps, out of a total of five, explain how the manufacturing process occurred. The first step is the mixing of the solid materials for 5 minutes and stirring at 600 RPM, the second stage is the homogenization of the alkaline activator for 5 minutes and 720 RPM, the third stage is the mixing of the solid materials with the alkaline activator, for 10 minutes and 2000 RPM, the fourth stage is the molding of the geopolymer mass and the fifth is the paste submission to the curing process. The cured process was as follow: samples were dried for 48 h at 65 °C, cooled to room temperature, removed from the molds and submerged in deionized water for 26d.

### 5.3.3 Capture of carbon dioxide ($CO_2$)

The adsorption data of carbon dioxide were obtained through the thermogravimetric analyzer DTG 60/60H (Shimadzu), which is composed by three parts: the first contains the furnace and thermal balance, the second is the gas flow control and third is the data collection system. In Figure 10 can be seen the layout of the part that includes the oven and thermal balance. The oven is ceramic and cylindrical geometry, the system can be operated in the ambient temperature range up to 1000 °C, at atmospheric pressure and heating rates up to 99.9 °C/min.

Figure 10 – First part of thermogravimetric analyzer.

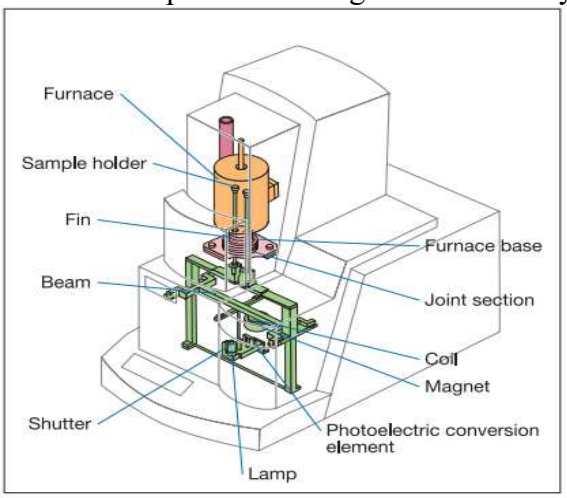


Source: Adapted from Shimadzu, 2019.

The second part of the thermogravimetric analyzer is the controller of the gas flows to be used in the process. The controller consists of three inputs (Dry, Purge 1 and Purge 2) and two outputs (Dry and Purge), the control in the Dry line is given manually and the Purge lines are automated by the equipment software. In Figure 11 we have the flow controller.

Figure 11 – Gas flow controller.


Source: Adapted from Shimadzu, 2019.

After the gases pass through the controller, it is directed to the reaction chamber, where the flow is given in a progressive manner. In Figure 12 the gas inlets are shown, the inert gas is inserted in the lower part of the balance, the reactive gas in the base of the oven and the outlet of the gases is located in the upper part of the chamber.

Figure 12. Design of gas flows in the reactive chamber.

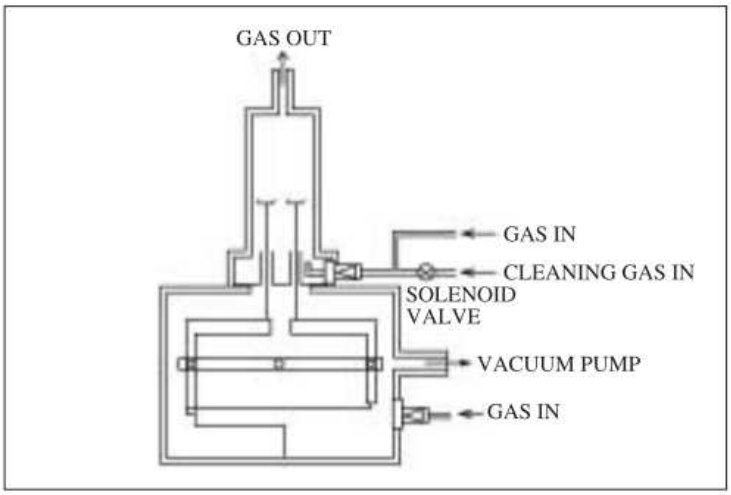


Source: Adapted from Shimadzu, 2019.

The last part of the thermogravimetric analyzer is to obtain the data of temperature and mass variation, Shimadzu Thermal Analysis Sotware TA-60WS is used and it is coupled to a computer. The software of the equipment is responsible for generating the thermograms, this same software is used to configure the desired programming.

This analysis was applied to the materials and to the synthesized geopolymers. The performance consists of zeroing the balance with the chamber closed with the inserted crucible, the system is opened, and the sample is inserted in the crucible, weighed and the chamber is

closed again. With the completion of the preparation process, the program to be executed is inserted. The present study is based on three fundamental phases: nitrogen purge ($N_2$), pre-treatment of the material and adsorption.

Through the first phase there is the elimination of gases that are inside the chamber, the purge, where one has the passage of the nitrogen gas with a constant flow and a period of 60 minutes.

The second stage is the pretreatment of the material, it is subjected to a set temperature, which is obtained with a constant rate of heating, a constant flow of inert gas, under these conditions for a period of 60 minutes. The realization of the first and second phases of the process is therefore indispensable as it intended to prepare the surface of the material for the adsorption phase of carbon dioxide.

Adsorption of the carbon dioxide is third stage of the process, the realization occurred isothermally at a temperature of 35 °C and atmospheric pressure (MINELLI *et al.*, 2016b). The programming performed in this analysis is show Table 5.

Table 5 – Programming for the analysis of $CO_2$ adsorption.

| **Process steps** | **Conditions** | | | |
|---|---|---|---|---|
| | **Temperature (°C)** | **Time (min)** | **Atmosphere** | **Flow (ml/min)** |
| **Purge** | 35 | 60 | $N_2$ | 100 |
| **Pre-treatment** | 110 | 60 | $N_2$ | 100 |
| **Cooling** | 35 | 10 | $N_2$ | 100 |
| **Adsorption** | 35 | 240 | $CO_2$ | 100 |

Source: Author's own elaboration.

The mass variation, in the adsorption adsorption process, is obtained through the data generated by TA-60WS software and are shown in milligram units. For a better understanding, it was modified to mmol$CO_2$/g of adsorbent, the calculation is presented Equation 9, where $m_{i,t}$ is the mass obtained in a given time, $m_i$ is the mass before the process of the beginning of the adsorption, $MM_{CO2}$ is the molecular weight of the carbon dioxide.

$$Q_{(mmol/g)} = \frac{m_{i,t} - m_i}{m_i \times MM_{CO_2}} \times 1000 \quad (9)$$

Source: Author's own elaboration.

# 6 RESULTS AND DISCUSSIONS

This chapter will present the results of characterization of precursor materials, geopolymers and evaluation of these materials as adsorbents of carbon dioxide, as well as relevant discussions.

## 6.1 CHARACTERIZATION OF PRECURSOR MATERIALS

### 6.1.1 Particle size

Particle size distribution is of great relevance in the development of geopolymers, as properties such as water demand, porosity, viscosity and degree of solubility are affected. Thus, impacting directly on matrix compaction and compressive strength (ASSI; EDDIE DEAVER; ZIEHL, 2018; MOOSAVI; ASADI; SHORAKI, 2019; SOUTSOS *et al.*, 2016). Materials with a $d_{0.5}$ <45m are considered satisfactory to obtain geopolymers with good strength (DUXSON *et al.*, 2007c; SOUTSOS *et al.*, 2016).

Figure 13 shows the cumulative distribution of precursor materials, metakaolin, fly ash, rice husk ash (black) and calcined rice husk ash (white), where $d_{0.5}$ values are 11.30, 27.50, 38.22 and 37.70 µm, respectively.

Figure 13 – Cumulative distribution of particle size for fly ash, metakaolin, rice husk ash and calcined rice husk ash.

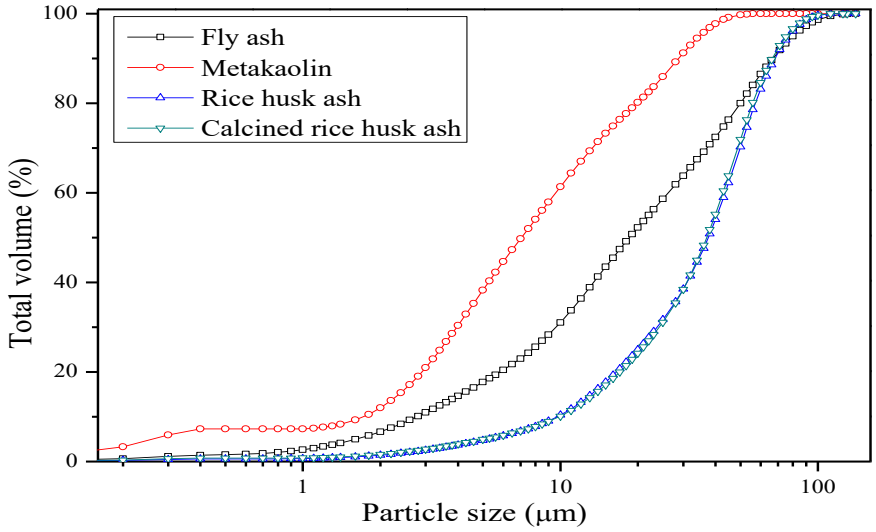


Source: Author's own elaboration.

### 6.1.2 Thermal behavior

Kaolinite claystone is not studied frequently as a raw material for geopolymer production, but it largely known that under thermal treatment, kaolinite is transformed into reactive metakaolin (AUTEF *et al.*, 2013b). As shown in Figure 14, kaolinite thermally decomposes at a temperature range 400 - 700 °C. The mass loss is the order of 13.70% and corresponds to the dehydroxylation process of the kaolinite, that is transformed into reactive metakaolin (PTÁČEK *et al.*, 2013). At temperature higher than 700 ºC, no significant variation in mass was observed (SANTOS, 1989).

So, after the thermal treatment of kaolin used in this study (900 °C, heating rate 5 ºC/min for 60 min), it is assumed that only reactive metakaolin was present in the solid.

Figure 14 – Thermogravimetric analysis of metakaolin.

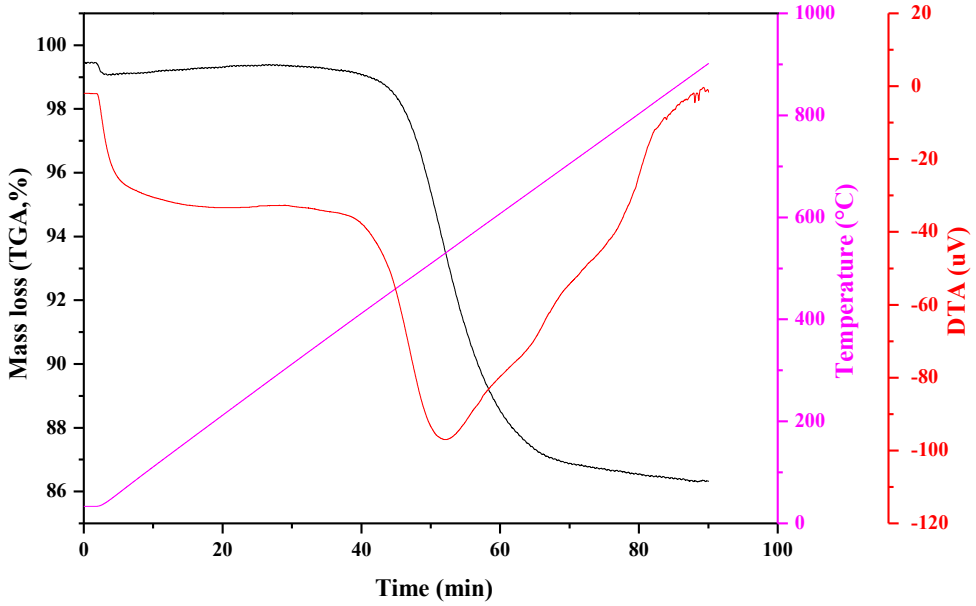


Source: Author's own elaboration.

The rice husk ash used in this study was black in color, indicating the presence of organic compounds residues in its composition. The presence of these carbonaceous materials could be useful to improve the adsorption, but its effect on the geopolymerization reactions must be investigated. So, black rice husk ash was calcinated to produce white calcinated rice husk ash. To guarantee complete elimination of organic compounds and no transformation of amorphous silica to crystalline silica, the thermal behavior of rice husk ash was investigated.

Figure 15 shows the thermal analysis of the rice husk ash, the loss of mass (6.60%) observed as the temperature increases may be attributed to the elimination of impurities and carbonaceous material. No phase transition phenomenon is observed from 500 °C to 240 min, thus ensuring that the material obtained after calcination is amorphous silica since the production of crystalline silica occurs above 900 °C (Zou; Yang, 2019).

Figure 15 – Thermogravimetric analysis of rice husk ash.

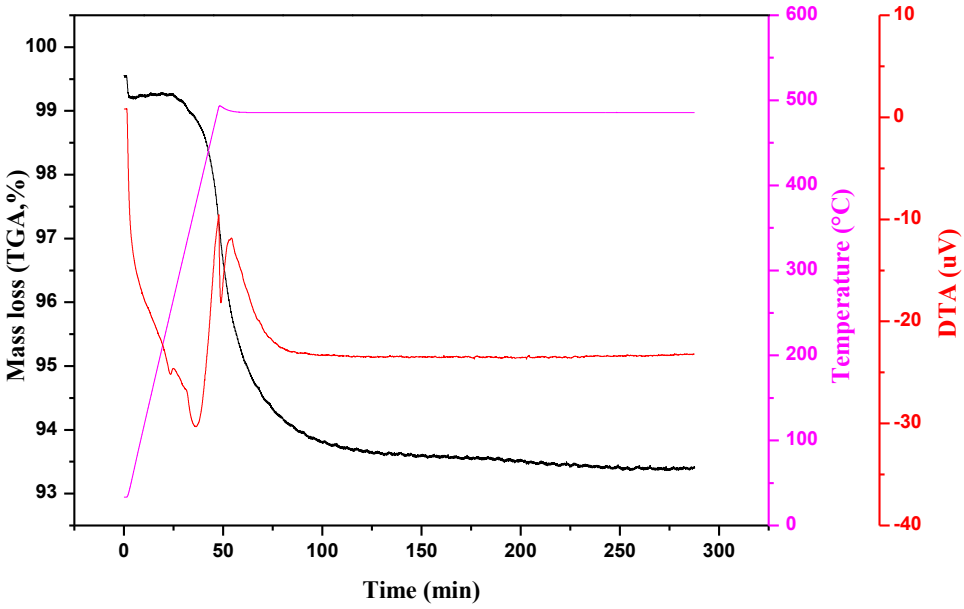


Source: Author's own elaboration.

### 6.1.3 Chemical composition and reactive oxides

The chemical compositions of precursor materials and reactive oxides are show in Table 6.

Table 6 – Composition of total and reactive oxides of precursor materials

| Chemical composition (% w/w) | | | | | | | | |
|---|---|---|---|---|---|---|---|---|
| **Compound** | **Metakaolin** | | **Fly ash** | | **Rice husk ash** | | **Calcined Rice husk ash** | |
| | **Total[a]** | **Reactive[b]** | **Total[a]** | **Reactive[b]** | **Total[a]** | **Reactive[b]** | **Total[a]** | **Reactive[b]** |
| **$SiO_2$** | 54.3 | 50.0 | 65.4 | 52.3 | 87.0 | 87.0 | 94.0 | 94.0 |
| **$Al_2O_3$** | 44.2 | 44.2 | 24.6 | 14.5 | 0 | | 0 | |
| **$Fe_2O_3$** | 0.3 | | 2.6 | | 0.1 | | 0.1 | |
| **$K_2O$** | 1.0 | | 2.8 | | 1.6 | | 1.7 | |
| **CaO** | 0 | | 1.4 | | 0.7 | | 0.8 | |
| **$Na_2O$** | 0 | | 0.5 | 0.5 | 0.1 | 0.1 | 0.1 | 0.1 |
| **MgO** | 0 | | 1.2 | | 1.0 | | 1.1 | |
| **$TiO_2$** | 0 | | 1.0 | | 0 | | 0 | |
| **$SO_3$** | 0 | | 0.5 | | 0 | | 0 | |
| **$P_2O_5$** | 0 | | 0 | | 0.7 | | 0.8 | |
| **MnO** | 0 | | 0 | | 0.2 | | 0.2 | |
| **LOI** | 0 | | 0 | | 7.5 | | 1.4 | |

a. Determined by FRX; b. Quantification by extraction Source: Author's own elaboration.

Alumina ($Al_2O_3$) and silica ($SiO_2$) oxides are the main constituents of the material in the metakaolin composition, while rice husk ash and calcined rice husk ash are almost entirely of silica oxide. Fly ash is also composed mostly of oxides of alumina and silica, but potassium ($K_2O$) and iron ($Fe_2O_3$) oxides are found, and it can be classified as type F, since it contains less than 10% of calcium oxide (ASTM, 2005).

The high content of silica and alumina in the solid residues (fly ash, rice husk ash and calcined rice husk ash enable them to be used in the geopolymerization. However, it is need to evaluate the reactive ratio of each oxide since the crystalline oxides has low reactivity in to be less reactive than amorphous materials during polymerization processes (LAU *et al.*, 2019). Moreover, the presence of organic impurities in the rice husk ash could be an additional resistance for the geopolymerization process.

Table 6 shows the quantification of reactive oxides in the metakaolin sample, fly ash, rice husk ash and calcined rice husk ash. As expected metakaolin has 92% of reactive oxide indicating that the thermal treatment applied to the kaolin precursor was efficient (DAVIDOVITS, 1991c; HELLER-KALLAI, 2006). Also $SiO_2$ present in the rice husk ash and in the calcined rice husk are completely reactive.

However, a high difference between total $SiO_2$ and $Al_2O_3$ content and oxides was measured for the fly ash. According to Fernández-Jiménez; Palomo; Criado, (2005b), the alkaline dissolution of the aluminosilicates in the fly ash occurs simultaneously to a precipitation process of alkaline hydroxides, which is deposited on solid surface and inhibits the dissolution of the aluminosilicates. So, the precipitation of alkaline hydroxides could explain the amount of reactive oxides in the fly ash.

### 6.1.4 Mineralogical composition and phase quantification

Figure 16 shows the diffractograms of the precursor materials. The XRD metakaolin pattern showed a considerable amorphous hump from 16° to 32°. The crystalline phases of quartz ($SiO_2$-JCPDS-46-1045) is also identified in the sample. It is also observed signals of fluorite ($CaF_2$- JCPDS-35-0816) used as internal standard. The absence of the kaolinite phase shows that the heat treatment was effective for the obtention of metakaolin (HELLER-KALLAI, 2006). The phase quantification 96.5% of amorphous material and 3.5% of quartz.

The fly ash diffractogram shows an amorphous hump from 17° to 30°, and it is composed of quartz ($SiO_2$-JCPDS-46-1045) (13.1%), mullite ($Al_6Si_2O_{13}$-JCPDS-15-0776)

(6.4%) and 80.5% are the amount of amorphous oxides.

It is observed in the diffractograms of the rice husk ash and the calcined rice husk ash an amorphous hump in the range from 17° to 27° for the two precursor materials. Opaline (BAYLISS; MALES, 1965) and fluorite ($CaF_2$-JCPDS-35-0816, internal standard), are the crystalline phases identified in both materials. The amorphous phase corresponds to 76.9 % of the rice husk ash composition that also contain 23.1% opaline, and the amorphous phase amount in the calcined husk ash decreases to 73.1 % while the opaline phase increases to 26.9 %. Although the thermal treatment applied to rice husk ash has increased the crystallinity, it is known that the opaline silica phase is also reactive in alkaline alkaline medium (HILLIER; LUMSDON, 2008).

Figure 16 – Diffractograms of metakaolin, fly ash, rice husk ash and calcined rice husk ash.

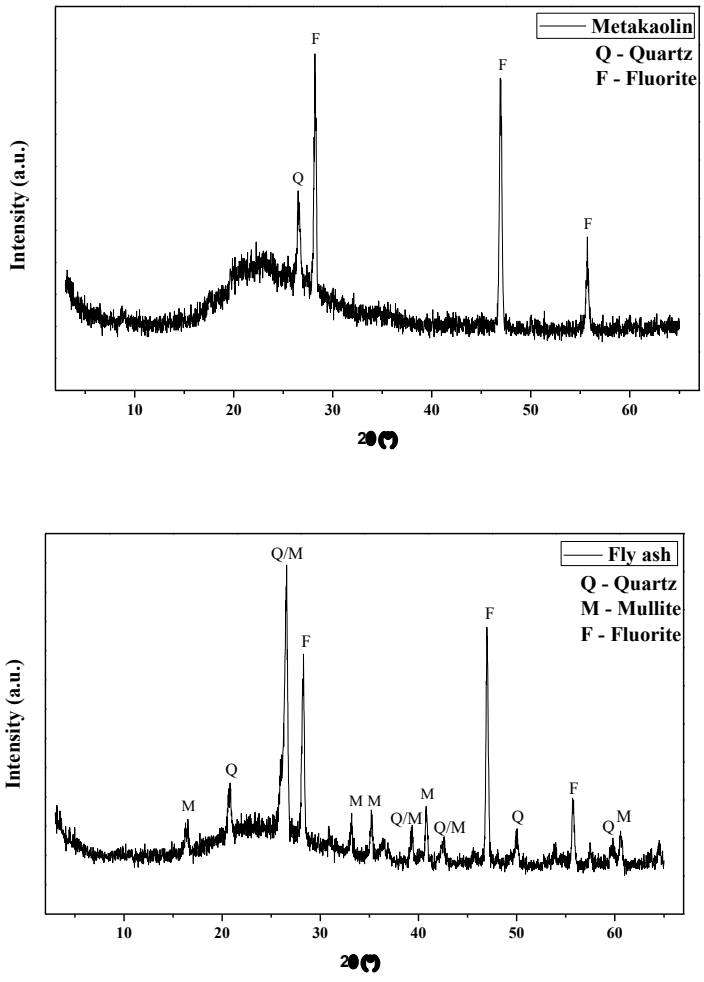

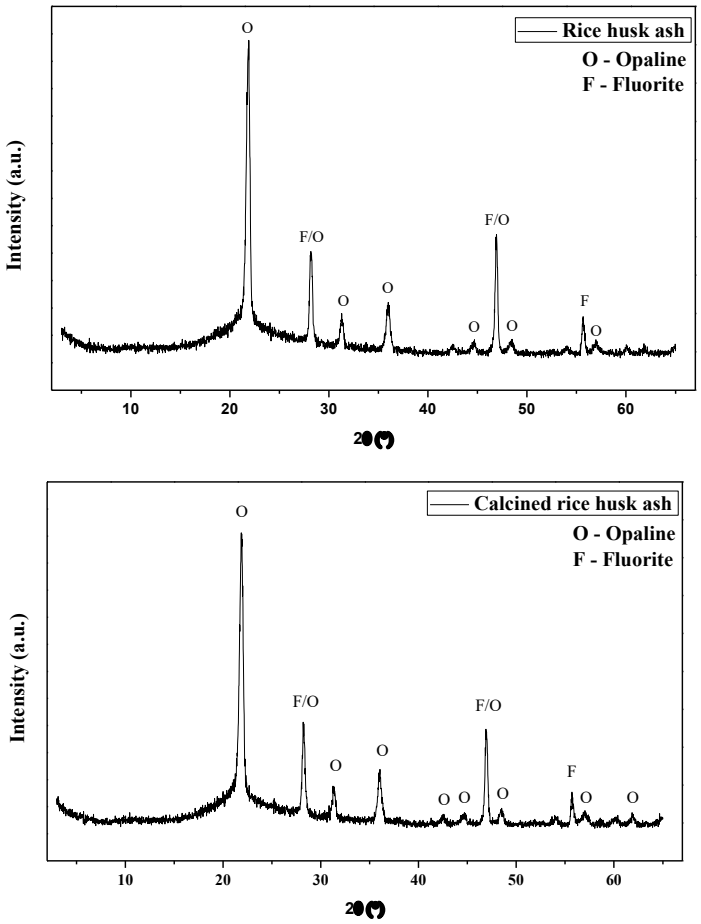


Source: Author's own elaboration.

### 6.1.5 Morphology

The morphology of the materials used in this study is shown in Figure 17. SEM images of metakaolin particles are composed of disorganized structures formed by the kaolinite dehydroxylation process (AUTEF *et al.*, 2013b). In the SEM image of fly ash it is possible to observe spherical particles of different sizes, while in the others materials some very rough and irregular particles may be observed. The expected honeycomb morphology can be seen in for the rice husk ash and calcined rice husk ash particles (ZOU; YANG, 2019). The difference between morphologies may contribute to the adsorption capacity of geopolymer, as in the case of rice husk ash, due to its relative surface area.

Figure 17 – Micrograph of precursor materials: metakaolin, fly ash, rice husk ash and calcined rice husk ash.

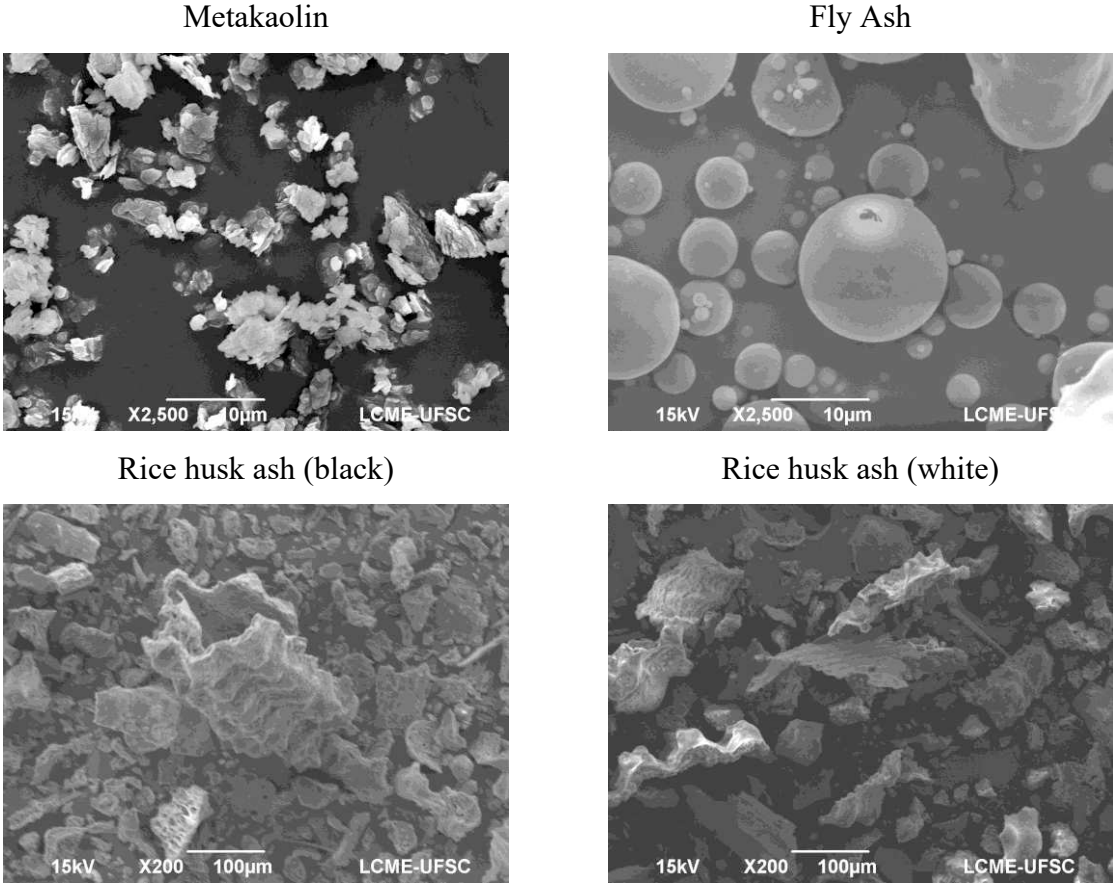


Source: Author's own elaboration.

## 6.2 CHARACTERIZATION OF GEOPOLYMERS

### 6.2.1 Mineralogical composition

New phases may have been formed in the prepared geopolymers under the thermal curing conditions (DAVIDOVITS, 1994), and with XRD analysis it is possible to observe the appearance of these phases.

Figure 18 shows the diffractograms of the MF-1 and MF-2 geopolymers. MF-1 and MF-2 present broad hump from 20° to 40° 2θ. Quartz ($SiO_2$-ICSD-027826) and mullite ($Al_{2.4}Si_{0.6}O_{4.8}$-ICSD-023867) are the phases identified in MF-1, being the same as the precursor materials. In MF-2 the phases identified are quartz ($SiO_2$-ICSD-027826), mullite ($Al_{2.4}Si_{0.6}O_{4.8}$-ICSD-023867) and sodalite ($Na_8(Al_6Si_6O_{24})(OH)_2(H_2O)_2$-ICSD-072059). Obtaining sodalite during the geopolymer synthesis process is related to three factors, reactive aluminosilicate materials, high sodium hydroxide concentration and thermal cure (DAVIDOVITS, 1994), and its presence would be advantageous for adsorptive properties (DING *et al.*, 2010; KHAJAVI; JANSEN; KAPTEIJN, 2009; KRÓL; MOZGAWA, 2019; NABAVI; MOHAMMADI; KAZEMIMOGHADAM, 2014).

Figure 18 – MF-1 and MF-2 diffractogram

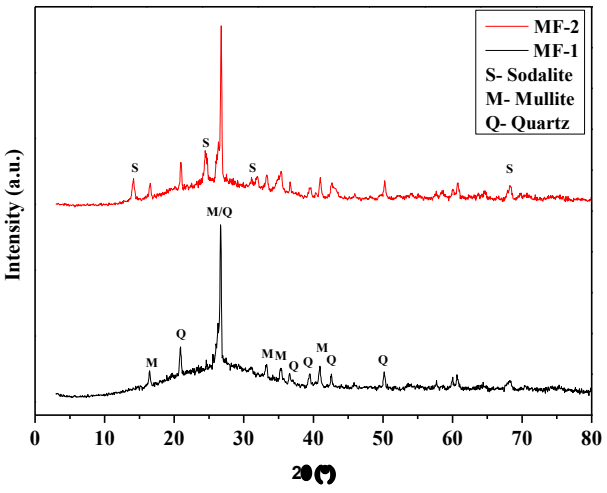


Source: Author's own elaboration.

Figure 19 shows the diffractograms of the MR-1, MR-2, MCR-1, MCR-2, MFR-1, MFR-2, MFCR-1 and MFCR-2 geopolymers. All geopolymers showed a broad hump from 20°

to 40°. The quartz ($SiO_2$- ICSD-027826), mullite ($Al_{2.4}Si_{0.6}O_{4.8}$-ICSD-023867) and opaline phases were identified.

Figure 19 – MR-1, MR-2, MCR-1, MCR-2, MFR-1, MFR-2, MFCR-1 and MFCR-2 diffractogram.

MR-1, MR-2, MCR-1, MCR-2

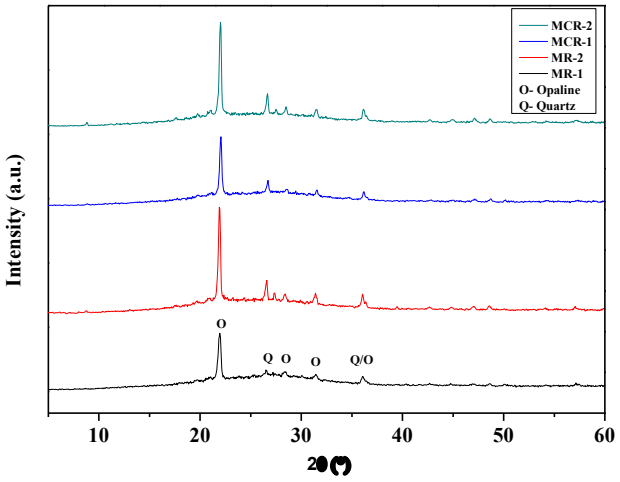


MFR-1, MFR-2, MFCR-1, MFCR-2

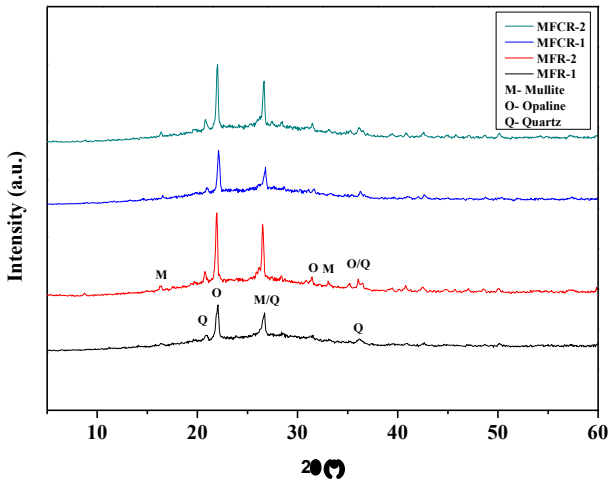


Source: Author's own elaboration.

The identification of the opaline phase after curing of the geopolymers, although reactive, suggests that the alkaline attack was not complete

The presence of broad hump from 20° to 40° in all geopolymer is characteristic of the formation of aluminosilicate gel, responsible for the characteristics of geopolymers as compressive strength. This phenomenon is most evident in the MF-1 and MF-2 geopolymers.

### 6.2.2 Morphology

The characterization by SEM is important to observed the homogeneity of the geopolymer, which changes due to unreacted particles of precursor materials, cracks and porosity (DUXSON *et al.*, 2005b), an important factor in the $CO_2$ capture process.

Figure 20 shows the SEM micrograph of geopolymers. A more homogeneous and denser structure is observed for sample MF-1 compared to MF-2. This fact is related to not using sodium silicate in the composition of MF-2, because, due to its high viscosity, a more compact microstructure is obtained (CRIADO; PALOMO; FERNANDEZ-JIMENEZ, 2005). In both samples a porous microstructure and partially attacked fly ash particles were observed. The presence of large cracks is noted in the MF-1 sample.

MR-1 shows a homogeneous part, given the formation of the gel. Several unreacted RHA particles, large cracks and pores are observed in their microstructure. In MR-2 small amounts of gel are observed, however, isolated. Most of it is a large cluster of partially reacted particles.

In the micrograph of the MCR-1 the gel formation is observed at different points, resulting in some homogeneous parts. Cracks, unreacted particles of RHAC and pores are observed. The MCR-2 has a microstructure similar to MR-2, with several agglomerated particles and a very small portion of gel.

As observed, in the samples MR-2 and MCR-2, the no addition of sodium silicate in the synthesis of the geopolymers, implies in a material with low gel production, in this way, the mechanical properties of the geopolymer are severely affected.

MFR-1 has a homogeneous and dense structure. Large cracks, partially reacted FA and RHA particles and pores are observed in its microstructure. MFR-2 has small amounts of gel, which does not result in a homogeneous material. However, a high agglomeration of partially reacted particles of the precursor materials is observed.

In the MFCR-1 gel formation is observed, however, they are not totally interconnected, thus, giving rise to a partially homogeneous structure. Small cracks, partially reacted precursor materials and pores of various sizes are observed. In the micrograph of MFCR-2 is noted a small amount of gel, however, most of the material is composed of agglomerated particles.

As already reported, the samples, MFR-2 and MFCR-2, which do not use silicate have a low gel content.

A high amount of precursor material that has not been fully reacted is observed in all

samples. Thus, could negatively affect the mechanical properties of the geopolymer. In general MF-1, MR-1 MCR-1, MFR-1, and MFCR-1 are more homogeneous with respect to MF-2, MR-2, MCR- 2, MFR-2, and MFCR-2. However, cracks are observed in all the microstructures of these samples, and although the samples have been sealed, these cracks may have been caused during the curing process, because with the evaporation of the water one has the contraction of the samples (HWANG; HUYNH, 2015a). As seen, samples MF-2, MR-2, MCR-2, MFR-2 and MFCR-2 showed little or no amount of gel in their matrix. The factor that may have caused this phenomenon is the non-use of sodium silicate, since it is a fast source of silica and favors the geopolymerization reaction (PACHECO-TORGAL; CASTRO-GOMES; JALALI, 2008b).

The presence of cracks on the MR-1 and MFR-1 sample could be related to low amount of water added, since water removal by evaporation is fast, and the mixture hardens quicker than in the other systems. The microstructure of the precursor materials may also have contributed to the occurrence of cracks.

Figure 20 – SEM images of geopolymers.

MF-1

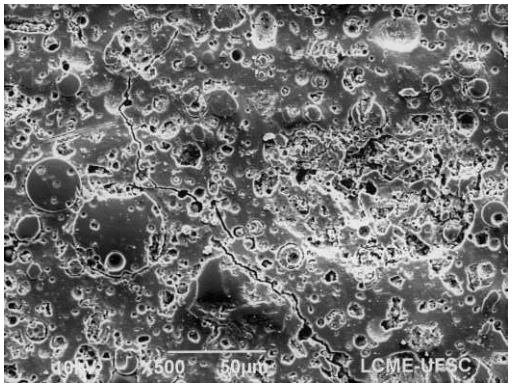


MF-2

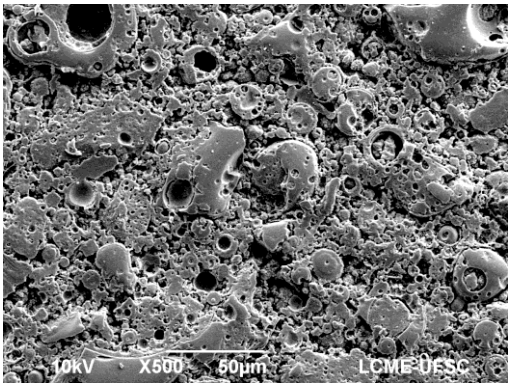


MR-1

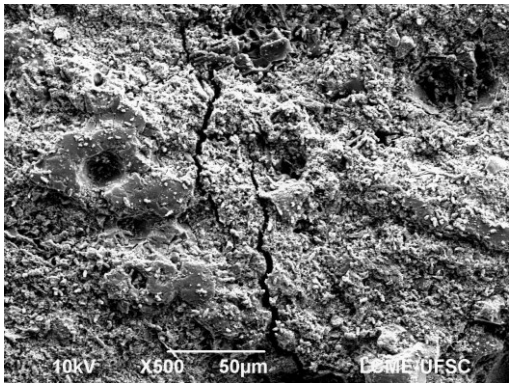


MR-2

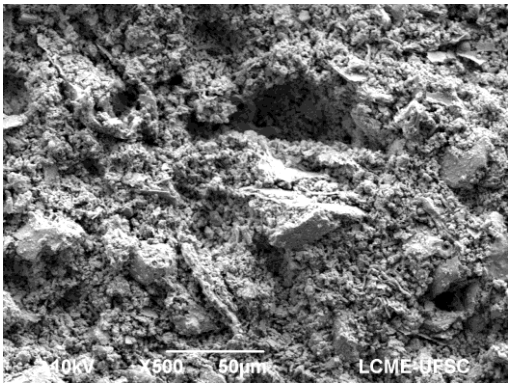

MCR-1 MCR-2

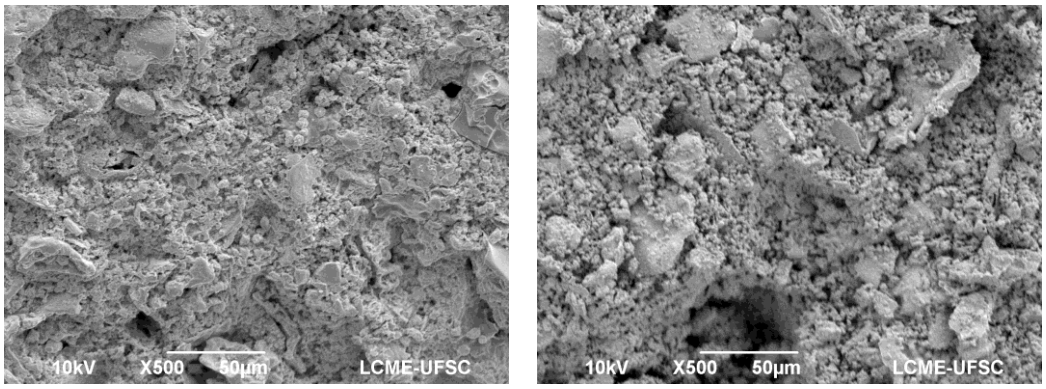


MFR-1 MFR-2

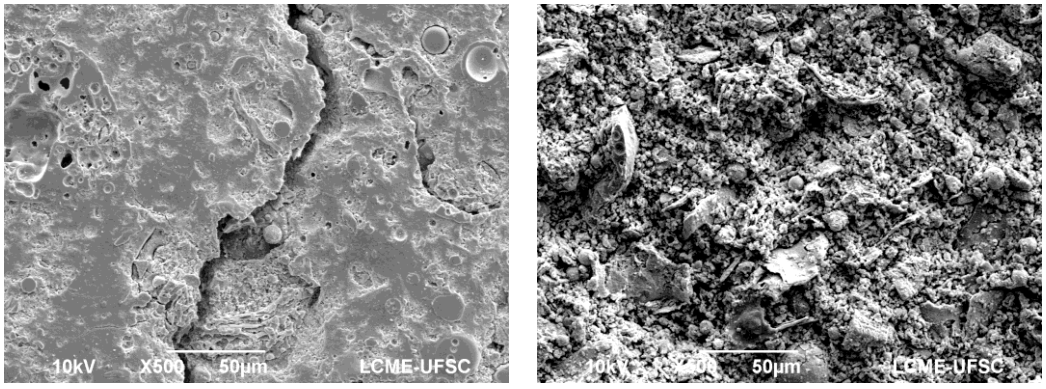


MFCR-1 MFCR-2

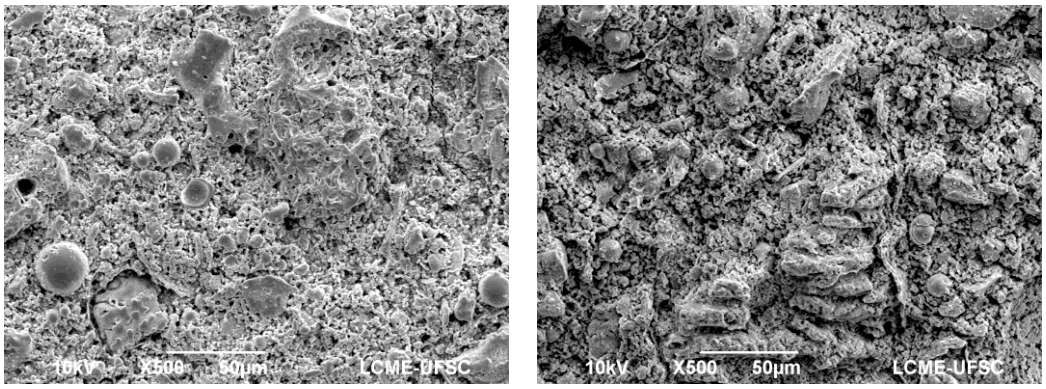


Source: Author's own elaboration.

### 6.2.3 Compressive strength

Compressive strength is an important factor to evaluate the viability of geopolymers to be used in $CO_2$ capture process, such as oil well cementation system or sealant of these wells. The compressive strength of the geopolymers depends on several factors such as: the difference in the degree of solubility between the precursor materials which affects the rate of dissolution and polycondensation; and the morphology and particle sizes of the reactant solids (metakaolin,

fly ash, rice husk ash and/or calcined rice husk ash) ) (DUXSON *et al.*, 2007b; KUSBIANTORO *et al.*, 2012b).

Figure 21 presents the compressive strength of MF-1 and MF-2. The MF-1 geopolymer exhibits a compressive strength of 16.5 MPa at 7 days of cure, however, at 28 days a decrease to 11 MPa is observed. This could be caused by the cure process used in this study, considering that when geopolymers containing metakaolin in its composition are submitted to a rapid aging, that is, high temperatures, tends to undergo a microstructural reorganization, leading to the formation of large pores that causes low compressive strength (LLOYD, 2009)

The MF-2 geopolymer showed no resistance to compression between the tests of 7 and 28 days of cure, obtaining a resistance of 7 MPa. However, it presented a lower resistance than MF-1 in the analyses of 7 and 28 d.

This difference in strength between MF-1 and MF-2 may be associated with the absence of sodium silicate in the synthesis of MF-2, because, due to its high viscosity, the silicate forms a geopolymer with a compacted microstructure, as seen in the SEM image for MF-1 which has a matrix denser than MF-2. Another factor related to this variation of resistance is the increase in the number of –Si—O—Si— bonds, which contribute to a better resistance, and the concentration of these bonds tends to increase when sodium silicate is used in the synthesis of the geopolymers (CRIADO; PALOMO; FERNANDEZ-JIMENEZ, 2005).

Figure 21 – Compressive strength with 7 and 28 d of cure. *Compressive strength of geopolymers after 7 days, developed for carbon dioxide storage, curing at 90 °C and 20.7 MPa

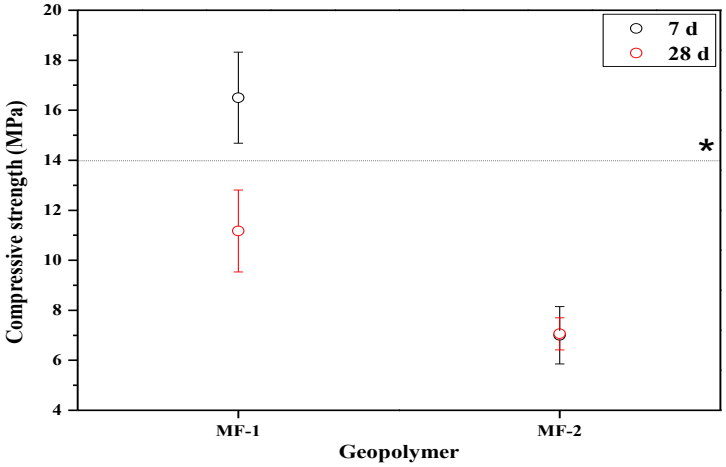


Source: Author's own elaboration.

Figure 22 shows the compressive strength of MR-1, MR-2, MCR- 1 and MCR-2.

The MR-1 shows a small variation of resistance between the performed tests, but within the error, where it exhibits a resistance of approximately 5.5 MPa. However, MR-2 dissolved in the submerged curing process, exhibiting no resistance.

MCR-1 showed a resistance of 2 MPa in the test performed at 7 days of cure and an increase was observed at 28 d of cure, exhibiting a resistance of 2.6 MPa. This gain may be associated with the dissolution of the reactive silica to the calcined rice husk ash and the sodium silicate, which will contribute to the increase of –Si—O—Si— bonds concentration and directly influence the resistance gain (HWANG; HUYNH, 2015a). The MCR-2 geopolymer dissolved in the submerged curing process, thus, not exhibiting resistance.

From the data obtained it can be concluded that the use of sodium silicate in the synthesis of the geopolymers is essential for obtaining geopolymers with resistance. Making it impossible to completely replace it with rice husk ash or calcined rice husk ash.

The resistance difference between MR-1 and MCR-1 may be associated with the carbonaceous materials that were removed in the calcination process, since both contain the same content of reactive silica.

Figure 22 – Compressive strength with 7 and 28 d of cure.

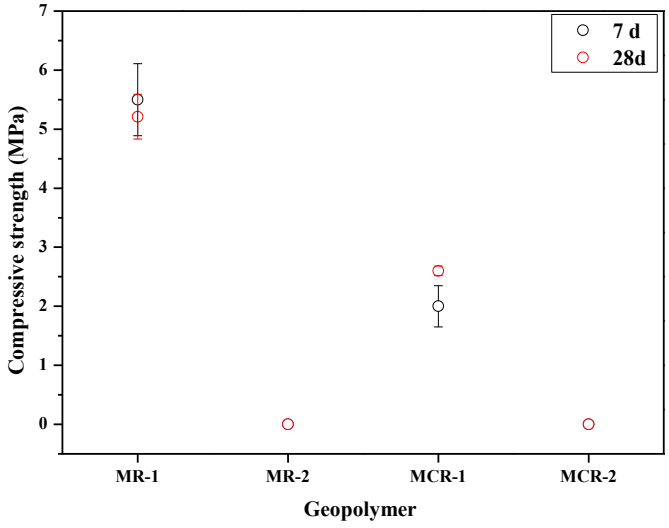


Source: Author's own elaboration.

The compressive strength of MFR-1, MFR-2, MFCR-1 and MFCR-2 is shown in Figure 23.

A resistance of 4.5 MPa is observed for the geopolymer MFR-1 at 7 d of cure, 28 d an increase to 5.3 MPa was observed. As already reported, a higher concentration of –Si—O—

Si— bonds during the curing period may lead to an increase in strength. The MFR-2 showed no resistance, disintegrating in the submerged curing process.

The MFCR-1 shows a resistance of 2.5 MPa at 7 d of cure and at 28 d presents a variation, however, contained within the error. It was not possible to evaluate the resistance of MFCR-2, since it decomposes in the submerged curing process.

Figure 23 – Compressive strength with 7 and 28 d of cure.

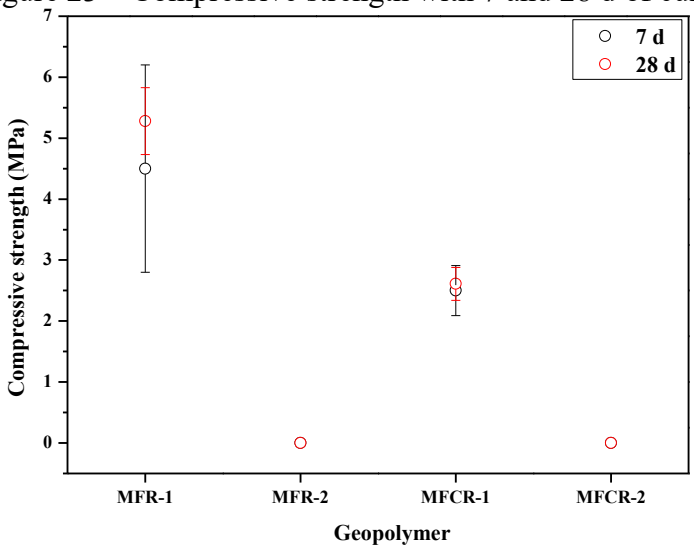


Source: Author's own elaboration.

The decomposition of the geopolymers (MR-2, MFR-2, MFCR-2, and MCR-2) during the submerged curing can be relate to the high content of rice husk ash and calcined rice husk ash used in the composition (He et al., 2013), since the incorporation of a high amount of rice husk ash results in lower resistance due to the uncomplete geopolymerization process. Also, the absence of sodium silicate in the formulation of those samples difficult the geopolymerization reactions. Beside this, the compressive strength and the decomposition of the geopolymers depends on the formation of –Si—O—Si— bonds, and the number of Si-O-Si bonds increases when the sodium silicate is used in the synthesis of the geopolymer (CRIADO; PALOMO; FERNANDEZ-JIMENEZ, 2005).

It should be noticed that the compressive strengths obtained in this study are lesser than the reference value suggested by Barlet-Gouedard et al.,2010 to application of functional geopolymers as well sealant and simultaneous $CO_2$ sorbent. In fact, the compressive strength is lower than several others studies to application of geopolymer as construction and building

material (HWANG; HUYNH, 2015b; ROWLES; O'CONNOR, 2003; STURM *et al.*, 2016a; YOUSEFI ODERJI; CHEN; JAFFAR, 2017), since all the geopolymers produced in this study are porous enabling its application in adsorptive process.

It can be observed that the compressive strength correlates with bulk density since geopolymers have similar bulk density values.

The MF-1 showed high compressive strength (>14 MPa) after 7 days cure enabling its application in carbon dioxide storage processes (BARLET-GOUEDARD; ZUSATZ-AYACHE; PORCHERIE, 2010). However, after 28 d cure, it was observed a decrease of its compressive strength.

The formation of zeolitic phase, as observed in MF-2, could also be explored in the geopolymer synthesis. Sodalite is a type of zeolite, has an octahedral structure and has very small pore sizes, around 2.4 Å, enabling its use in membranes for $H_2/CH_4$ separation processes and water selectivity (DING *et al.*, 2010; KHAJAVI; JANSEN; KAPTEIJN, 2009; KRÓL; MOZGAWA, 2019; NABAVI; MOHAMMADI; KAZEMIMOGHADAM, 2014).

### 6.2.4 Water absorption and bulk density

Water absorption and bulk density are relevant factors to determine the applicability of geopolymers, as it influences the durability of the material. Several factors such as precursor material morphology, porosity, cracks and unreacted material are related to water absorption and bulk density of the geopolymer.

In Table 7 is presented the water absorption of geopolymer MF- 1, MF-2, MR-1, MCR-1, MFR-1 and MFCR-1, and the compressive strength obtained at 28 days. It was not possible to perform analyzes for the MR-2, MCR-2, MFR-2 and MFCR-2 geopolymers due to dissolution in submerged cure.

It is noted an inverse behavior between the water absorption a decrease in resistance, since while the compressive strength follows the order:

MF-1 > MF-2 > MFR-1 ~ MR-1 > MFCR-1 ~ MCR-1

the water absorption follows the opposite order:

MF-1 < MF-2 < MFR-1 < MFR-1 ~ MR-1 < MFCR-1 < MCR-1

Table 7 – Water absorption and compressive strength

| | Geopolymers | | | | | |
|---|---|---|---|---|---|---|
| | **MF-1** | **MF-2** | **MFR-1** | **MFCR-1** | **MR-1** | **MCR-1** |
| **Water absorption (%)** | 36.56 | 39.80 | 45.30 | 53.23 | 54.44 | 62.37 |
| **Compressive strength (MPa)** | 11 | 7 | 5.3 | 2.5 | 5.5 | 2.6 |

Source: Author's own elaboration.

These results partially agree with the order of bulk density shown in Table 8, being the MCR-1 the lowest compressive strength resistant, the highest water absorbent and lowest dense geopolymer. So, it is expected that MCR-1 is the best $CO_2$ adsorbent, as it will be discussed in the following sections.

Table 8 – Bulk density of geopolymers

| | Geopolymers | | | | | |
|---|---|---|---|---|---|---|
| | **MF-1** | **MF-2** | **MFR-1** | **MFCR-1** | **MR-1** | **MCR-1** |
| **Bulk density ($g/cm^3$)** | 1.69 | 1.68 | 1.74 | 1.83 | 1.79 | 1.63 |

Source: Author's own elaboration.

### 6.2.5 Electrical conductivity and sodium and silicon leaching

The electrical conductivity technique can qualitatively evaluate the leaching of chemical elements to the medium during the submerged curing process. Figure 24 and Table 9 shows the electrical conductivity of all geopolymers.

Figure 24 – Electrical conductivity during the submerged curing process

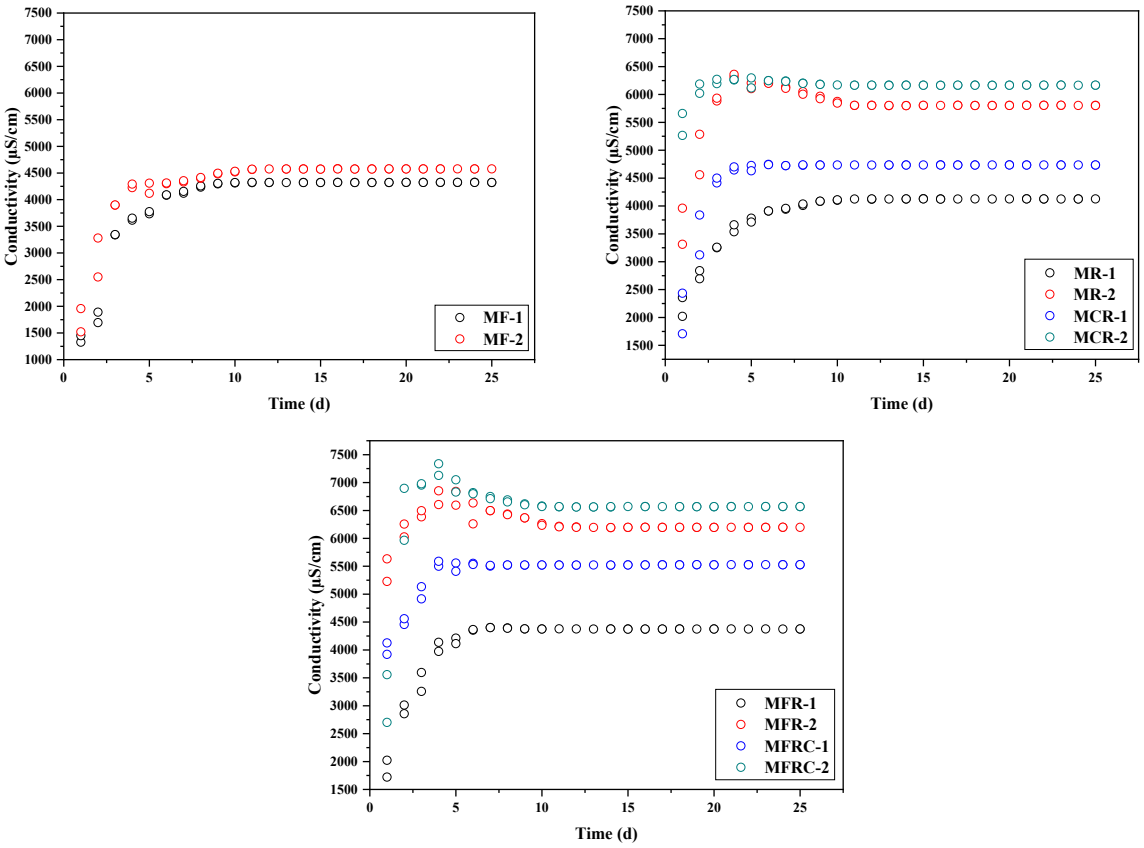


Source: Author's own elaboration.

Table 9 – Electrical conductivity during the submerged curing process

| Geopolymer | Electrical conductivity after 28 d (µS/cm) | Na ions leached after 7 days (% w/w) | Si ions leached after 7 days (% w/w) |
|---|---|---|---|
| **MF-1** | 4357 | 25 | 6 |
| **MF-2** | 4566 | 25 | 9 |
| **MR-1** | 4101 | 4 | 10 |
| **MR-2** | 5104 | 33 | 21 |
| **MCR-1** | 4759 | 51 | 14 |
| **MCR-2** | 6184 | 77 | 21 |
| **MFR-1** | 4101 | 31 | 11 |
| **MFR-2** | 6296 | 96 | 20 |
| **MFCR-1** | 4759 | 37 | 15 |
| **MFCR-2** | 6676 | 23 | 17 |

Source: Author's own elaboration.

Geopolymers that dissolve in the submerged curing process (MR- 2, MFR-2, MFCR- 2, and MCR-2) have the highest values of conductivity and high sodium and silica leaching, due to the low geopolymerization degree. However, the geopolymers that maintained the physical structure showed the following conductivity order:

MR-1 ~ MFR-1 < MF-1 < MF-2 < MFCR-1 ~ MCR-1

Na ions leaching order:

MR-1 < MF-1 ~MF-2 < MFR-1 < MFCR-1 < MCR-1

and Si ions leaching order:

MF-1 < MF-2 < MFR-1 ~ MR-1 < MFCR-1 ~MCR-1

So, it is possible to conclude that the silicon ions leaching is directly related to the geopolymerization degree, once the compressive strength order is exactly the same MF-1 > MF-2 > MFR-1 ~ MR-1 > MFCR-1 ~ MCR-1.

### 6.2.6 Surface area and porosity

The characterization by BET allows to study the microstructural characteristics of geopolymers as surface area, total pore volume and average pore size (Table 10).

The $N_2$ adsorption-desorption isotherms are shown in Figure 25. The MF-1, MF-2, MR-1, MCR-1, MFR-1 and MFCR-1 geopolymers exhibit type II isotherms according to classification from IUPAC (THOMMES *et al.*, 2015). In MR-1 it can be seen a small volume of gas adsorbed at low pressures, which corresponds to the fill region of the micropores, and it can contribute to its largest BET surface area (Table 10). The surface area ($S_{BET}$) of the MF-1, MF-2, MCR-1 and MFCR-1 geopolymers showed similar values, while MR-1 and MFR-1 presented higher values of surface area, and these results could be related to the presence of unreacted rice husk ash particles in MR-1 and MFR-1 as can be observed in SEM images (ZOU; YANG, 2019).

All geopolymers showed very low pore volume. The MF-2, MCR-1 MFCR-1 and MR- 1 geopolymers showed no significant differences in total pore volume (Vp), with MFR-1 and MF-1 having the highest values, 0.060 and 0.048 $cm^3/g$. In accordance, the average pore size of all materials are quite similar.

The average pore size difference between geopolymers is due to the monomeric units formed during the geopolymerization reaction, being Polysialate-PS (Si-O-Al-O), Polysialatesiloxo-PSS (Si-O-Al-O-Si-O) and Polysialatedisiloxo-PSDS (Si-O-Al-O-Si-O-Si-O) (CIOFFI; MAFFUCCI; SANTORO, 2003). According to the results shown in Table 7, it is possible to assume that the monomeric units are similar.

Table 10 – Surface area, total pore volume and average pore size of geopolymers

| Geopolymer | $S_{BET}$ ($m^2/g$) | Vp ($cm^3/g$) | Ps (nm) |
|---|---|---|---|
| **MF-1** | 10.3 | 0.048 | 2.09 |
| **MF-2** | 11.8 | 0.036 | 2.06 |
| **MR-1** | 20.9 | 0.042 | 2.08 |
| **MCR-1** | 8.4 | 0.036 | 2.08 |
| **MFR-1** | 17.4 | 0.060 | 2.09 |
| **MFCR-1** | 8.8 | 0.036 | 1.64 |

Source: Author's own elaboration.

Table 11 is a compiled of the main geopolymers results after the curing time has elapsed.

Figure 25 – $N_2$ adsorption-desorption isotherms for the prepared geopolymers at 77 K

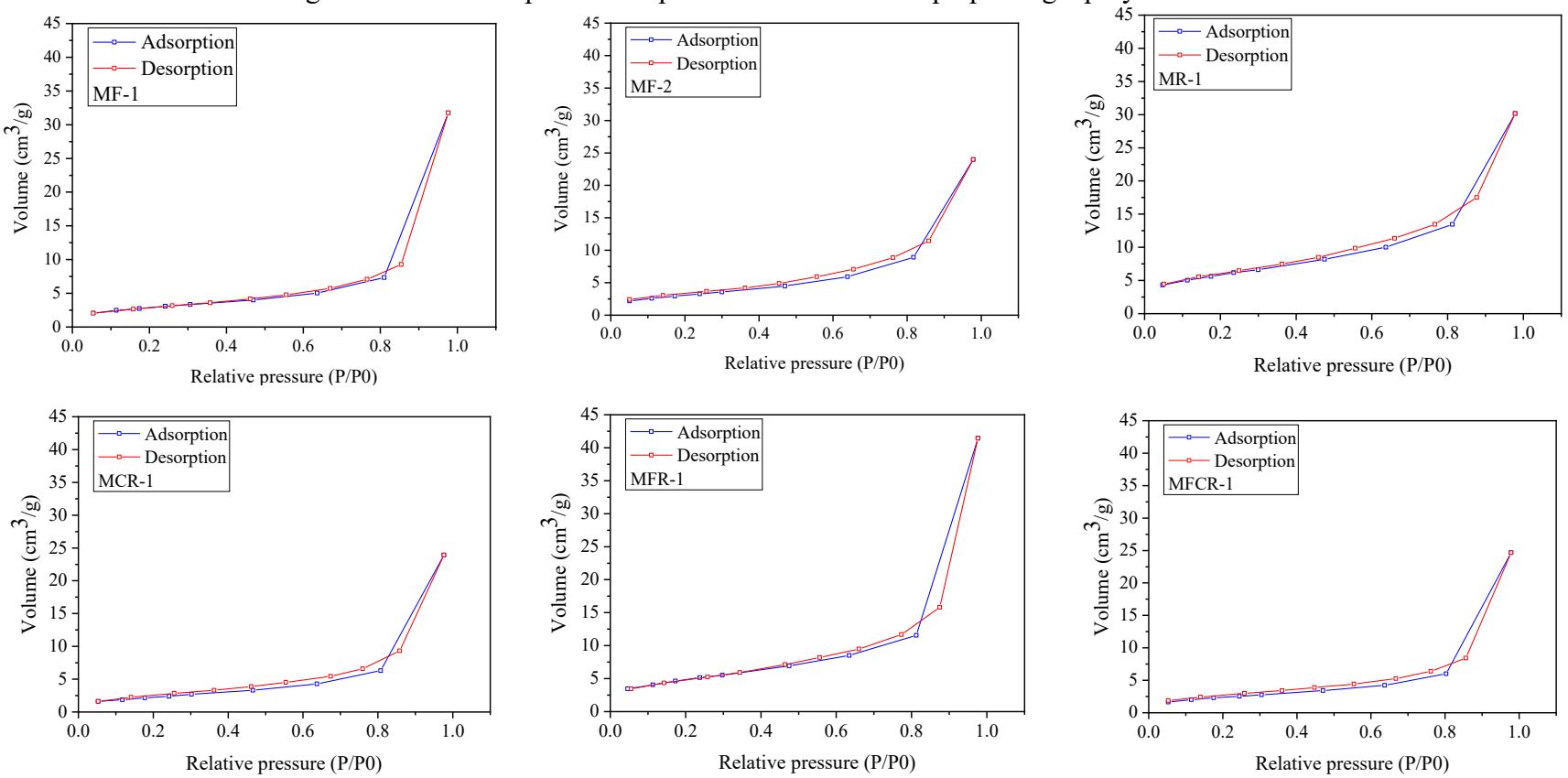


Source: Author's own elaboration.

Table 11 – Compiled from geopolymers results.

| | Geopolymer | | | | | | | | | |
|---|---|---|---|---|---|---|---|---|---|---|
| | **MF-1** | **MF-2** | **MR-1** | **MR-2** | **MCR-1** | **MCR-2** | **MFR-1** | **MFR-2** | **MFCR-1** | **MFCR-2** |
| **Compressive strength (Mpa)** | 11 | 7 | 5.5 | - | 2.6 | - | 5.3 | - | 2.5 | - |
| **Water absorption (%)** | 36.56 | 39.80 | 54.44 | - | 62.37 | - | 45.30 | - | 53.23 | - |
| **Bulk density (g/cm3)** | 1.69 | 1.68 | 1.79 | - | 1.63 | - | 1.74 | - | 1.83 | - |
| **Electrical conductivity (µS/cm)** | 4357 | 4566 | 4101 | 5104 | 4759 | 6184 | 4101 | 6296 | 4759 | 6676 |
| **Na ions leached - 7d (% w/w)** | 25 | 25 | 4 | 33 | 51 | 77 | 31 | 96 | 37 | 23 |
| **Si ions leached - 7d (% w/w)** | 6 | 9 | 10 | 21 | 14 | 21 | 11 | 20 | 15 | 17 |
| **$S_{BET}$ (m2/g)** | 10.3 | 11.8 | 20.9 | - | 8.4 | - | 17.4 | - | 8.8 | - |
| **$V_p$ (cm3/g)** | 0.048 | 0.036 | 0.042 | - | 0.036 | - | 0.060 | - | 0.036 | - |
| **$P_s$ (nm)** | 2.09 | 2.06 | 2.08 | - | 2.08 | - | 2.09 | - | 1.64 | - |

Source: Author's own elaboration.

# 7 GEOPOLYMER APPLICATION

## 7.1 $CO_2$ ADSORPTION AND DESORPTION

This stage of the study will present the data obtained from the $CO_2$ adsorption process for the precursor materials and the compressive strength geopolymers. The desorption process was evaluated only for the geopolymers. As it presented a good fit to the experimental data, the pseudo-first order kinetic model was used to obtain the kinetic parameters.

### 7.1.1 Adsorption of $CO_2$ on the precursor materials

Figure 26 shows the $CO_2$ capture process of metakaolin, fly ash, rice husk ash and calcined rice husk ash, at 35 °C. The metakaolin showed a noticeable instability at the end of the process, probably related to its physicochemical properties, and it would deserve special investigation since this oscillating behaviour was confirmed in triplicate measurements. The amount of $CO_2$ adsorbed increases regularly at about 50 minutes and achieve the value ~ 0.33 mmol/g, but saturation equilibrium is not achieved even after 240 min. The same behavior was observed in the adsorption of $CO_2$ on rice husk ash (black) and calcined rice husk ash (white) (Figure 26), while a less irregular adsorption behavior was measured on fly ash

.

Figure 26 – $CO_2$ adsorption on the precursor materials at 35 °C and pressure of 1 bar.

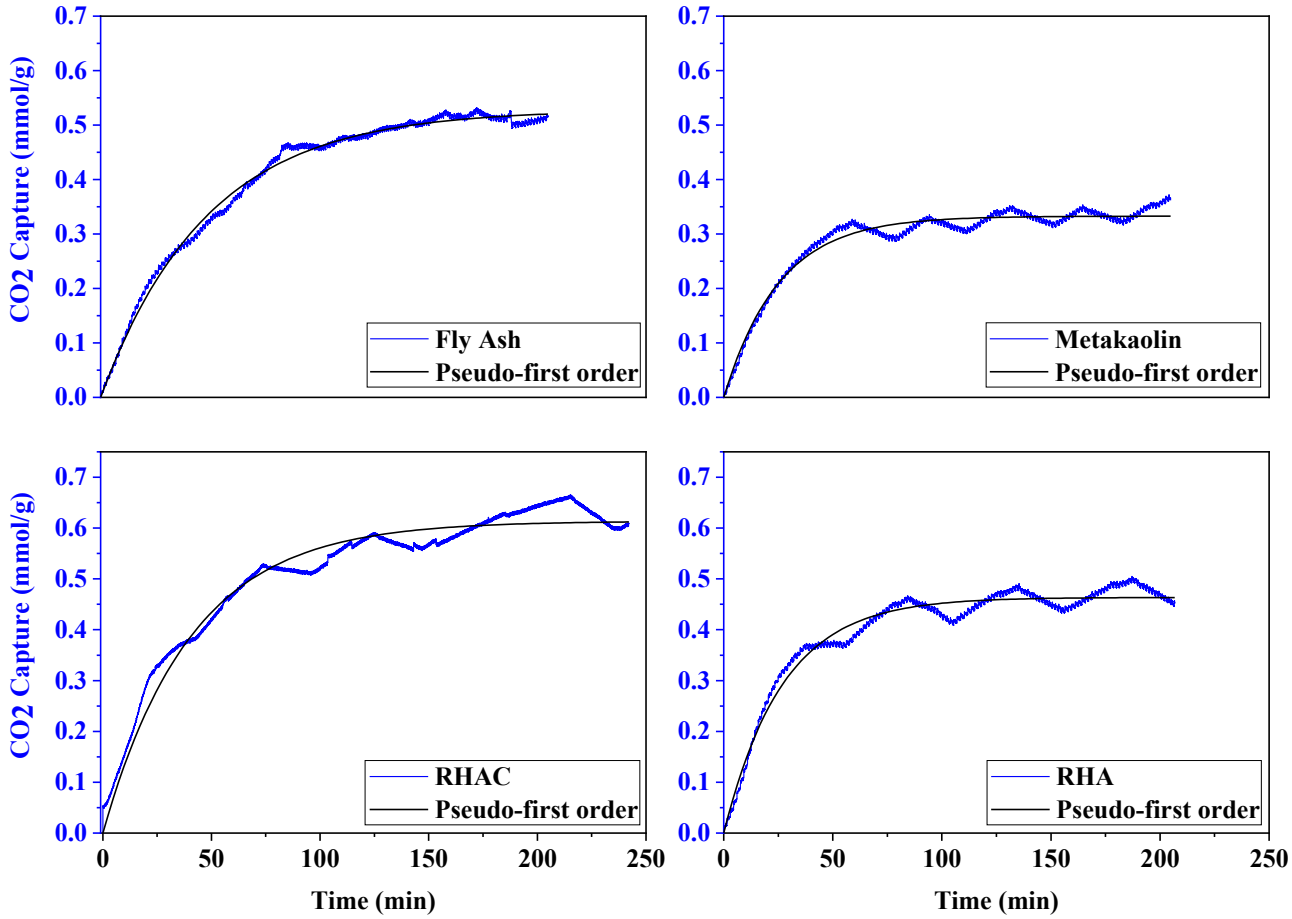


Source: Author's own elaboration.

Table 12 summarizes the kinetic parameters obtained by the fitting of the pseudo-first order model to the adsorption data.

Table 12 – Kinect parameters of the pseudo-first order model.

| | $q_e$ (mmol/g) | k ($min^{-1}$) | $R^2$ |
|---|---|---|---|
| **Metakaolin** | 0.33 ± 1.56E-4 | 0.040 ± 9.60E-5 | 0.97 |
| **Rice husk ash** | 0.46 ± 2.30E-4 | 0.037 ± 9.11E-5 | 0.97 |
| **Calcined rice husk ash** | 0.61 ± 3.40E-4 | 0.024 ± 5.73E-5 | 0.97 |
| **Fly Ash** | 0.53 ± 2.10E-4 | 0.020 ± 2.66E-5 | 0.99 |

Source: Author's own elaboration.

As seen, the materials that presented the highest adsorption capacities were F and CR. The morphology and specific area of the particles are the main factors re0sponsible for this capacity, and as already seen, fly ash is composed of spheres and several have holes, leaving a hollow sphere, thus assigning large areas, while CR also has a high specific area (CHEN *et al.*, 2018; ZOU; YANG, 2019).

Considering the mass proportion of each precursor material in the geopolymer formulations, the expected value considering the weighted average value to each geopolymer is shown in Figure 27. So, if different $CO_2$ adsorption capacity for the geopolymers produced in this study is obtained, it is due to the geopolymerization reaction. Equation 10 was used, where $PM_i$ is the amount used of each precursor material and $X_{CO2i}$ is the adsorption capacity of each precursor material.

$$Q_{CO_2\,PM} = \frac{\sum PM_i \times X_{CO_2 i}}{\sum PM_i} \tag{10}$$

Figure 27 – Weighted average value for the adsorption capacity expected for each geopolymer

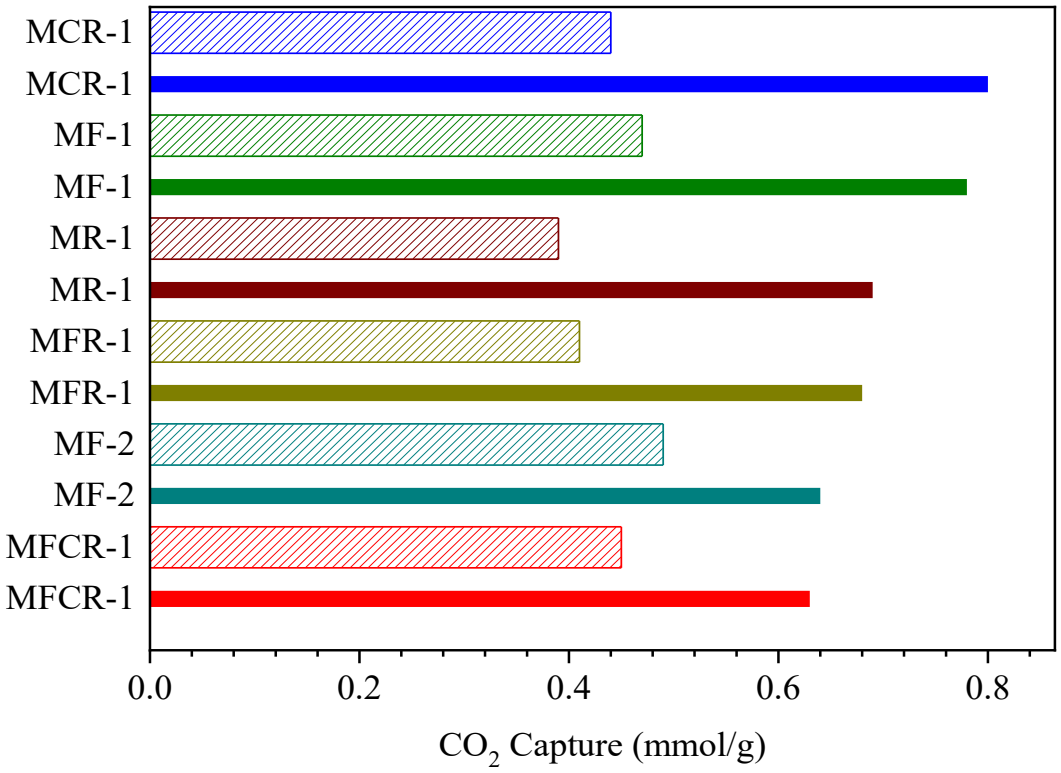


Source: Author's own elaboration.

### 7.1.2 Adsorption of $CO_2$ on the geopolymers

The adsorption capacities of adsorbent materials depends on various factors such as volume, pore size and the connectivity between pores, surface area and material density, since the higher the density the lower the porosity (NASCIMENTO *et al.*, 2014). As the geopolymers produced in this study are very similar in physico-chemical character, it is not expected significant $CO_2$ adsorptive/desorptive characteristics.

As shown in Figure 28, the $CO_2$ adsorption achieves the saturation equilibrium at about 2 h at 35 °C and 1 bar pressure, and differently from the precursor materials, the adsorption curve is smooth and monotonically increasing, according to a pseudo-first order kinetic model (Table 13).

Figure 28 – Adsorption of $CO_2$ on different geopolymers at 35 °C and pressure of 1 bar.

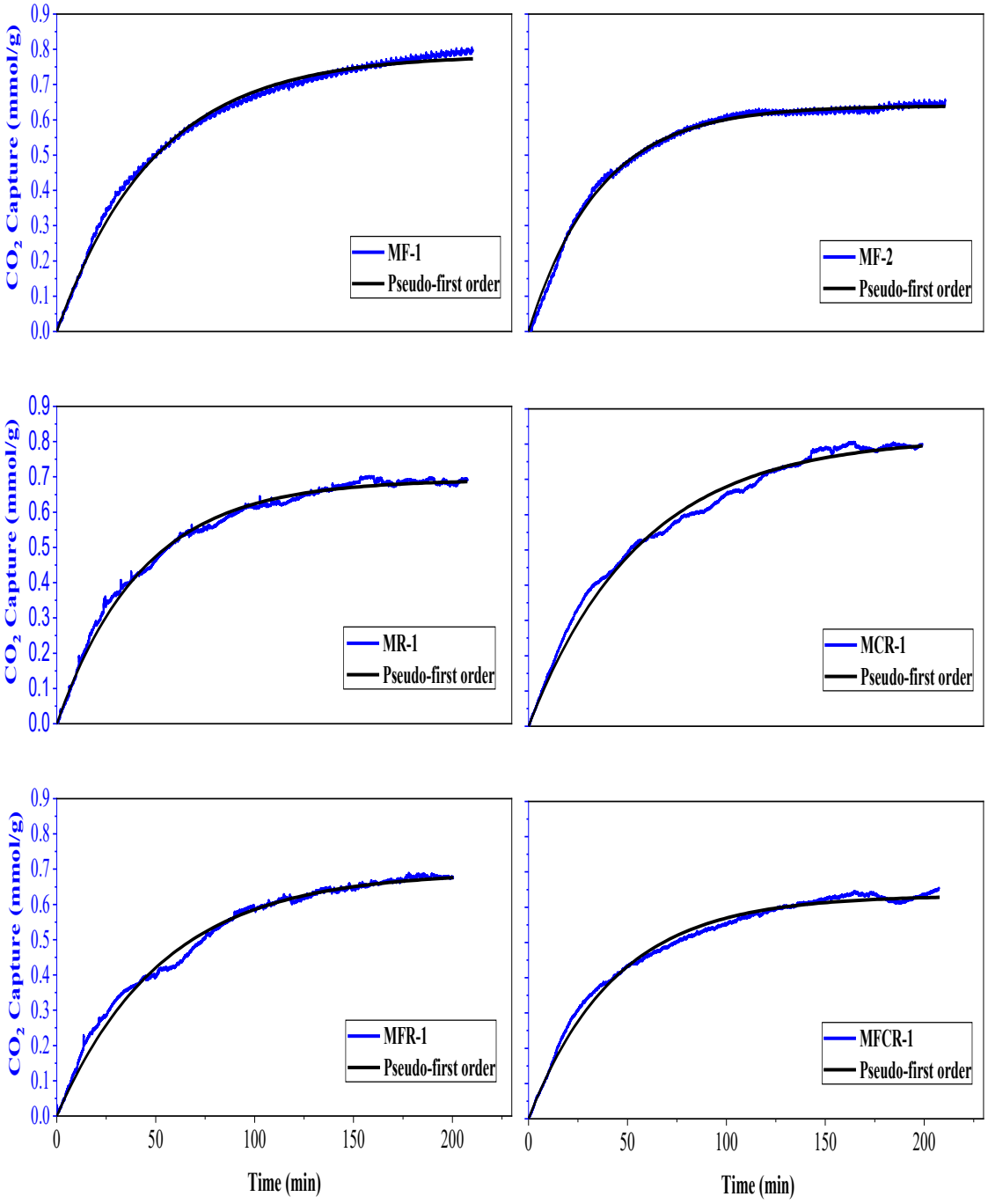


Source: Author's own elaboration.

The pseudo-first order kinetic constants are quite similar, although the adsorptive capacity depends on the raw materials or alkaline activator (Table 12).

Table 13 – Weighted average value for the adsorption capacity expected for each geopolymer.

| Geopolymers | $q_e$ (mmol/g) | k ($min^{-1}$) | $R^2$ |
|---|---|---|---|
| **MF-1** | 0.78 ± 2.50E-4 | 0.020 ± 2.14E-5 | 0.99 |
| **MF-2** | 0.64 ± 1.36E-4 | 0.028 ± 2.49E-5 | 0.99 |
| **MR-1** | 0.69 ± 2.35E-4 | 0.023 ± 2.86E-5 | 0.99 |
| **MCR-1** | 0.82 ± 5.13E-4 | 0.018 ± 3.24E-5 | 0.99 |
| **MFR-1** | 0.69 ± 4.00E-4 | 0.019 ± 3.30E-5 | 0.99 |
| **MFCR-1** | 0.63 ± 2.54E-4 | 0.023 ± 3.33E-5 | 0.99 |

Source: Author's own elaboration.

No evident relationship between the BET surface area and adsorptive capacity was observed. Even the formation of a zeolitic phase, sodalite, in MF-2 did not increase the $CO_2$ adsorption capacity.

Some authors have observed that there is a relationship between the $CO_2$ adsorption capacity and concentration of basic sites on the geopolymer surface, since carbon dioxide is acidic and a higher concentration of accessible basic sites increase the adsorbed amount (EMDADI *et al.*, 2017; MALEKI *et al.*, 2018; NOVAIS *et al.*, 2016).

MCR-1, the best $CO_2$ adsorbent, probably has the lowest sodium content, since it presented the highest sodium leaching during the cure. It should be noted that the $CO_2$ adsorption capacity of the geopolymers followed the same order that measured for their precursors (calcinated rice husk ash > fly ash > rice husk ash) (Table 11), indicating that the nature of the solid residue determine the $CO_2$ adsorption capacity.

### 7.1.3 Desorption of $CO_2$ on the geopolymers

The adsorptive process is reversible, as shown by the desorption curves (Figure 29), and the desorption pseudo-first order constant are similar than for the adsorptive process (Table 14). The $CO_2$ is almost completely recovered by desorption under $N_2$ atmosphere and the time required to complete desorption is almost the same utilized by the adsorptive process (Figure 28 and Table 13).

Figure 29 – $CO_2$ desorption at 35 °C and pressure 1 of bar.

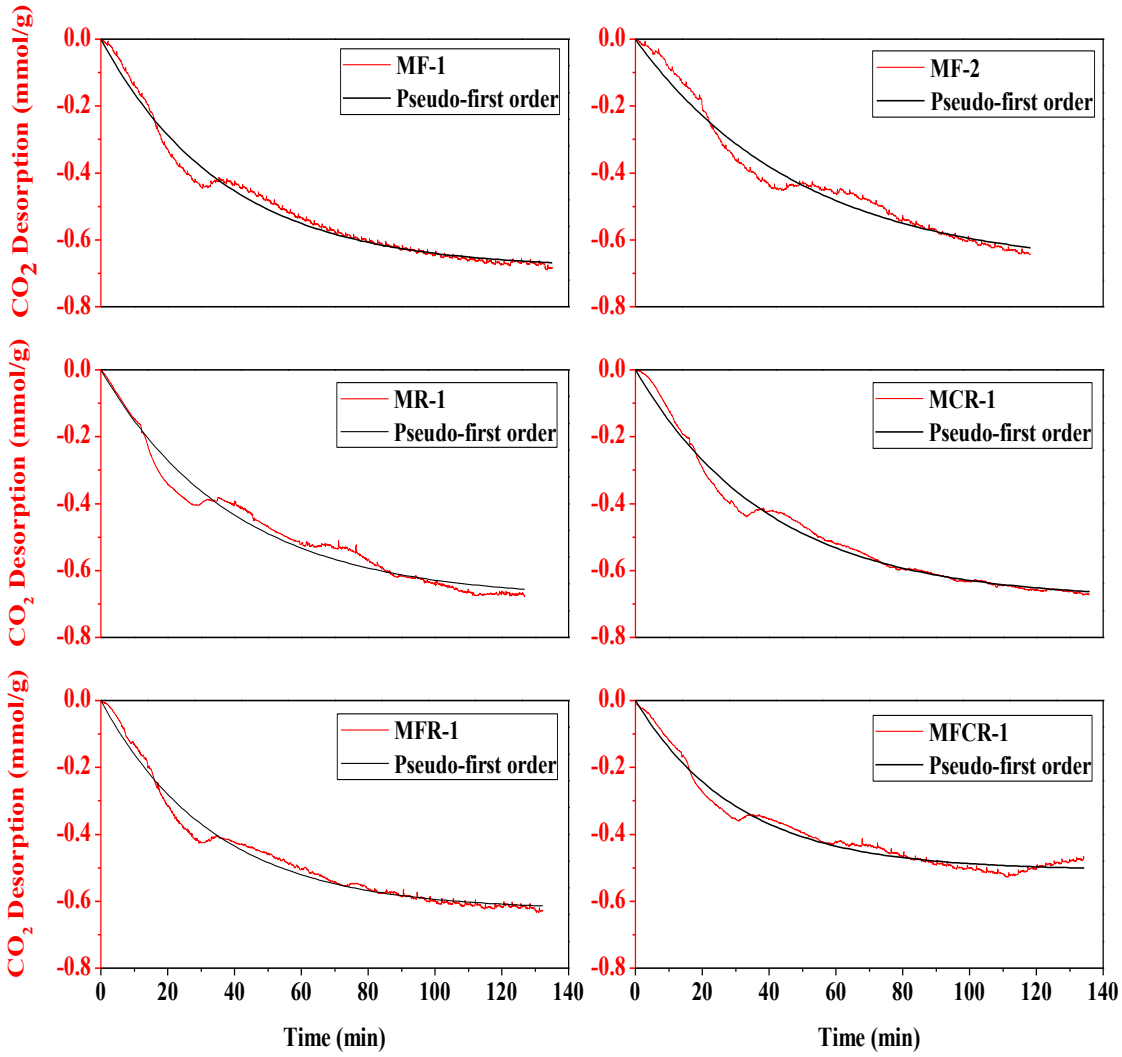


Source: Author's own elaboration.

Table 14 – Pseudo-first order kinetic parameters for the $CO_2$ desorption at 35 °C and pressure 1 bar (under $N_2$ atmosphere).

| Geopolymers | $q_e$ (mmol/g) | k ($min^{-1}$) | $R^2$ |
|---|---|---|---|
| **MF-1** | 0.68 ± 6.35E-4 | 0.027 ± 7.53E-5 | 0.98 |
| **MF-2** | 0.68 ± 1.05E-2 | 0.024 ± 9.21E-5 | 0.97 |
| **MR-1** | 0.68 ± 1.02E-2 | 0.025 ± 1.02E-4 | 0.97 |
| **MCR-1** | 0.69 ± 6.36E-4 | 0.025 ± 6.60E-5 | 0.99 |
| **MFR-1** | 0.63 ± 5.60E-4 | 0.030 ± 8.40E-5 | 0.98 |
| **MFCR-1** | 0.51 ± 4.40E-4 | 0.032 ± 9.55E-5 | 0.98 |

Source: Author's own elaboration.

### 7.1.4 Comparison of $CO_2$ adsorptive capacity of different geopolymers and others aluminosilicate adsorbents

The adsorption capacity is similar for all geopolymers evaluated confirming that the microstructural characteristics of geopolymers, such as surface area, pore volume and pore size, do not contribute to the adsorption capacity. Table 15 summarizes the adsorptive capacity of the geopolymers produced in this dissertation and some other aluminosilicate adsorbents, using the same experimental conditions.

Table 15 – Comparison of the adsorptive capacity of geopolymers developed in this study and other adsorbent materials.

| Adsorbent | $CO_2$ adsorption (mmol/g) 35 °C 1 bar | Precursor material | Reference |
|---|---|---|---|
| **MCR-1** | 0.80 | Metakaolin/calcined rice husk ash | This study |
| **MF-1** | 0.78 | Metakaolin/fly ash | This study |
| **MR-1** | 0.69 | Metakaolin/rice husk ash | This study |
| **MFR-1** | 0.68 | Metakaolin/fly ash/ rice husk ash | This study |
| **MF-2** | 0.64 | Metakaolin/fly ash | This study |
| **MFCR-1** | 0.63 | Metakaolin/fly ash/calcined rice husk ash | This study |
| **G10** | 0.62 | Metakaolin | Minelli *et al.*, 2016b |
| **G13** | 0.58 | Metakaolin | |
| **G23** | 0.57 | Metakaolin | |
| **MOF - MIL-101** | 0.65 | Cr(NO3)3.9H20/terephthalic acid/ natrium acetium | Zhang *et al.*, 2015 |
| **ZIF** | 0.59 | Zeolitic imidazolate framework (ZIF-8Sigma-Aldrich) | Huang *et al.*, 2011 |

Source: Author's own elaboration.

Calcinated rice husk ash (white) activated by NaOH and sodium silicate is the material precursor most suitable to produce a $CO_2$ geopolymer adsorbent, and its $CO_2$ capacity is 22.5% higher than the best geopolymeric adsorbent reported in the literature up to now (MINELLI *et al.*, 2016a), and 100% higher than the $CO_2$ which would be adsorbed by the weighted average value of adsorptive capacity of the raw materials

### 7.1.5 Economic analyze

Table 16 is showed the economic analysis for geopolymers and precursor materials. Geopolymers have a lower cost compared to precursor materials. This is due to the use of waste such as fly ash and rice husk ash to replace commercial products such as metakaolin and sodium silicate, thereby making the geopolymer manufacturing process cheaper. In addition, the incorporation of these materials benefited the $CO_2$ capture process.

Table 16 – Economic analysis of geopolymers and precursor materials.

| **Geopolymer** | | | | | | |
|---|---|---|---|---|---|---|
| | **MF-1** | **MF-2** | **MR-1** | **MCR-1** | **MFR-1** | **MFCR-1** |
| **Cost of geopolymer (U$D[A]/100g)** | 0.44 | 0.37 | 0.46 | 1.01 | 0.45 | 1.00 |
| **$CO_2$ Capture (mmol/100g)** | 78.0 | 64.0 | 69.0 | 82.0 | 69.0 | 63.0 |

| **Precursor materials** | | | | |
|---|---|---|---|---|
| | **Metakaolin** | **Fly ash** | **Rice husk ash (black)** | **Calcined rice husk ash (white)** |
| **Cost (U$D[A]/100g)** | 1.87 | 0.00067 | 0 | 2.18 |
| **$CO_2$ Capture (mmol/100g)** | 33.0 | 53.0 | 46.0 | 61.0 |

A. Dollar quote held on September 16, 2019.

Source: Author's own elaboration.

# 8 CONCLUSION

In this study, the synthesis of geopolymers employing residues, fly ash, rice husk ash and calcined rice husk ash, in part of the composition, was successful.

The extraction of oxides, $SiO_2$, $Al_2O_3$ and $Na_2O$, aims to correctly quantify the composition of reactive oxides in the precursor materials, and therefore available for the geopolymerization process. Factor of great importance for the final properties of the geopolymer. Accurate quantification of oxides helps to lower process costs since alkaline activator dosing is not done in high excess. The metakaolin showed a high reactivity, where 92% $SiO_2$ and 100% $Al_2O_3$ are available for reaction. The rice husk ash and calcined rice husk ash showed 100% reactivity. Fly ash presented the lowest reactivity among the precursor materials, being 80 and 59%, for $SiO_2$ and $Al_2O_3$, respectively. Thus, confirming the difference between the total amount of oxides quantified by XRF, XRD- Rietveld and the reactive amount obtained by the extraction process.

Ten geopolymer compositions were formulated. Aiming at a lower use of commercialized materials such as metakaolin, high percentages of residues were incorporated in the geopolymer formulations. The geopolymers, MF-1 and MF-2, using metakaolin and fly ash presented the best compressive strength values, 11 and 7 MPa, respectively. Fact attributed to the high content of aluminosilicate gel obtained. In MF-2, the formation of zeolitic phase, sodalite was observed, a fact already reported in the literature, due to the high reactivity of metakaolin and fly ash in alkaline and thermal conditions. The MR-1 geopolymer containing metakaolin and rice husk ash had a compressive strength value of 5.5 MPa, when using the calcined rice husk ash, the geopolymer obtained negatively affected mechanical properties, obtaining a resistance of 2.6 MPa. Thus, noting that the removal of the carbonaceous material affected the compressive strength. Geopolymers containing two residues in the same composition had worse mechanical properties, attributed to the difference between particle sizes.

The non-use of sodium silicate as part of the alkaline activator suggests that a higher percentage of precursor material, and mainly residues, should be incorporated into the geopolymer compositions, thus causing a low cost and low environmental aggression process. Among the formulations that did not use sodium silicate, only MF-2, which contained

metakaolin and fly ash, showed good compression results (7 MPa), however, lower than MF-1 that used silicate. The other compositions (MR-2, MCR-2, MFR-2 and MFCR-2), which had rice husk ash and calcined rice husk ash, dissolved during submerged cure and could not have the properties evaluated. Thus, noting that the use of sodium silicate is fundamental for a better geopolymerization process.

From the leaching analysis it was possible to quantify the percentage of unreacted oxides during the geopolymerization process. Which directly impacts the final properties of geopolymers. The geopolymers that dissolved during submerged cure showed the highest percentages of leached oxides. It was found that the different degrees of solubility of precursor materials directly affect the percentage of leached oxides.

Considering the $CO_2$ capture process, the geopolymers presented different carbon dioxide adsorption capacities. The use of calcined rice husk ash increased the adsorption capacity of the geopolymer, expected phenomenon, since this material has a high specific area. No evident relationship between the BET surface area and adsorptive capacity was observed. The zeolitic phase obtained in MF-2 did not show significant adsorption gain. It should be noted that the $CO_2$ adsorption capacity of the geopolymers followed the same order that measured for their precursors (calcinated rice husk ash (white) > fly ash > rice husk ash (black)), indicating that the nature of the solid residue determine the $CO_2$ adsorption capacity.

The pseudo-first order kinetic model used to validate the experimental data of desorption adsorption processes obtained under the conditions of 35 °C and 1 bar presented a good fit.

Overall, it can be concluded that geopolymers are promising adsorbent materials for carbon dioxide capture.

The geopolymers showed good results as compressive strength and $CO_2$ adsorption. However specific studies to analyze cure conditions, amount of incorporated residue, alkaline activator and Si: Al ratio are suggested as future studies to obtain improved properties of geopolymers.

New conditions (temperature and pressure) in the adsorption and desorption process should be analyzed to evaluate the behavior of geopolymers. Another future study is its evaluation on the selectivity of gases such as $N_2$, $CH_4$, $H_2$.

## REFERENCES


AHSAN, M. B.; HOSSAIN, Z. Supplemental use of rice husk ash (RHA) as a cementitious material in concrete industry. **Construction and Building Materials**, v. 178, p. 1–9, jul. 2018.

ALLAHVERDI, A.; NAJAFI KANI, E.; HOSSAIN, K. M. A.; LACHEMI, M. **Methods to control efflorescence in alkali-activated cement-based materials**. [s.l.] Woodhead Publishing Limited, 2014.

ANTIOHOS, S. K.; TAPALI, J. G.; ZERVAKI, M.; SOUSA-COUTINHO, J.; TSIMAS, S.; PAPADAKIS, V. G. Low embodied energy cement containing untreated RHA: A strength development and durability study. **Construction and Building Materials**, v. 49, p. 455–463, 2013.

ASSI, L. N.; EDDIE DEAVER, E.; ZIEHL, P. Effect of source and particle size distribution on the mechanical and microstructural properties of fly Ash-Based geopolymer concrete. **Construction and Building Materials**, v. 167, p. 372–380, 2018.

ASTM. **Standard Specification for Coal Fly Ash and Raw or Calcined Natural Pozzolan for Use in Concrete**. West Conshohocken, PA: [s.n.].

AUTEF, A.; JOUSSEIN, E.; POULESQUEN, A.; GASGNIER, G.; PRONIER, S.; SOBRADOS, I.; SANZ, J.; ROSSIGNOL, S. Influence of metakaolin purities on potassium geopolymer formulation: The existence of several networks. **Journal of Colloid and Interface Science**, v. 408, n. 1, p. 43–53, 2013a.

AUTEF, A.; JOUSSEIN, E.; GASGNIER, G.; PRONIER, S.; SOBRADOS, I.; SANZ, J.; ROSSIGNOL, S. Role of metakaolin dehydroxylation in geopolymer synthesis. **Powder Technology**, v. 250, p. 33–39, dez. 2013b.

BAI, C.; COLOMBO, P. Processing, properties and applications of highly porous geopolymers: A review. **Ceramics International**, v. 44, n. 14, p. 16103–16118, out. 2018.

BAKHAREV, T. Geopolymeric materials prepared using Class F fly ash and elevated temperature curing. **Cement and Concrete Research**, v. 35, n. 6, p. 1224–1232, 2005.

BARLET-GOUEDARD, V.; ZUSATZ-AYACHE, B.; PORCHERIE, O. **Geopolymer composition and application for carbon dioxide storage**United States, 2010.

BAYLISS, P.; MALES, P. A. The mineralogical similarity of precious and common opal from Australia. **Mineralogical Magazine and Journal of the Mineralogical Society**, v. 35, n. 270, p. 429–431, 14 jun. 1965.

BILLONG, N.; KINUTHIA, J.; OTI, J.; MELO, U. C. Performance of sodium silicate free geopolymers from metakaolin (MK) and Rice Husk Ash (RHA): Effect on tensile strength and microstructure. **Construction and Building Materials**, v. 189, p. 307–313, 2018.

BURUBERRI, L. H.; TOBALDI, D. M.; CAETANO, A.; SEABRA, M. P.; LABRINCHA, J. A. Evaluation of reactive Si and Al amounts in various geopolymer precursors by a simple method. **Journal of Building Engineering**, v. 22, n. November 2018, p. 48–55, 2019.

CARVALHO, A. M. G. DE. **Introdução ao estudo dos Minerais**. [s.l: s.n.].

CHEN, A. N.; LI, M.; XU, J.; LOU, C. H.; WU, J. M.; CHENG, L. J.; SHI, Y. S.; LI, C. H. High-porosity mullite ceramic foams prepared by selective laser sintering using fly ash hollow spheres as raw materials. **Journal of the European Ceramic Society**, v. 38, n. 13, p. 4553–4559, 2018.

CHENG, T. W.; LEE, M. L.; KO, M. S.; UENG, T. H.; YANG, S. F. The heavy metal adsorption characteristics on metakaolin-based geopolymer. **Applied Clay Science**, v. 56, p. 90–96, fev. 2012.

CHINDAPRASIRT, P.; JATURAPITAKKUL, C.; CHALEE, W.; RATTANASAK, U. Comparative study on the characteristics of fly ash and bottom ash geopolymers. **Waste Management**, v. 29, n. 2, p. 539–543, 2009.

CIOFFI, R.; MAFFUCCI, L.; SANTORO, L. Optimization of geopolymer synthesis by calcination and polycondensation of a kaolinitic residue. **Resources, Conservation and Recycling**, v. 40, n. 1, p. 27–38, dez. 2003.

CONAB, C. N. DE A.-. **HISTÓRICO MENSAL DE ARROZ**Brasília, 2018. Dispon&#65533;vel em: <https://www.conab.gov.br/info-agro/analises-do-mercado-agropecuario-e-extrativista/analises-do-mercado/historico-mensal-de-arroz>

CRIADO, M.; PALOMO, A.; FERNÁNDEZ-JIMÉNEZ, A. Alkali activation of fly ashes. Part 1: Effect of curing conditions on the carbonation of the reaction products. **Fuel**, v. 84, n. 16, p. 2048–2054, nov. 2005.

D'ALESSANDRO, D. M.; SMIT, B.; LONG, J. R. Carbon Dioxide Capture: Prospects for New Materials. **Angewandte Chemie International Edition**, v. 49, n. 35, p. 6058–6082, 16 ago. 2010.

DANTAS, T. L. P. **Separação de dióxido de carbono por adsorção a partir de misturas sintéticas do tipo gás de exaustão**. [s.l.] Universidade Federal de Santa Catarina, 2009.

DAVIDOVITS, JOSEPH; DAVIDOVICS, MICHAEL; DAVIDOVITS, N. **Process for Obtaining a Geopolymeric Alumino-Silicate and Products thus Obtained**United States, 1994. Dispon&#65533;vel em: <https://patents.google.com/patent/US5342595A/en>

DAVIDOVITS, J. GEOPOLYMERS: INORGANIC POLYMERIC NEW MATERIALS. **THERMAL ANALYSIS**, v. 37, p. 1633–1656, 1991a.

DAVIDOVITS, J. Geopolymers. **Journal of Thermal Analysis**, v. 37, n. 8, p. 1633–1656, ago. 1991b.

DAVIDOVITS, J. Geopolymers. **Journal of Thermal Analysis**, v. 37, n. 8, p. 1633–1656, ago. 1991c.

DAVIDOVITS, J. GEOPOLYMERS: Man-Made Rock Geosynthesis and the Resulting Development of Very Early High Strength Cement. **Journal Materials Education**, v. 16, p. 91–139, 1994.

DAVIDOVITS, J. 30 Years of Successes and Failures in Geopolymer Applications . Market Trends and Potential Breakthroughs . **Geopolymer 2002 Conference, October 28-29, 2002, Melbourne, Australia**, p. 1–16, 2002.

DIMAS, D. D.; GIANNOPOULOU, I. P.; PANIAS, D. Utilization of alumina red mud for synthesis of inorganic polymeric materials. **Mineral Processing and Extractive Metallurgy Review**, v. 30, n. 3, p. 211–239, 2009.

DING, L.; YANG, H.; RAHIMI, P.; OMOTOSO, O.; FRIESEN, W.; FAIRBRIDGE, C.; SHI, Y.; NG, S. Solid transformation of zeolite NaA to sodalite. **Microporous and Mesoporous Materials**, v. 130, n. 1–3, p. 303–308, maio 2010.

DONG, M.; FENG, W.; ELCHALAKANI, M.; LI, G. (KEVIN); KARRECH, A.; MAY, E. F. Development of a High Strength Geopolymer by Novel Solar Curing. **Ceramics International**, v. 43, n. 14, p. 11233–11243, 2017.

DUXSON, P.; LUKEY, G. C.; SEPAROVIC, F.; VAN DEVENTER, J. S. J. Effect of alkali cations on aluminum incorporation in geopolymeric gels. **Industrial and Engineering Chemistry Research**, v. 44, n. 4, p. 832–839, 2005a.

DUXSON, P.; PROVIS, J. L.; LUKEY, G. C.; MALLICOAT, S. W.; KRIVEN, W. M.; VAN DEVENTER, J. S. J. Understanding the relationship between geopolymer

composition, microstructure and mechanical properties. **Colloids and Surfaces A: Physicochemical and Engineering Aspects**, v. 269, n. 1–3, p. 47–58, nov. 2005b.

DUXSON, P.; MALLICOAT, S. W.; LUKEY, G. C.; KRIVEN, W. M.; VAN DEVENTER, J. S. J. The effect of alkali and Si/Al ratio on the development of mechanical properties of metakaolin-based geopolymers. **Colloids and Surfaces A: Physicochemical and Engineering Aspects**, v. 292, n. 1, p. 8–20, 2007a.

DUXSON, P.; FERNÁNDEZ-JIMÉNEZ, A.; PROVIS, J. L.; LUKEY, G. C.; PALOMO, A.; VAN DEVENTER, J. S. J. Geopolymer technology: The current state of the art. **Journal of Materials Science**, v. 42, n. 9, p. 2917–2933, 2007b.

DUXSON, P.; FERNÁNDEZ-JIMÉNEZ, A.; PROVIS, J. L.; LUKEY, G. C.; PALOMO, A.; VAN DEVENTER, J. S. J. Geopolymer technology: the current state of the art. **Journal of Materials Science**, v. 42, n. 9, p. 2917–2933, 19 maio 2007c.

DUXSON, P.; PROVIS, J. L. Designing precursors for geopolymer cements. **Journal of the American Ceramic Society**, v. 91, n. 12, p. 3864–3869, 2008.

EMDADI, Z.; ASIM, N.; AMIN, M.; AMBAR YARMO, M.; MALEKI, A.; AZIZI, M.; SOPIAN, K. Development of Green Geopolymer Using Agricultural and Industrial Waste Materials with High Water Absorbency. **Applied Sciences**, v. 7, n. 5, p. 514, 2017.

FAQIR, N. M.; ELKATATNY, S.; MAHMOUD, M.; SHAWABKEH, R. Fabrication of kaolin-based cement plug for CO 2 storage wells. **Applied Clay Science**, v. 141, p. 81–87, jun. 2017.

FERNÁNDEZ-JIMÉNEZ, A.; PALOMO, A.; CRIADO, M. Microstructure development of alkali-activated fly ash cement: A descriptive model. **Cement and Concrete Research**, v. 35, n. 6, p. 1204–1209, 2005a.

FERNÁNDEZ-JIMÉNEZ, A.; PALOMO, A.; CRIADO, M. Microstructure development of alkali-activated fly ash cement: a descriptive model. **Cement and Concrete Research**, v. 35, n. 6, p. 1204–1209, jun. 2005b.

FOGLER, H. S. **Elements of Chemical Reaction Engineering**. 4. ed. Pennsylvania: [s.n.].

GHARZOUNI, A.; JOUSSEIN, E.; SAMET, B.; BAKLOUTI, S.; ROSSIGNOL, S. Effect of the reactivity of alkaline solution and metakaolin on geopolymer formation. **Journal of Non-Crystalline Solids**, v. 410, p. 127–134, 2015.

GOMEZ-ZAMORANO, L. Y.; VEGA-CORDERO, E.; STRUBLE, L. Composite geopolymers of metakaolin and geothermal nanosilica waste. **Construction and Building Materials**, v. 115, p. 269–276, 2016.

GUARÍN ROMERO, J.; MORENO-PIRAJÁN, J.; GIRALDO GUTIERREZ, L. Kinetic and Equilibrium Study of the Adsorption of CO2 in Ultramicropores of Resorcinol-Formaldehyde Aerogels Obtained in Acidic and Basic Medium. **Journal of Carbon Research**, v. 4, n. 4, p. 1–19, 2018.

HAJIMOHAMMADI, A.; VAN DEVENTER, J. S. J. Dissolution behaviour of source materials for synthesis of geopolymer binders: A kinetic approach. **International Journal of Mineral Processing**, v. 153, p. 80–86, 2015.

HELLER-KALLAI, L. Chapter 7.2 Thermally Modified Clay Minerals. In: **Developments in Clay Science**. [s.l: s.n.]. v. 1p. 289–308.

HILLIER, S.; LUMSDON, D. G. Distinguishing opaline silica from cristobalite in bentonites: a practical procedure and perspective based on NaOH dissolution. **Clay Minerals**, v. 43, n. 3, p. 477–486, 9 set. 2008.

HO, Y. S.; MCKAY, G. A Comparison of chemisorption kinetic models applied to pollutant removal on various sorbents. **Process Safety and Environmental Protection**, v. 76, n. 4, p. 332–340, 1998.

HO, Y. S.; MCKAY, G. Pseudo-seconf order model for sorption process. **Process Biochemistry**, v. 34, p. 451–465, 1999.

HOY, M.; HORPIBULSUK, S.; RACHAN, R.; CHINKULKIJNIWAT, A.; ARULRAJAH, A. Recycled asphalt pavement – fly ash geopolymers as a sustainable pavement base material: Strength and toxic leaching investigations. **Science of The Total Environment**, v. 573, p. 19–26, dez. 2016.

HUANG, H.; ZHANG, W.; LIU, D.; LIU, B.; CHEN, G.; ZHONG, C. Effect of temperature on gas adsorption and separation in ZIF-8: A combined experimental and molecular simulation study. **Chemical Engineering Science**, v. 66, n. 23, p. 6297–6305, dez. 2011.

HWANG, C.-L.; HUYNH, T.-P. Effect of alkali-activator and rice husk ash content on strength development of fly ash and residual rice husk ash-based geopolymers. **Construction and Building Materials**, v. 101, p. 1–9, dez. 2015a.

HWANG, C. L.; HUYNH, T. P. Effect of alkali-activator and rice husk ash content on strength development of fly ash and residual rice husk ash-based geopolymers. **Construction and Building Materials**, v. 101, p. 1–9, 2015b.

IPCC. **Climate Change 2014 Synthesis Report - IPCCClimate Change 2014: Synthesis Report. Contribution of Working Groups I, II and III to the Fifth Assessment Report of the Intergovernmental Panel on Climate Change**. Geneva, Switzerland: [s.n.].

J., D. 30 Years of successes and failures in geopolymer applications. Market trends and potential breakthroughs. Geopolymer 2002: Turn Potential Into Profit, Melbourne, Australia: Siloxo Pty Ltd., G.C. Lukey, Ed., CD-ROM Proceedings. p. 1–16, 2002.

KAUR, K.; SINGH, J.; KAUR, M. Compressive strength of rice husk ash based geopolymer: The effect of alkaline activator. **Construction and Building Materials**, v. 169, p. 188–192, 2018.

KHAJAVI, S.; JANSEN, J. C.; KAPTEIJN, F. Application of hydroxy sodalite films as novel water selective membranes. **Journal of Membrane Science**, v. 326, n. 1, p. 153–160, jan. 2009.

KHAN, R.; JABBAR, A.; AHMAD, I.; KHAN, W.; KHAN, A. N.; MIRZA, J. Reduction in environmental problems using rice-husk ash in concrete. **Construction and Building Materials**, v. 30, p. 360–365, 2012.

KOLEŻYŃSKI, A.; KRÓL, M.; ŻYCHOWICZ, M. The structure of geopolymers – Theoretical studies. **Journal of Molecular Structure**, v. 1163, p. 465–471, 2018.

KOMNITSAS, K.; ZAHARAKI, D. Geopolymerisation: A review and prospects for the minerals industry. **Minerals Engineering**, v. 20, n. 14, p. 1261–1277, 2007.

KOSHY, N.; DONDROB, K.; HU, L.; WEN, Q.; MEEGODA, J. N. Synthesis and characterization of geopolymers derived from coal gangue, fly ash and red mud. **Construction and Building Materials**, v. 206, p. 287–296, 2019.

KRÓL, M.; MOZGAWA, W. Zeolite layer on metakaolin-based support. **Microporous and Mesoporous Materials**, v. 282, n. March, p. 109–113, jul. 2019.

KUSBIANTORO, A.; NURUDDIN, M. F.; SHAFIQ, N.; QAZI, S. A. The effect of microwave incinerated rice husk ash on the compressive and bond strength of fly ash based geopolymer concrete. **Construction and Building Materials**, v. 36, p. 695–703, 2012a.

KUSBIANTORO, A.; NURUDDIN, M. F.; SHAFIQ, N.; QAZI, S. A. The effect of microwave incinerated rice husk ash on the compressive and bond strength of fly ash based geopolymer concrete. **Construction and Building Materials**, v. 36, p. 695–703, nov. 2012b.

LAHOTI, M.; WONG, K. K.; YANG, E. H.; TAN, K. H. Effects of Si/Al molar ratio

on strength endurance and volume stability of metakaolin geopolymers subject to elevated temperature. **Ceramics International**, v. 44, n. 5, p. 5726–5734, 2018.

LAU, C. K.; ROWLES, M. R.; PARNHAM, G. N.; HTUT, T.; NG, T. S. Investigation of geopolymers containing fly ash and ground-granulated blast-furnace slag blended by amorphous ratios. **Construction and Building Materials**, v. 222, p. 731–737, out. 2019.

LEE, B.; KIM, G.; KIM, R.; CHO, B.; LEE, S.; CHON, C.-M. Strength development properties of geopolymer paste and mortar with respect to amorphous Si/Al ratio of fly ash. **Construction and Building Materials**, v. 151, p. 512–519, out. 2017.

LLOYD, R. R. Accelerated ageing of geopolymers. In: **Geopolymers**. [s.l.] Elsevier, 2009. p. 139–166.

MA, S.-H.; XU, M.-D.; QIQIGE; WANG, X.-H.; ZHOU, X. Challenges and Developments in the Utilization of Fly Ash in China. **International Journal of Environmental Science and Development**, v. 8, n. 11, p. 781–785, 2018.

MALEKI, A.; MOHAMMAD, M.; EMDADI, Z.; ASIM, N.; AZIZI, M.; SAFAEI, J. Adsorbent materials based on a geopolymer paste for dye removal from aqueous solutions. **Arabian Journal of Chemistry**, set. 2018.

MEDRI, V.; FABBRI, S.; DEDECEK, J.; SOBALIK, Z.; TVARUZKOVA, Z.; VACCARI, A. Role of the morphology and the dehydroxylation of metakaolins on geopolymerization. **Applied Clay Science**, v. 50, n. 4, p. 538–545, 2010.

MINELLI, M.; MEDRI, V.; PAPA, E.; MICCIO, F.; LANDI, E.; DOGHIERI, F. Geopolymers as solid adsorbent for CO2 capture. **Chemical Engineering Science**, v. 148, p. 267–274, 2016a.

MINELLI, M.; MEDRI, V.; PAPA, E.; MICCIO, F.; LANDI, E.; DOGHIERI, F. Geopolymers as solid adsorbent for CO2 capture. **Chemical Engineering Science**, v. 148, p. 267–274, jul. 2016b.

MINJIGMAA, A.; TEMUUJIN, J.; DARKHIJAV, B.; DAVAABAL, B.; RUESCHER, C.; BATTSETSEG, B. E. Characterization of Effloresences of Ambient and Elevated Temperature Cured Fly Ash Based Geopolymer Type Concretes. **Advanced Materials Research**, v. 1139, p. 25–29, 2016.

MO, B. H.; ZHU, H.; CUI, X. M.; HE, Y.; GONG, S. Y. Effect of curing temperature on geopolymerization of metakaolin-based geopolymers. **Applied Clay Science**, v. 99, p. 144–148, 2014.

MODAK, A.; JANA, S. Advancement in porous adsorbents for post-combustion CO2 capture. **Microporous and Mesoporous Materials**, v. 276, n. September 2018, p. 107–132, mar. 2019.

MOOSAVI, A.; ASADI, S.; SHORAKI, H. J. Microstructure and mechanical properties of tabular alumina composites with geopolymer binder at elevated temperatures. **Ceramics International**, v. 45, n. 7, p. 9092–9098, 2019.

MUÑIZ-VILLARREAL, M. S.; MANZANO-RAMÍREZ, A.; SAMPIERI-BULBARELA, S.; GASCA-TIRADO, J. R.; REYES-ARAIZA, J. L.; RUBIO-ÁVALOS, J. C.; PÉREZ-BUENO, J. J.; APATIGA, L. M.; ZALDIVAR-CADENA, A.; AMIGÓ-BORRÁS, V. The effect of temperature on the geopolymerization process of a metakaolin-based geopolymer. **Materials Letters**, v. 65, n. 6, p. 995–998, 2011.

NABAVI, M. S.; MOHAMMADI, T.; KAZEMIMOGHADAM, M. Hydrothermal synthesis of hydroxy sodalite zeolite membrane: Separation of H2/CH4. **Ceramics International**, v. 40, n. 4, p. 5889–5896, maio 2014.

NAJAFI KANI, E.; ALLAHVERDI, A.; PROVIS, J. L. Efflorescence control in geopolymer binders based on natural pozzolan. **Cement and Concrete Composites**, v. 34, n. 1, p. 25–33, 2012.

NASCIMENTO, R. F. DO; LIMA, A. C. A. DE; VIDAL, C. B.; MELO, D. DE Q.; RAULINO, G. S. C. **Adsorção: aspectos teóricos e aplicações ambientais**. Fortaleza: Imprensa Universitária, 2014.

NASVI, M. C. M.; RANJITH, P. G.; SANJAYAN, J.; BUI, H. Effect of temperature on permeability of geopolymer: A primary well sealant for carbon capture and storage wells. **Fuel**, v. 117, n. PART A, p. 354–363, jan. 2014.

NASVI, M. C. M.; RANJITH, P. G.; SANJAYAN, J. Effect of different mix compositions on apparent carbon dioxide (CO2) permeability of geopolymer: Suitability as well cement for CO2 sequestration wells. **Applied Energy**, v. 114, p. 939–948, fev. 2014.

NIC, M.; JIRAT, J.; KOSATA, B. **Compendium of Chemical Terminology Gold Book**. 2.3.2 ed. Washington: ACS Publications & ACS CINF, 2012.

NOVAIS, R. M.; BURUBERRI, L. H.; SEABRA, M. P.; LABRINCHA, J. A. Novel porous fly-ash containing geopolymer monoliths for lead adsorption from wastewaters. **Journal of Hazardous Materials**, v. 318, p. 631–640, nov. 2016.

NURUDDIN, M. F.; ABDUL RAHIM, R. H.; MAN, Z.; RAHMIATI, T.; ISMAIL, L.; AZIZLI, K. A. Comparison of Using NaOH and KOH Activated Fly Ash-Based Geopolymer on the Mechanical Properties. **Materials Science Forum**, v. 803, p. 179–184, 2014.

ONUTAI, S.; KOBAYASHI, T.; THAVORNITI, P.; JIEMSIRILERS, S. Porous fly ash-based geopolymer composite fiber as an adsorbent for removal of heavy metal ions from wastewater. **Materials Letters**, v. 236, p. 30–33, fev. 2019.

PACHECO-TORGAL, F.; CASTRO-GOMES, J.; JALALI, S. Alkali-activated binders: A review. Part 1. Historical background, terminology, reaction mechanisms and hydration products. **Construction and Building Materials**, v. 22, n. 7, p. 1305–1314, 2008a.

PACHECO-TORGAL, F.; CASTRO-GOMES, J.; JALALI, S. Alkali-activated binders: A review. Part 2. About materials and binders manufacture. **Construction and Building Materials**, v. 22, n. 7, p. 1315–1322, jul. 2008b.

PAIVA, M. D. M.; SILVA, E. C. C. M.; MELO, D. M. A.; MARTINELLI, A. E.; SCHNEIDER, J. F. A geopolymer cementing system for oil wells subject to steam injection. **Journal of Petroleum Science and Engineering**, v. 169, n. June, p. 748–759, out. 2018.

PALOMO, A., M. GRUTZECK, AND M. B. Alkali-activated fly ashes: a cement for the future. Cement and concrete research. **Cement and Concrete Research**, v. 29(8):, p. 1323-1329., 1999.

PALOMO, A.; FERNÁNDEZ-JIMÉNEZ, A.; ALONSO, S.; FERNANDEZ-JIME, A. Alkaline Activation of Fly Ashes : NMR Study of the Reaction Products Alkaline Activation of Fly Ashes : NMR Study of the Reaction Products. **Journal of the …**, v. 1145, n. November 2015, p. 1141–1145, 2008.

PANAGIOTOPOULOU, C.; KONTORI, E.; PERRAKI, T.; KAKALI, G. Dissolution of aluminosilicate minerals and by-products in alkaline media. **Journal of Materials Science**, v. 42, n. 9, p. 2967–2973, 2007.

PROVIS, J. L. **Modeling the Formation of Geopolymers**. [s.l.] The University of Melbourne, 2006.

PROVIS, J. L.; BERNAL, S. A. Geopolymers and Related Alkali-Activated Materials. **Annual Review of Materials Research**, v. 44, n. 1, p. 299–327, 2014.

PROVIS, J. L.; YONG, S. L.; DUXSON, P. Nanostructure/microstructure of metakaolin geopolymers. In: PROVIS, J. L.; VAN DEVENTER, J. S. J. (Eds.). . **Geopolymers: Structures, Processing, Properties and Industrial Applications**. 1. ed. Melbourne: [s.n.]. p.

72–88.

PTÁČEK, P.; OPRAVIL, T.; ŠOUKAL, F.; WASSERBAUER, J.; MÁSILKO, J.; BARÁČEK, J. The influence of structure order on the kinetics of dehydroxylation of kaolinite. **Journal of the European Ceramic Society**, v. 33, n. 13–14, p. 2793–2799, nov. 2013.

RANJBAR, N.; MEHRALI, M.; ALENGARAM, U. J.; METSELAAR, H. S. C.; JUMAAT, M. Z. Compressive strength and microstructural analysis of fly ash/palm oil fuel ash based geopolymer mortar under elevated temperatures. **Construction and Building Materials**, v. 65, p. 114–121, 2014.

RASAKI, S. A.; BINGXUE, Z.; GUARECUCO, R.; THOMAS, T.; MINGHUI, Y. Geopolymer for use in heavy metals adsorption, and advanced oxidative processes: A critical review. **Journal of Cleaner Production**, v. 213, p. 42–58, mar. 2019.

RATTANASAK, U.; CHINDAPRASIRT, P. Influence of NaOH solution on the synthesis of fly ash geopolymer. **Minerals Engineering**, v. 22, n. 12, p. 1073–1078, 2009.

REDFERN, S. A. T. The kinects of dehydroxylation of kaolinite. **Clay Minerals**, v. 22, n. 4, p. 447–456, 1987.

ROWLES, M.; O'CONNOR, B. Chemical optimisation of the compressive strength of aluminosilicate geopolymers synthesised by sodium silicate activation of metakaolinite. **Journal of Materials Chemistry**, v. 13, n. 5, p. 1161–1165, 2003.

SAMANTA, A.; ZHAO, A.; SHIMIZU, G. K. H.; SARKAR, P.; GUPTA, R. Post-Combustion CO 2 Capture Using Solid Sorbents: A Review. **Industrial & Engineering Chemistry Research**, v. 51, n. 4, p. 1438–1463, 21 fev. 2012.

SAMANTASINGHAR, S.; SINGH, S. P. Effect of synthesis parameters on compressive strength of fly ash-slag blended geopolymer. **Construction and Building Materials**, v. 170, p. 225–234, 2018.

SANTOS, P. DE S. **Ciência e Tecnologia de Argilas**. 2.ª ed. São Paulo: Blucher, Edgard, 1989.

SHEN, Y.; SHI, W.; ZHANG, D.; NA, P.; FU, B. The removal and capture of CO2 from biogas by vacuum pressure swing process using silica gel. **Journal of CO2 Utilization**, v. 27, n. July, p. 259–271, out. 2018.

SHI, C.; JIMÉNEZ, A. F.; PALOMO, A. New cements for the 21st century: The pursuit of an alternative to Portland cement. **Cement and Concrete Research**, v. 41, n. 7, p. 750–763, 2011.

ŠKVÁRA, F.; KOPECKÝ, L.; MYŠKOVÁ, L.; ŠMILAUER, V. Í. T.; ALBEROVSKÁ, L.; VINŠOVÁ, L. Aluminosilicate polymers - Influence of elevated temperatures, efflorescence. **Ceramics - Silikaty**, v. 53, n. 4, p. 276–282, 2009.

SORE, S. O.; MESSAN, A.; PRUD'HOMME, E.; ESCADEILLAS, G.; TSOBNANG, F. Synthesis and characterization of geopolymer binders based on local materials from Burkina Faso – Metakaolin and rice husk ash. **Construction and Building Materials**, v. 124, p. 301–311, 2016.

SOUTSOS, M.; BOYLE, A. P.; VINAI, R.; HADJIERAKLEOUS, A.; BARNETT, S. J. Factors influencing the compressive strength of fly ash based geopolymers. **Construction and Building Materials**, v. 110, p. 355–368, 2016.

STRYDOM, C. A.; SWANEPOEL, J. C. Utilisation of fly ash in a geopolymeric material. **Applied Geochemistry**, v. 17, n. 8, p. 1143–1148, 2002.

STURM, P.; GLUTH, G. J. G.; BROUWERS, H. J. H.; KÜHNE, H. C. Synthesizing one-part geopolymers from rice husk ash. **Construction and Building Materials**, v. 124, p. 961–966, 2016a.

STURM, P.; GLUTH, G. J. G.; BROUWERS, H. J. H.; KÜHNE, H.-C. Synthesizing one-part geopolymers from rice husk ash. **Construction and Building Materials**, v. 124, p.

961–966, out. 2016b.

SUN, Z.; VOLLPRACHT, A. One year geopolymerisation of sodium silicate activated fly ash and metakaolin geopolymers. **Cement and Concrete Composites**, v. 95, n. October 2018, p. 98–110, 2019.

THOMMES, M.; KANEKO, K.; NEIMARK, A. V.; OLIVIER, J. P.; RODRIGUEZ-REINOSO, F.; ROUQUEROL, J.; SING, K. S. W. Physisorption of gases, with special reference to the evaluation of surface area and pore size distribution (IUPAC Technical Report). **Pure and Applied Chemistry**, v. 87, n. 9–10, p. 1051–1069, 1 out. 2015.

TONIOLO, N.; RINCÓN, A.; AVADHUT, Y. S.; HARTMANN, M.; BERNARDO, E.; BOCCACCINI, A. R. Novel geopolymers incorporating red mud and waste glass cullet. **Materials Letters**, v. 219, p. 152–154, 2018.

VAN DEVENTER, J. S. J.; PROVIS, J. L.; DUXSON, P.; LUKEY, G. C. Reaction mechanisms in the geopolymeric conversion of inorganic waste to useful products. **Journal of Hazardous Materials**, v. 139, n. 3, p. 506–513, 2007.

VAN JAARSVELD, J. G. S.; VAN DEVENTER, J. S. J.; LUKEY, G. C. The effect of composition and temperature on the properties of fly ash- and kaolinite-based geopolymers. **Chemical Engineering Journal**, v. 89, n. 1–3, p. 63–73, 2002.

WAN, Q.; RAO, F.; SONG, S. Reexamining calcination of kaolinite for the synthesis of metakaolin geopolymers - roles of dehydroxylation and recrystallization. **Journal of Non-Crystalline Solids**, v. 460, p. 74–80, 2017.

WANG, Q.; LUO, J.; ZHONG, Z.; BORGNA, A. CO2 capture by solid adsorbents and their applications: current status and new trends. **Energy Environ. Sci.**, v. 4, n. 1, p. 42–55, 2011.

UNITED STATES. National Oceanic & Atmospheric Administration. U.s. Department Of Commerce. **Trends in Atmospheric Carbon Dioxide.** 2018. Disponível em: <https://www.esrl.noaa.gov/gmd/ccgg/trends/global.html>. Acesso em: 10 out. 2019.

WILLIAMS, R. P.; VAN RIESSEN, A. Determination of the reactive component of fly ashes for geopolymer production using XRF and XRD. **Fuel**, v. 89, n. 12, p. 3683–3692, dez. 2010.

WIRAWAN, S. K.; CREASER, D. CO2 adsorption on silicalite-1 and cation exchanged ZSM-5 zeolites using a step change response method. **Microporous and Mesoporous Materials**, v. 91, n. 1–3, p. 196–205, 2006.

XU, H.; DEVENTER, J. S. J. VAN. The geopolymerisation of alumino-silicate minerals. **International Journal of Mineral Processing**, v. 59, p. 247–266, 2000.

YANG, T.; ZHU, H.; ZHANG, Z.; GAO, X.; ZHANG, C.; WU, Q. Effect of fly ash microsphere on the rheology and microstructure of alkali-activated fly ash/slag pastes. **Cement and Concrete Research**, v. 109, n. January, p. 198–207, 2018a.

YANG, T.; ZHU, H.; ZHANG, Z.; GAO, X.; ZHANG, C.; WU, Q. Effect of fly ash microsphere on the rheology and microstructure of alkali-activated fly ash/slag pastes. **Cement and Concrete Research**, v. 109, n. January, p. 198–207, 2018b.

YOUSEFI ODERJI, S.; CHEN, B.; JAFFAR, S. T. A. Effects of relative humidity on the properties of fly ash-based geopolymers. **Construction and Building Materials**, v. 153, p. 268–273, out. 2017.

ZHANG, P.; XUE, X.; DAI, J.-G.; ZHANG, W.-D.; POON, C.-S.; LIU, Y.-L. Inhibiting efflorescence formation on fly ash–based geopolymer via silane surface modification. **Cement and Concrete Composites**, v. 94, n. August, p. 43–52, 2018.

ZHANG, Y.; SU, W.; SUN, Y.; LIU, J.; LIU, X.; WANG, X. Adsorption Equilibrium of N 2 , CH 4 , and CO 2 on MIL-101. **Journal of Chemical & Engineering Data**, v. 60, n. 10, p. 2951–2957, 8 out. 2015.

ZHANG, Z.; WANG, H.; YAO, X.; ZHU, Y. Effects of halloysite in kaolin on the formation and properties of geopolymers. **Cement and Concrete Composites**, v. 34, n. 5, p. 709–715, 2012.

ZHANG, Z.; PROVIS, J. L.; REID, A.; WANG, H. Fly ash-based geopolymers: The relationship between composition, pore structure and efflorescence. **Cement and Concrete Research**, v. 64, p. 30–41, 2014.

ZHANG, Z. H.; ZHU, H. J.; ZHOU, C. H.; WANG, H. Geopolymer from kaolin in China: An overview. **Applied Clay Science**, v. 119, p. 31–41, 2016.

ZHOU, W.; YAN, C.; DUAN, P.; LIU, Y.; ZHANG, Z.; QIU, X.; LI, D. A comparative study of high- and low-Al2O3fly ash based-geopolymers: The role of mix proportion factors and curing temperature. **Materials and Design**, v. 95, p. 63–74, 2016.

ZHU, H.; LIANG, G.; XU, J.; WU, Q.; ZHAI, M. Influence of rice husk ash on the waterproof properties of ultrafine fly ash based geopolymer. **Construction and Building Materials**, v. 208, p. 394–401, 2019.

ZHUANG, X. Y.; CHEN, L.; KOMARNENI, S.; ZHOU, C. H.; TONG, D. S.; YANG, H. M.; YU, W. H.; WANG, H. Fly ash-based geopolymer: Clean production, properties and applications. **Journal of Cleaner Production**, v. 125, p. 253–267, 2016.

ZIBOUCHE, F.; KERDJOUDJ, H.; DE LACAILLERIE, J. B. D. E.; VAN DAMME, H. Geopolymers from Algerian metakaolin. Influence of secondary minerals. **Applied Clay Science**, v. 43, n. 3–4, p. 453–458, 2009.

ZOU, Y.; YANG, T. Rice Husk, Rice Husk Ash and Their Applications. In: **Rice Bran and Rice Bran Oil**. Shanghai: Elsevier, 2019. p. 207–246.